

Stratigraphy of Part of the Lunar Near Side

GEOLOGICAL SURVEY PROFESSIONAL PAPER 1046-A

*Prepared on behalf of the
National Aeronautics and Space Administration.*



Stratigraphy of Part of the Lunar Near Side

By DON E. WILHELMS

A P O L L O 1 5 — 1 7 O R B I T A L I N V E S T I G A T I O N S

G E O L O G I C A L S U R V E Y P R O F E S S I O N A L P A P E R 1 0 4 6 - A

*Prepared on behalf of the
National Aeronautics and Space Administration*



UNITED STATES DEPARTMENT OF THE INTERIOR

CECIL D. ANDRUS, *Secretary*

GEOLOGICAL SURVEY

H. William Menard, *Director*

Library of Congress Cataloging in Publication Data

Wilhelms, Don E.
Stratigraphy of part of the lunar nearside

Apollo 15-17 orbital investigations. Geological Survey Professional Paper 1046-A

Bibliography: p. A66-A71

Supt. of Docs. No.: I 19.16:1046-A

1. Lunar stratigraphy. 2. Project Apollo. I. United States. National Aeronautics and Space Administration.

II. Title. III. Series. IV. Series: United States. Geological Survey. Professional Paper 1046-A

QB592.W52

551.7'00999'1

80-607099

**For sale by the Superintendent of Documents, U.S. Government Printing Office
Washington, D.C. 20402**

CONTENTS

	Page		Page
Abstract	A1	Taruntius region	A35
Introduction	1	Terra units	35
Previous work	2	Low albedo of some terra units	38
Scope	2	Northern Nectaris basin rim	39
Data sources	3	Theophilus	39
Stratigraphic terminology	3	Orientale analogs	43
Acknowledgments	6	Secondary impact craters of Imbrium	43
Mare Imbrium and northern Oceanus Procellarum	6	Deposits	45
Introduction	6	Post-Imbrium features	45
Superposition relations	8	Central highlands	45
Mare ages on basis of small craters	14	Grooves	46
Flooding of small craters	14	Subcircular Imbrium secondary craters	46
Morphology of small superposed craters	14	Other possible secondary craters	47
Other properties	17	Primary impact craters	47
Color	17	Descartes mountains	51
Radar	17	Other hummocky deposits and hills	51
Reflectivity	17	Plains deposits	52
Correlations with time-stratigraphic units	17	Southern Oceanus Procellarum	56
Apeninus-Haemus region	19	Fra Mauro Formation	56
Terra materials—Imbrium basin	19	Mare properties	57
Massif material	22	Age	57
Material of Montes Archimedes	23	Color	60
Blocky ejecta	23	Reflectivity	61
Lineated and smooth ejecta	23	Thickness	61
Grooved material	24	Correlations of mare properties	62
Possible impact melt	25	Age versus thickness	63
Slump deposits	26	Age versus color	63
Dark materials	26	Color versus reflectivity	63
Mare materials	26	Reflectivity versus thickness	64
Mare and dark mantling material in Montes Haemus	27	Color versus thickness	64
Sources	27	Age versus reflectivity	64
Terra east of Mare Serenitatis, west of Crisium, and north of Tranquillitatis	27	Very red terra	64
Pre-Imbrian materials	31	Summary and conclusions	65
Possible Imbrium effects	31	Imbrium impact	65
Internal versus basin origin of structures	31	Mare materials	66
Craters	34	References cited	67

ILLUSTRATIONS

	Page
FIGURE 1. Shaded relief map of part of the lunar nearside showing location of text figures	A4
2. Geologic map of northern Oceanus Procellarum, Montes Harbinger, and Aristarchus plateau	6
3. Geologic map of part of southern Mare Imbrium	8
4-7. Photographs of:	
4. Young lava flows in Mare Imbrium	10
5. Crater Euler	11
6. Crater Lambert	12
7. Craters Delisle and Diophantus	13
8. Stereoscopic photographs showing stratigraphic relations between older Eratosthenian mare material and secondary craters of Timocharis and Eratosthenes	15
9. Photograph of area in northern Oceanus Procellarum	16
10. Color-difference photograph including region mapped in figures 2 and 3	18
11. Geologic map of terra materials in Apeninus-Haemus region	20

	Page
FIGURE 12. Stereoscopic photographs of central part of area mapped in figure 11A	A22
13. Photograph showing varieties of ejecta and mare features on southeast-sloping flank of Montes Apenninus	24
14. Photograph of area on flank of Orientale basin analogous to area in figure 13	25
15. Geologic map of dark materials in parts of Apenninus-Haemus region, Mare Serenitatis, and Mare Tranquillitatis ..	28
16. Color-difference photograph including region mapped in figure 11	30
17. Geologic map of eastern Serenitatis, western Crisium, and northern Tranquillitatis region	32
18. Stereoscopic photographs showing east-central part of area covered by figure 17A	34
19. Photograph showing part of area mapped in figure 17	35
20. Photograph of area 900 km east-southeast of Orientale basin center	36
21. Geologic map of Taruntius region	37
22. Stereoscopic photographs showing southwestern corner of area in figure 21	38
23. Geologic map of part of northern Nectaris rim	40
24. Stereoscopic photographs of part of area mapped in figure 23	41
25. Stereoscopic photographs showing features of crater Theophilus	42
26. Photograph of Orientale secondary craters and basin deposits southeast of Orientale basin	44
27. Geologic map of part of central highlands	48
28. Stereoscopic photographs of part of central highlands	52
29. Photograph of Orientale analogs of many features in study area	54
30. Photograph of crater Struve L	55
31. Photograph of plains deposits in floor of crater Albategnius	55
32. Geologic map of part of southern Oceanus Procellarum	56
33. Stereoscopic photographs of central part of area covered by figure 32A	58
34. Stereoscopic photographs of western part of area covered by figure 32B	58
35. Stereoscopic photographs of eastern part of area covered by figure 32B	59
36. Color-difference photograph including area mapped in figure 32	60
37. Histograms showing relations between pairs of properties of mare soil mapped in figure 32	62

TABLES

	Page
TABLE 1. D_L values in the areas mapped in figures 2 and 3	A17
2. Crater age assignments in the northern Oceanus Procellarum-southern Mare Imbrium region	19
3. List of mare units mapped in figure 32	63

APOLLO 15-17 ORBITAL INVESTIGATIONS

STRATIGRAPHY OF PART OF THE LUNAR NEAR SIDE

By DON E. WILHELMS

ABSTRACT

The geology of the part of the lunar near side west of longitude 50°E. photographed by Apollos 15, 16, and 17 has been remapped and reinterpreted. Emphasis is on the stratigraphy of the mare materials and on genetic and stratigraphic interpretations of terra units and landforms believed related to the Imbrium basin. The key data sets are stereoscopic orbital pictures taken by the three Apollo missions, Lunar Orbiter IV photographs of the Orientale basin, Earth-based telescopic color-difference images, and the Apollo 16 rock analyses.

In northern Oceanus Procellarum and southern Mare Imbrium, a detailed stratigraphic sequence of 20 crater and mare units has been determined. Working definitions of the Imbrian-Eratosthenian and Eratosthenian-Copernican systemic boundaries based on this sequence are proposed. The sequence is correlated with relative mare ages that are calibrated against absolute rock ages, and values of 3.3 ± 0.1 and $\leq 2.3 \pm 0.1$ billion years, respectively, are estimated for the system boundaries.

The terrae of the north-central near side are dominated by the rings and continuous ejecta of the Imbrium basin. The crest of Montes Apenninus is part of the main rim crest of the Imbrium crater of excavation, modified by slumps. Blocky primary basin ejecta lofted or thrust onto the Apennine flank grades outward to lineated and smooth ejecta that flowed along the surface and overrode pre-basin features and Imbrium-basin secondary impact craters. Grooves in the overridden high terrain are flow lineations in the continuous ejecta blanket. Flowing deposits obstructed by pre-existing terrain apparently piled up as small knobs and ridges. Impact melt was deposited on the Apennine flank and inside the basin on the Apennine bench; parts of the bench deposits are superposed on slump material, indicating slumping immediately after basin formation. The terra east of Serenitatis, west of Crisium, and north and east of Tranquillitatis consists of overlapping deposits and intersecting rings of pre-Imbrian basins modified by superposition of Imbrium secondary craters, secondary or primary deposits, and northwest-oriented grooves and other landforms previously attributed to faulting.

In Maria Serenitatis and Tranquillitatis and on bordering terrae, the oldest dark units are mare and dark mantling materials that appear both red and blue on color-difference photographs. An early generalization that darkness and youth correlate for these materials is in error, and a later conclusion that lava eruptions progressed in time from blue (high titanium) in the east to red (low titanium) in the central near side to blue again in the west in Eratosthenian time also has many exceptions. Other studies have shown that color and reflectivity are both determined by composition in mature regoliths derived from mare lavas. Mantling materials are common on the terra borders of all maria studied and probably occur within maria as well. Many deposits considered mare because of their flatness may be pyroclastic accumulations. Sources can be identified for many mantling deposits but not for most maria. Adjacent mare patches occur at

several levels, and so have no common hydrostatic level. Mare or mantling materials have flowed from one level to another in several localities. Superposition of mantles on terrae gives rise to mixed telescopic properties.

The central highlands, northern Nectaris basin rim, and other outer terrae were largely shaped by Imbrium ejecta. Conspicuous Imbrium-radial grooves appear on the stereoscopic photographs to consist of coalescing elliptical secondary impact craters. Other grooves and ridges were formed by flow of material along the surface. Very few faults were found in the terrae of the entire mapped region. With increasing distance from Imbrium, the Imbrium secondary craters appear more circular, more widely spaced, and topographically sharper. Many sharp and degraded craters once considered primary impact craters here and elsewhere are now believed secondary to Imbrium. Complex and diverse landforms including mounds seemingly superposed on irregular craters, deposits that bury or partly fill craters, and various basin-radial ridges and grooves are explained by the nearly simultaneous impact of many closely spaced ejecta fragments and by interaction with primary ejecta. Many of the pits near the Apollo 16 site are Imbrium secondary craters superposed on Nectaris basin ejecta, but the Descartes mountains material at the site could have been emplaced as a flow containing much primary ejecta, as suggested by others. Such flows probably produced other thick, hummocky deposits including the Fra Mauro Formation and also contributed to some of the larger plains deposits in the transition zone between continuous Imbrium ejecta and secondary features. Distal plains deposits are probably composed mostly of secondary ejecta. Some small plains patches in the central highlands could be of Orientale origin.

Southern Oceanus Procellarum includes a complex patchwork of mare units and terra islands geologically like the central highlands. Color and reflectivity correlate closely for most units, blue mare units being dark and red units light. Apparently the regoliths are mature, and composition is the only factor controlling reflectivity for most units. A few anomalously bright blue units may have been contaminated by underlying terra materials that may include fresh crystalline fragments. A few anomalously dark red units may have been contaminated or may contain titanium-rich pyroclastic glass whose optical properties result from a certain degree of devitrification.

INTRODUCTION

This is the first chapter of a series describing investigations by the U.S. Geological Survey based on data acquired from lunar orbit, chiefly by Apollo missions 15, 16, and 17. The stratigraphy of the near side of the Moon west of 50° east longitude as determined by

photogeological techniques is the principal topic of this chapter. Subsequent chapters, by other authors, describe remote-sensing studies (chapter B), crater geometry (chapter C), and experimental photogrammetry (chapter D) and include results from earlier Apollo missions as well as the last three.

PREVIOUS WORK

The Apollo orbital photographs provide a close look at an area that has been studied geologically for many years starting with Gilbert (1893). Astronomers Baldwin (1949, 1963) and Kuiper (1954, 1959) also contributed many geological insights in their general lunar studies. Geologic mapping in the space age began with three near-side maps by Hackman and Mason (1961), followed by an intensive program of detailed mapping based on systematic application of stratigraphic principles developed by Shoemaker (1962) and Shoemaker and Hackman (1962). Maps at 1:1,000,000 scale in the area covered by the present study were prepared by Marshall (1963), Eggleton (1965), Carr (1965, 1966), Moore (1965, 1967), Hackman (1966), Morris and Wilhelms (1967), Milton (1968), Howard and Masursky (1968), Wilhelms (1968, 1972a), Scott and Pohn (1972), and Elston (1972). The telescopic phase of this mapping was summarized by Wilhelms (1970), and the rest of the pre-Apollo 15 mapping was summarized and updated on a near-side map at 1:5,000,000 scale by Wilhelms and McCauley (1971). Numerous other maps and topical studies cover parts of the area, including large-scale pre-mission maps (Eggleton and Offield, 1970; Carr and others, 1971; Milton and Hodges, 1972; Scott and others, 1972). Among the achievements of this previous work are (1) recognition of the temporal gap between formation of the Imbrium basin and Mare Imbrium, (2) correct interpretation of the impact origin of the basin, (3) correct volcanic interpretation of the mare material, and (4) correct general prediction of the lithology of the rocks collected by Apollos 11, 12, 14, 15, and 17. The lunar geologic framework established by these studies gave direction to surface exploration by Apollo and unmanned missions.

Despite the pre-Apollo photogeologic effort, however, many aspects of lunar geology were not understood. Predictive failures included (1) reversal by most mappers of the stratigraphic relations between light-colored mare materials of central Mare Serenitatis and the dark mantling and mare materials at its margin, (2) misinterpretation of light-colored terra plains material, (3) misinterpretation of terra landforms such as pits, furrows, and domes, and (4) a failure to predict the impact nature of the rocks sampled by Apollo 16

that was a consequence of (2) and (3). The first error might have been avoided by more persistent application of the principles of superposition and more sophisticated crater counts—entirely within the discipline of photogeology. More timely and intensive photogeologic work—specifically, on the Orientale basin—might also have mitigated the Apollo 16 error by raising alternatives to the volcanic interpretations of the plains and other terra landforms. However, the origin of material units at the Apollo 16 site probably could not have been unambiguously specified by remote methods, and our present understanding is dependent on analyses of the returned rocks. This reality illustrates the need for interaction between “ground truth” and photogeology, which can identify and classify lunar material units, determine relative ages, identify problems, and propose multiple working hypotheses, but which can rarely prove origins (Greeley and Carr, 1976). When origins and absolute ages are learned by onsite exploration, photogeologists can then construct new models for testing.

SCOPE

This paper presents a new set of detailed and general interpretations for the terrae in the Apollo zone by taking into account the Apollo and Luna sample analyses and other information acquired or interpreted since the earlier synoptic mapping of the region (Wilhelms and McCauley, 1971). Many of the stratigraphic relations and landforms observed in the terrae here might still be interpreted logically by volcanic or other endogenic processes, but the Apollo 16 analyses, in particular, are regarded as requiring impact interpretations. No fundamentally new genetic interpretations of the maria are required by the sample analyses, but refinements in their stratigraphy that have emerged from photogeology and radiometric dating are reported. The paper includes more explicit and detailed explanations of photogeologic reasoning than do earlier descriptions of lunar mapping principles (Shoemaker, 1962; Shoemaker and Hackman, 1962; McCauley, 1967; Wilhelms, 1970, 1972b; Wilhelms and McCauley, 1971; Mutch, 1973; also see Varnes, 1974, for a penetrating abstract analysis of the logic of geologic maps in general).

For report purposes the overflown area west of long 50° E. is divided into seven regions (fig. 1, heavy lines). Each is described by one or more geologic maps and annotated photographs. Topics of greatest interest within the regions are stressed, and the maps vary somewhat in methods of portrayal, symbolization, and subdivision of units. Because of adequate previous treatment, primary impact craters are not subdivided extensively by age except in the first region (figs. 2, 3)

or by material subunit except for the large crater Theophilus (figs. 23, 25). The study area includes three Apollo landing sites (15, 16, 17) and is near the other three (11, 12, 14), but the geology of the sites is not stressed because of extensive existing literature. The division into regions is based partly on natural geologic provinces and partly on the desire to retain the compilation scales for all maps (1:3,300,000 at the equator to 1:3,800,000 at 30° latitude, good mapping scales for lunar studies in my opinion). The black and white reproduction prohibits adequate portrayal of two superposed units, so where dark mantling materials and terra materials are both significant, separate maps are drawn (figs. 11, 15).

The photographed strips (fig. 1) cover two principal features, the volcanic maria and the Imbrium impact basin and its flanks. The Apollo 15 and 17 strips of photographs on one hand and the Apollo 16 strip on the other, although oriented differently and separated widely in most of the area, happen to compose a radial sample of the Imbrium basin and its periphery. The Apollo 15 and 17 strips cover the basin from its buried center to a point about 2,000 km from the center except for a mare-covered gap. The Apollo 16 strip, which makes an obtuse angle with the radial directions, covers the basin periphery from about 1,350 km from the basin center in the west to about 2,350 km at the border of Mare Fecunditatis. Inner basin features are described first in this paper and outer, mostly secondary-impact features in later sections. Mare materials are described in detail only in the first, second, and last of the seven regions. Part of Mare Tranquillitatis that was photographed by Apollo 15 west of long 39° E. is not discussed because of a photographic sun illumination too high to provide new information. Summaries and conclusions about the detailed regional studies are collected at the end of the report.

DATA SOURCES

Vertical stereoscopic metric photographs taken by Apollo 15, 16, and 17 mapping cameras are the chief but not sole data source for this work. Stereoscopies aids in estimating the three-dimensional form of contacts and volumes of deposits and in qualitatively assessing a scene, to the extent that stereoscopic photographs are superior to others when taken vertically (or subsequently rectified) at low-angle illuminations. However, the invaluable Lunar Orbiter IV photographs that cover most of the near side monoscopically were necessary supplements to the Apollo photographs, which cover relatively narrow strips. The Orbiter IV photographs provide the regional context that has proved vital in lunar studies because of the coarse scale

of the Moon's most significant features. Also, high-resolution (100–150 m) Orbiter IV photographs were used to fill out small map areas along the edges of the Apollo strips (fig. 1) and were helpful inside the Apollo coverage, especially where the Apollo photographs were taken at sun illuminations higher than about 45°. Furthermore, the most important single basis for interpretations of lunar terrae has proved to be the relatively unmodified Orientale basin, photographed by Orbiter IV but not Apollo. An attempt was made to reinterpret the near-side terrae solely from relations exposed within them, but many ambiguities remained that were not resolved until comparable features of Orientale were examined in detail. Accordingly, this report includes numerous photographs of features at distances from Orientale that are proportional to distances of similar features from Imbrium.

Apollo panoramic photographs, which have higher resolution than the mapping photographs, were used to check certain detailed relations but are not well suited to areal mapping because of their narrow format.

Important data for studies of the maria are contained in color-difference images (Whitaker, 1972a, b, c) prepared by combining Earth-based telescopic photographs taken at two wavelengths—one at the ultraviolet end of the spectrum (0.31 to 0.40 μm with a maximum at about 0.37 μm) and the other at the near infrared end (0.73 to 0.90 μm , with a maximum at about 0.82 μm). The resulting image shows the relative blueness or redness of surface areas at these two wavelengths: relatively blue areas appear dark, and relatively red areas are bright. Throughout this paper such areas are referred to for simplicity as "blue" or "red" although these terms are only relative, as all lunar colors are reddish.

STRATIGRAPHIC TERMINOLOGY

Ages of lunar material units are currently defined as follows. Pre-Nectarian units are older than the Nectaris basin. The Nectarian System includes materials of the Nectaris basin and other, younger units that are older than the Imbrium basin (Stuart-Alexander and Wilhelms, 1975). The term pre-Imbrian is equivalent to pre-Nectarian plus Nectarian. The Imbrian System includes materials of the Imbrium basin and other, younger units that are older than the Eratosthenian System. The adjectival form "Imbrian" refers to this time-stratigraphic system or to the corresponding time period, whereas "Imbrium" refers only to the basin and its materials. The Imbrian-Eratosthenian boundary has never been formally defined (Wilhelms, 1970), nor has the boundary between the Eratosthenian System and the Copernican System, the youngest lunar time-

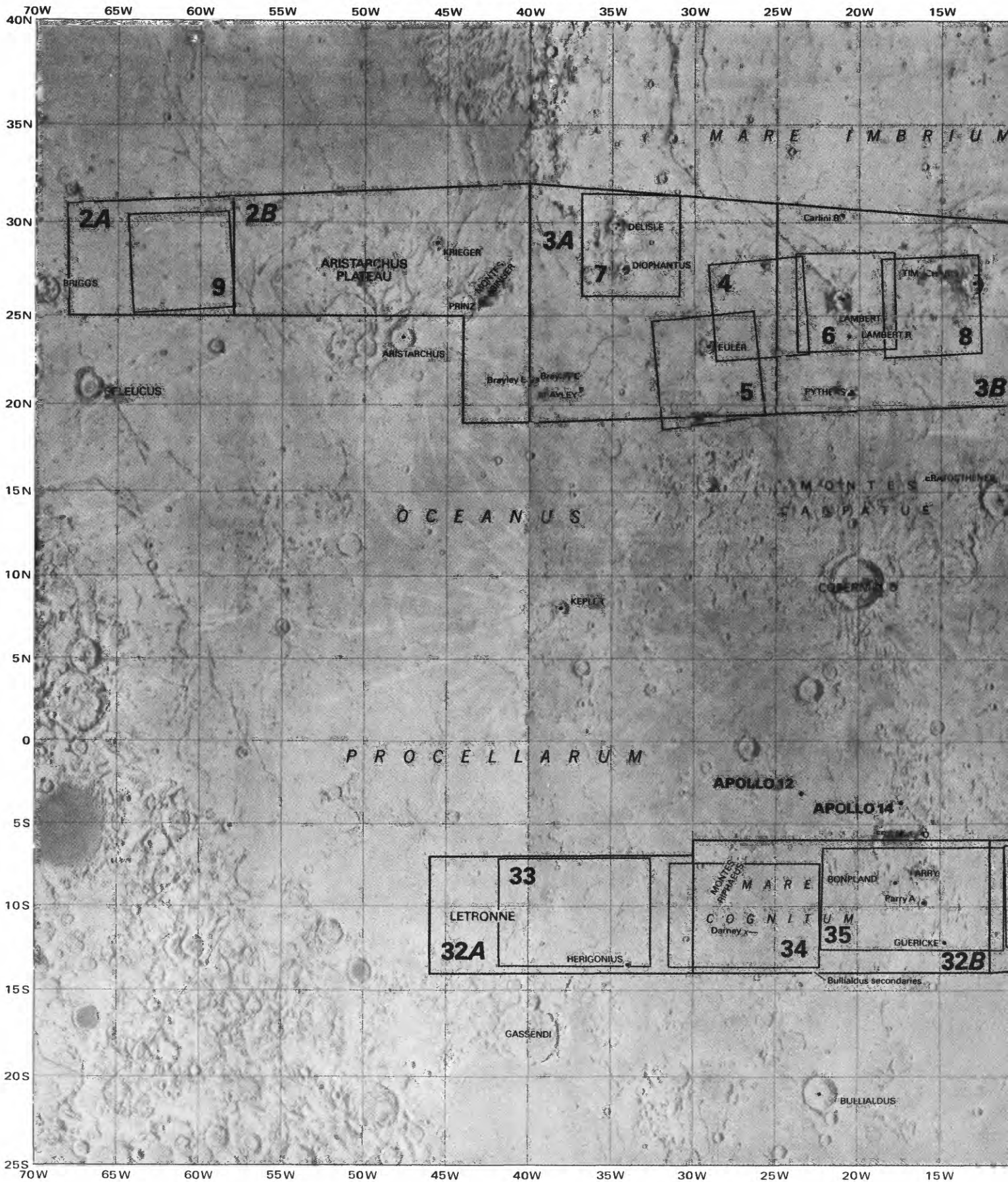
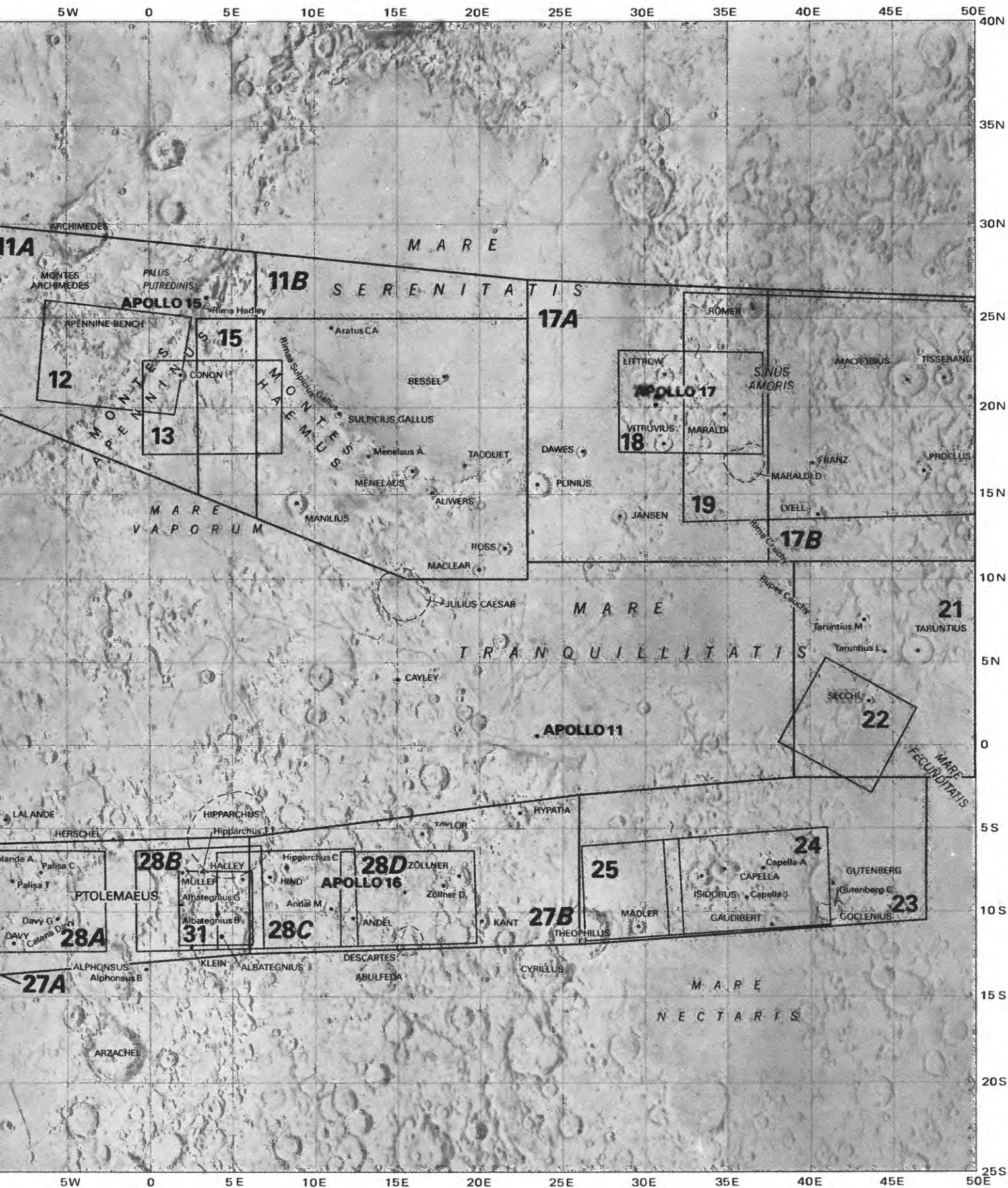


FIGURE 1.—Location of text figures including geologic maps (figs. 2, 3, 11, 15, 17, 21, 23, 27, 32; heavy lines) and photographs except those of Orientale (figs. 14, 20, 26, 27, 28, 29, 30) and the color-difference images (figs. 10, 16, 36). Illustration covers area between latitudes 40° N. and 25° S. and longitudes 50° E. and 70° W. Base maps are from the Apollo 15-17 mission.

STRATIGRAPHY OF PART OF THE LUNAR NEAR SIDE

A5



LOC-1 (west of long 50° W.) and LOC-2, original scale 1:2,750,000 at the equator, first edition, May 1971, prepared by U.S. Air Force Aeronautical Chart and Information Center (now part of the Defense Mapping Agency).

stratigraphic system, usually considered to consist of materials of rayed craters. New working definitions of the Imbrian-Eratosthenian and Eratosthenian-Copernican boundaries are proposed in the following section.

ACKNOWLEDGMENTS

This study was conducted on behalf of the National Aeronautics and Space Administration from 1973 to 1976. Most of the work was done as part of Experiment S-222, H. J. Moore, Principal Investigator, under NASA contract T-1167B. The regional studies that provided important feedback were performed under NASA contract W13,130. The work was facilitated by the excellent base maps of the LOC series prepared by

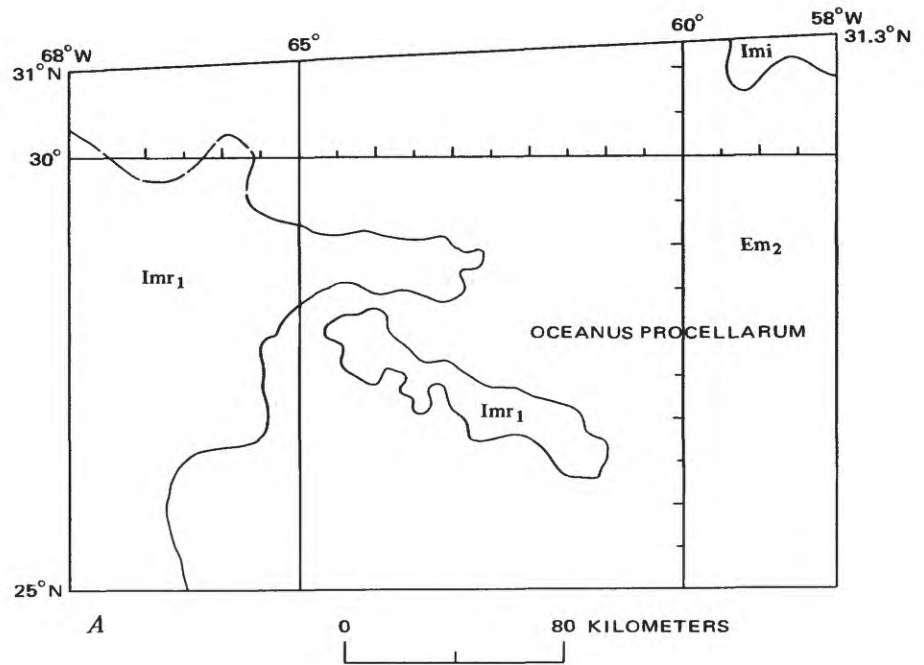
the Defense Mapping Agency, which portray the finest detail needed for the present purposes with good representational fidelity and locational accuracy. The manuscript benefited greatly from reviews by C. A. Hodges and H. J. Moore.

MARE IMBRIUM AND NORTHERN OCEANUS PROCELLARUM

INTRODUCTION

The northwesternmost area of the near side photographed by Apollo includes the Aristarchus plateau (Moore, 1967), Montes Harbinger, and the surrounding mare of Oceanus Procellarum (fig. 2). The unusual fea-

DETAILED SEQUENCE	
Ca	Ejecta and secondary-crater materials of crater Aristarchus
Csk	Secondary-crater materials of crater Kepler
Cp	Materials of crater Pytheas
Csc	Secondary-crater materials of crater Copernicus
Edi	Materials of crater Diophantus
Em ₃	Eratosthenian mare material, youngest
Em ₂	Eratosthenian mare material, intermediate age
Ede	Materials of crater Delisle
Ee	Materials of crater Euler
Em ₁	Eratosthenian mare material, oldest
Et	Materials of crater Timocharis
Ese	Secondary-crater materials of crater Eratosthenes
Ei	Materials of crater Lambert
Imi	Imbrian mare material, intermediate color
Ik	Materials of crater Krieger
Imr ₂	Imbrian mare material, red, younger
Imr ₁	Imbrian mare material, red, older
Idr	Dark mantling material, red
Ip	Wall and secondary-crater materials of crater Prinz
≡	Materials of Imbrium basin



EXPLANATION

	Mare and dark-mantling materials
	Materials of Imbrian and younger craters
	Materials of Imbrium basin rings

UNDIVIDED UNITS

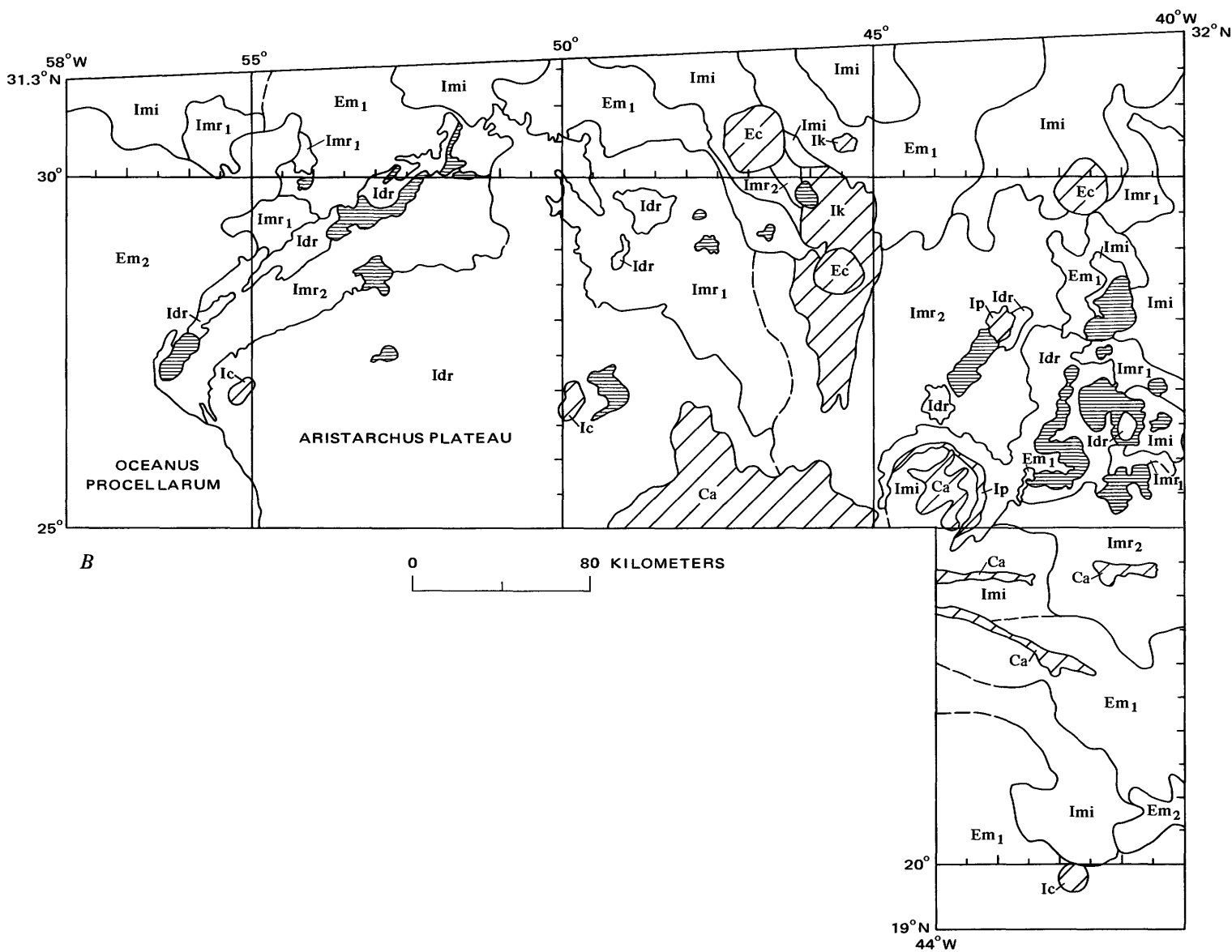
Ec	Materials of small Eratosthenian craters
Ic	Materials of small Imbrian craters
d	Dark mantling material
---	Indefinite contact

FIGURE 2.—Geologic map of part of northern Oceanus Procellarum, Montes Harbinger (right), and the Aristarchus plateau. Sources of data: Apollo 15 mapping-camera frames 2077-2091,

tures of this region, studied by a variety of remote sensing techniques (Zisk and others, 1977), include a markedly reddish mantle that may be a loosely fragmental deposit, numerous sinuous rilles, and other endogenic features. The part of Mare Imbrium photographed by Apollo (fig. 3), especially its well-developed volcanic flow features, has also been extensively studied (R. G. Strom, fig. 18 in Kuiper, 1965; Moore, 1965; Carr, 1965; Fielder and Fielder, 1968; Whitaker, 1972a, b; Hodges, 1973; Young and others, 1973a, b; Schaber, 1973; Schaber and others, 1975, 1976; Boyce and Dial, 1973, 1975; Boyce and others, 1975). The present study integrates the stratigraphic conclusions of these works and adds new observations of mare and crater units made on the excellent Apollo photographs.

The terra materials, which are parts of Imbrium basin rings exposed in relatively small islands, are not discussed.

The ejecta blanket of each crater is a discrete, laterally continuous layer of material that has a definite position in the lunar stratigraphic column. Secondary craters and their ejecta form deposits that are contemporaneous with each primary crater. For convenience, on most lunar geologic maps, the materials of a group of craters are together classed as a geologic map unit. For example, materials of all rayed craters are usually lumped as crater materials of the Copernican System, and all nonrayed post-mare crater materials are assigned to the Eratosthenian System (Shoemaker and Hackman, 1962; McCauley, 1967; Wilhelms, 1970). In



2190-2205, 2334-2350, 2473-2493, and 2741-2751; Apollo 17 mapping-camera frames 2929-2935 (the part south of lat 25° N.).

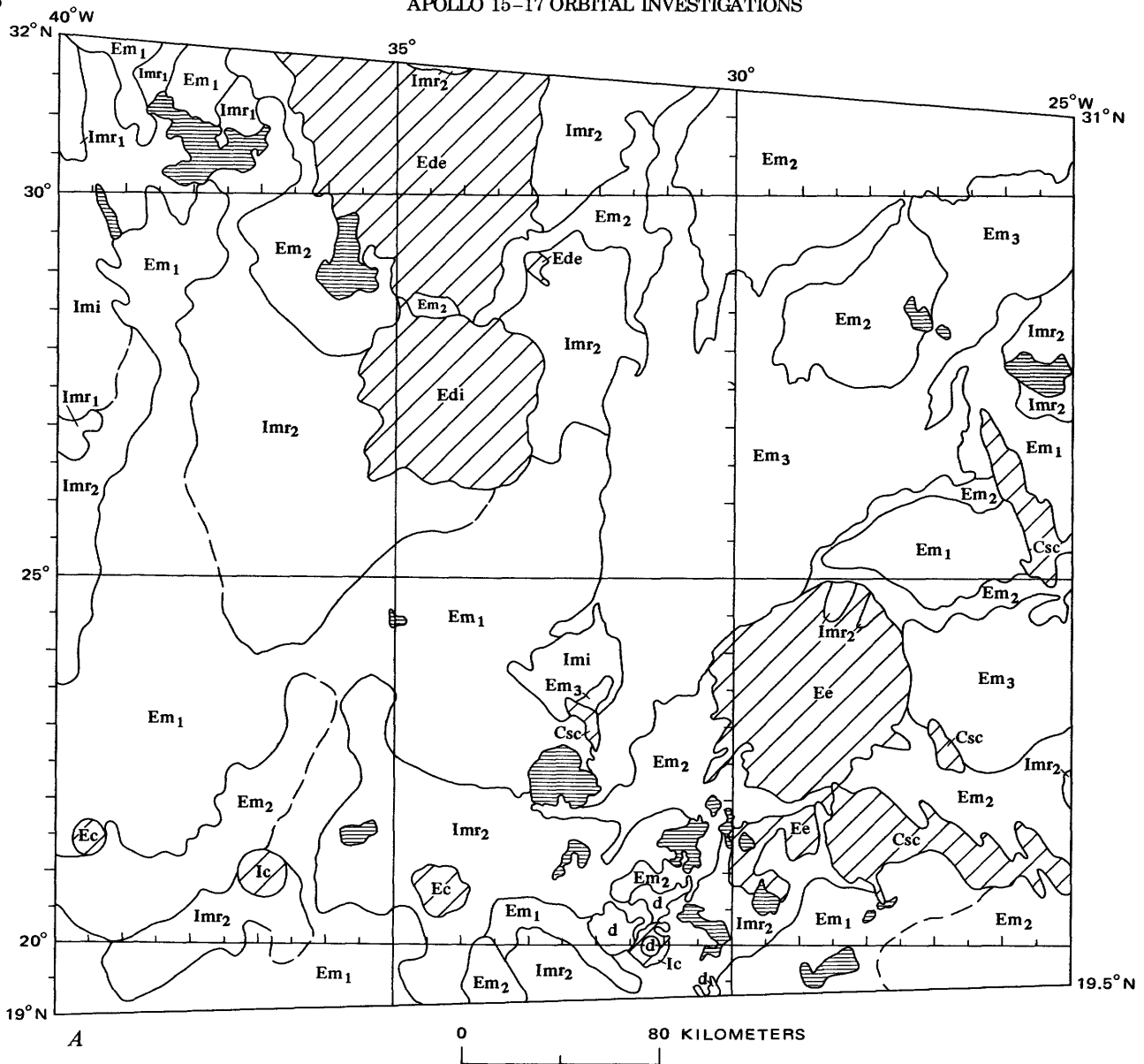


FIGURE 3.—Geologic map of part of southern Mare Imbrium. Explanation given with figure 2. Feature names can be determined from geologic unit symbols and figure 1. Sources of data: Apollo 15 mapping camera frames 595-602, 1002-1013, 1144-1160, 1685-1703, 1827-1851,

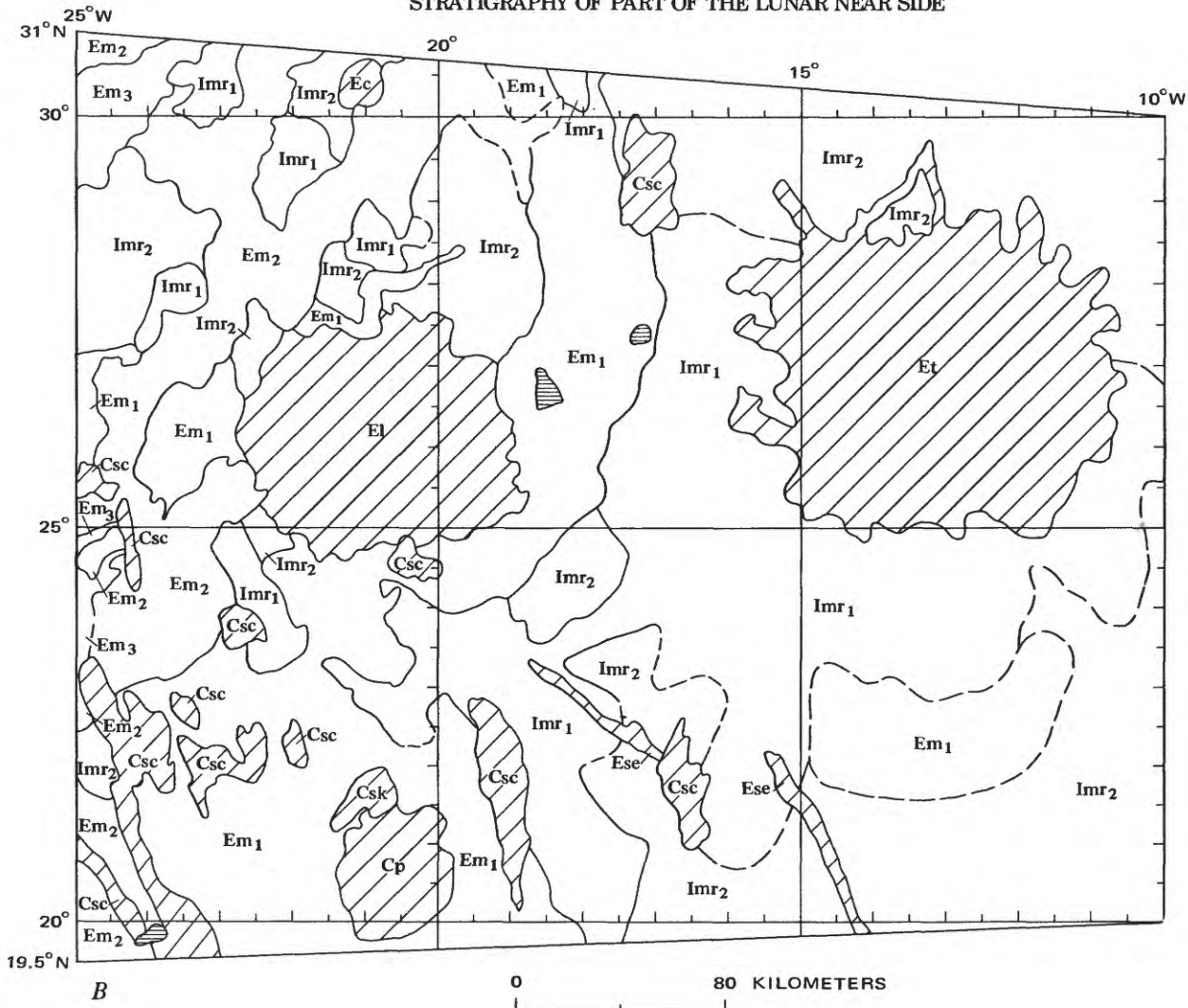
this report, 12 individual craters larger than 15 km are ranked in their proper stratigraphic place among eight mare or dark mantling units.

This detailed stratigraphic sequence was determined by a series of iterations among various types of data. First, the most obvious contacts were established on the basis of geometric superposition and transection relations among units visible as three-dimensional deposits or readily distinguishable by differing densities of small superposed craters. Such contacts amount to about half the total. Color-difference photographs and

data on small superposed craters were then consulted to locate additional boundaries. When the stereoscopic photographs were re-examined, subtle topographic and crater-density contacts not previously detected were commonly found at these boundaries. The complete sequence is given in the caption of figure 2.

SUPERPOSITION RELATIONS

Central Mare Imbrium contains distinct flow lobes that are much like those of terrestrial volcanic flows (R. G. Strom, fig. 18, in Kuiper, 1965; Fielder and



2063–2079, 2174–2192, 2330–2337, 2460–2475, and 2734–2742; Apollo 17 mapping-camera frames 2115–2123, 2278–2296, 2714–2735, 2907–2932.

Fielder, 1968; Schaber, 1969, 1973; Schaber and others, 1975, 1976; Wilhelms, 1970; Whitaker, 1972a, b). The two youngest Eratosthenian mare material units, in particular, have many distinct flow fronts that are clearly superposed on lobes of the same unit or a more heavily cratered older unit (figs. 4–8).

Several elevated and deformed mare patches called "kipukas" (Nichols and others, 1974) are embayed by obviously younger, flat mare units. Large shieldlike kipukas such as that west of Euler (fig. 5) are fractured, whereas the surrounding maria are not. A patch

of old reddish Imbrian mare material (fig. 3B, map symbol Imr₁) seems to follow the raised circular structure Lambert R (Young and others, 1973b; Hodges, 1973) and to be embayed by younger, flat, blue mare material (figs. 3B, 6). The older units, after covering the elevations, apparently subsided into the adjacent depressions, probably while shrinking during cooling. These relations and relations between ridges and sinuous rilles (Young and others, 1973a, b) indicate an extended deformational history of mare materials in the region.

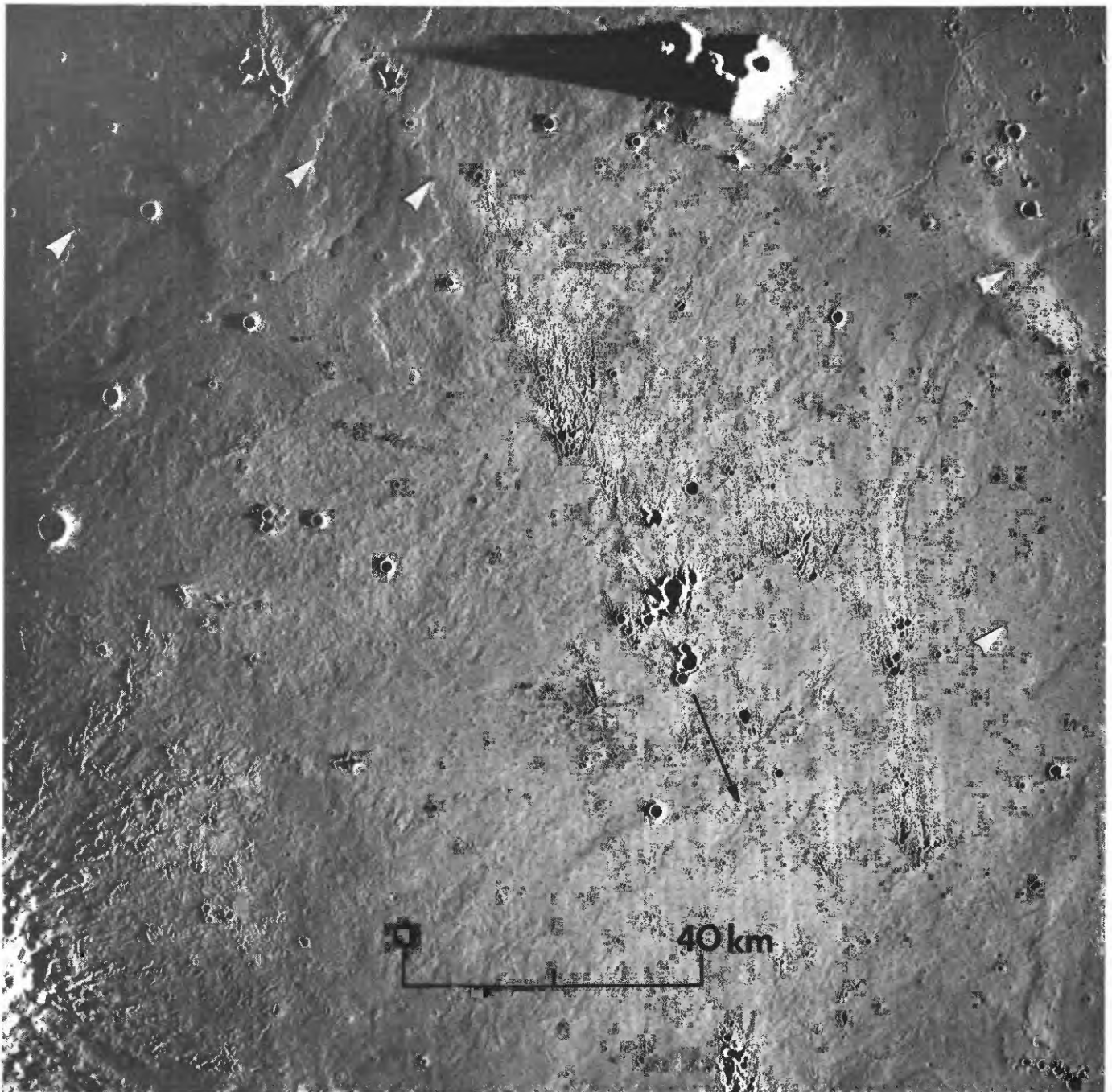


FIGURE 4.—Young lava flows in Mare Imbrium (white arrowheads). Fine texture visible on most mare surfaces. Secondary craters of Copernicus (500 km in direction of black arrow) have cast conspicuous "herringbone" ejecta away from Copernicus. Rim and secondary craters of crater Euler partly visible along lower left edge. Apollo 15 mapping-camera frame 1157, sun illumination from right (east) 2° above horizontal.

The age of the dark red mantling material in the Aristarchus-Harbinger region is better determined by superposition relations than by densities of small superposed craters, because craters acquire indistinct shapes on weak fragmental mantling deposits (Lucchitta and Sanchez, 1975; Zisk and others, 1977).

Moore (1967) assigned a Copernican or Eratosthenian age to the mantle because, on telescopic photographs, rays of Aristarchus were visible on adjacent units but not the mantle. However, Apollo and Lunar Orbiter photographs show that subdued Aristarchus secondaries are superposed and that Imbrian mare material

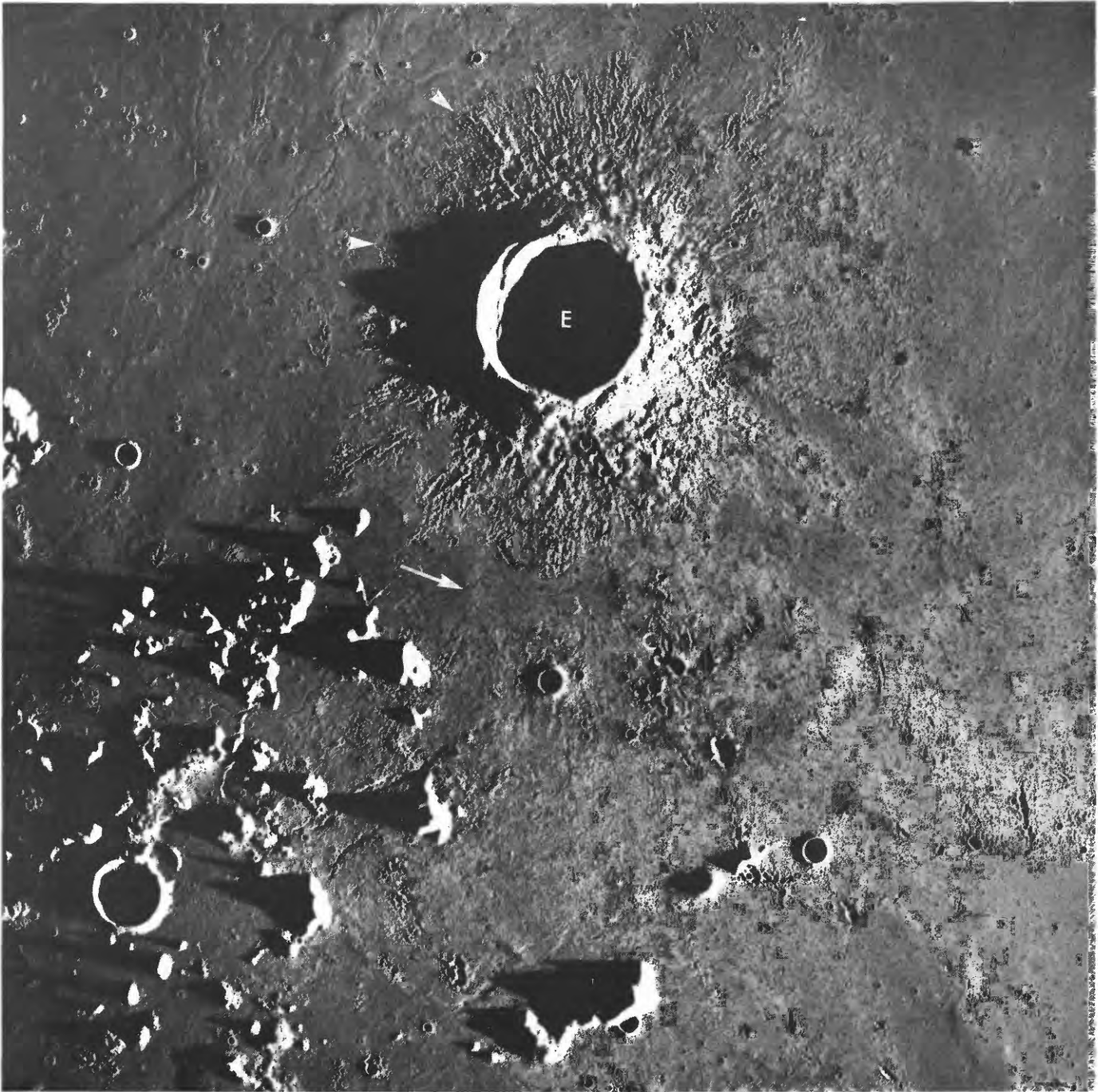


FIGURE 5.—Crater Euler, 27.5 km diameter (E). A tongue of intermediate-age Eratosthenian mare material containing a sinuous rille (arrow) cuts across the southern ejecta and isolates a patch of ejecta. Copernicus secondaries (C) are superposed on the Euler ejecta. Lobate flows of youngest Eratosthenian basalt containing lava channels truncate western ejecta of Euler (arrowheads), and the ejecta around the entire remaining periphery also seems partly inundated by mare material. The rugged hills in the lower left quadrant are islands of Imbrium basin rings. North of the hills is an elevated, fractured “kipuka” of old mare material (k). Apollo 17 mapping frame 2293; sun illumination from right (east), 3° above horizontal.

is younger than most of the red mantle (Zisk and others, 1977). Therefore, the mantle is Imbrian.

Ejecta or secondary craters of major impact craters are commonly superposed on one mare unit but partly

flooded by another (figs. 5–8). The difference between a slightly flooded secondary and an unmodified one superposed on the lavas may be subtle and detectable only on the best photographs, yet this distinction is



FIGURE 6.—Crater Lambert, 30 km diameter. Ring structure south of Lambert is Lambert R. Ejecta and secondary craters are superposed on mare materials in some places (A, B) but flooded by mare in others (C, D). The flooding at C was by thick flows of the intermediate-age Eratosthenian mare unit, whereas at D the flows (oldest Eratosthenian mare) were thin and did not obliterate the secondaries. The unit at D contains a sinuous rille and possibly small endogenic pits and a volcanic ridge (between letters D and E). A gashlike endogenic feature (arrowhead) is in the older unit to the east. Secondary craters at E seem to be outer secondaries of Eratosthenes 375 km to the southeast and, like Lambert secondaries, are flooded by the oldest Eratosthenian mare material. Apollo 15 mapping-camera frame 1153; sun illumination from right (east) 7° above horizontal.

often required to determine an age sequence. Secondary impact craters are very useful in establishing stratigraphic relations because of their wide extent.

The entire periphery of the crater Euler is embayed by mare material; its secondary craters and ejecta ex-

tend out to nearly a crater diameter but are truncated or filled by lava (fig. 5). South of the crater, a tongue of young mare material containing a sinuous rille has flooded the ejecta. South of the tongue, however, extensive unflooded ejecta and secondaries reappear and

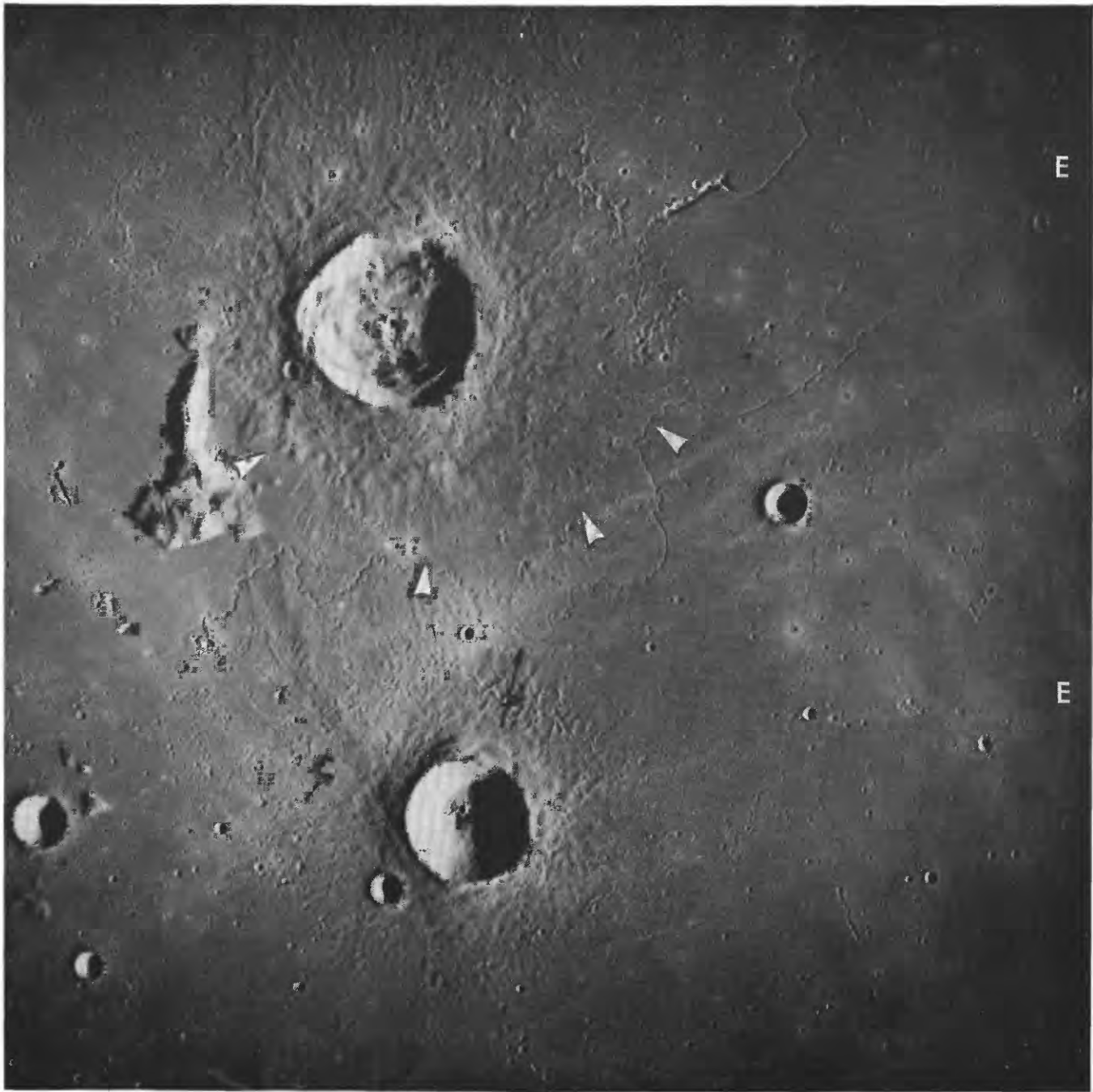


FIGURE 7.—Craters Delisle (above, 25 km) and Diophantus (below, 18.5 km). The intermediate Eratosthenian mare unit containing a sinuous rille between the two craters partly inundates the Delisle ejecta (white arrowheads) but is overlain by Diophantus ejecta (black arrow). Secondaries superposed on Diophantus ejecta (C) lie on a ray radial to Copernicus and date Diophantus as older than Copernicus. Part of the youngest mapped mare unit lies along the right edge of the photograph (E). Apollo 15 mapping-camera frame 2074; sun illumination from right (east) 19° above horizontal.

show that the mare units there (oldest Eratosthenian and younger red Imbrian) are older than Euler.

The crater Lambert is embayed by all nearby Eratosthenian materials but is superposed on Imbrian mare in several places (fig. 6). As the oldest Eratosthe-

nian mare embays Lambert but is overlain by Euler secondaries, Lambert is older than Euler.

Diophantus secondaries are superposed on Delisle ejecta, establishing Diophantus as the younger crater (fig. 7). This relation is confirmed by the fact that a

mare unit (intermediate Eratosthenian) flooded the southern and western ejecta of Delisle (as noted by Moore, 1965) but did not flood materials of the immediately adjacent Diophantus. Secondaries of Diophantus transect a sinuous rille in the part of the intermediate Eratosthenian mare unit that floods the southern Delisle ejecta. Both craters are superposed on the younger Imbrian red mare unit. Secondaries of Diophantus are also superposed on the youngest Eratosthenian mare unit. Thus the age sequence here, from oldest to youngest, is younger red Imbrian mare, Delisle, intermediate Eratosthenian mare, youngest Eratosthenian mare, Diophantus.

The crater Timocharis is also probably older than the old Eratosthenian mare unit that embays Lambert; that unit seems to truncate outer secondaries of Timocharis (fig. 8). Secondary craters of Eratosthenes also overlie the two Imbrian mare units in the southeast corner of the map area (fig. 3B) but are truncated by the old Eratosthenian unit (fig. 8).

Ejecta of the crater Krieger overlies the younger Imbrian red mare and is in turn overlain by the oldest Eratosthenian unit and probably the intermediate-color Imbrian unit (fig. 2B). Therefore, Krieger is Imbrian in age but younger than the Imbrian crater Prinz that formed before the dark, reddish mantle.

Some small craters can also be ranked by relations to mare units but are not included in the detailed sequence. For example, the Eratosthenian crater at 30.5° N., 21° W. (Carlini B) is superposed on the younger Imbrian red mare unit but is embayed by the intermediate Eratosthenian unit. The entire periphery of the Eratosthenian crater at 21.5° N., 39.5° W. (Brayley C) is embayed, whereas the small adjacent crater (Brayley E, unmapped) is completely untouched (Neukum and others, 1975a). Four other mapped small Eratosthenian craters are superposed on all nearby units. Four small mapped craters are embayed by Imbrian mare materials, and so are also Imbrian.

In summary, superposition relations yield the following stratigraphic relations:

Diophantus
 Youngest Eratosthenian mare material
 Intermediate Eratosthenian mare material
 Delisle-Euler
 Oldest Eratosthenian mare material
 Timocharis-Eratosthenes-Lambert
 Imbrian mare material of intermediate color
 Krieger
 Younger Imbrian red mare material
 Older Imbrian red mare material
 Dark, red mantling material
 Prinz

The ambiguous cases can be resolved by size-frequency counts of small superposed craters. Neukum and König (1976) determined that Delisle is younger than Euler and Eratosthenes younger than Lambert. Other relations found by Neukum and König agree with those determined here; their complete list in the region is:

Aristarchus
 Copernicus-Diophantus
 Delisle
 Euler
 Timocharis-Eratosthenes
 Lambert

Ambiguities in the results of Neukum and König are resolved by the superposition of Copernicus secondaries on Diophantus (fig. 7) and apparently, of Timocharis secondaries on those of Eratosthenes (fig. 8). Superposition relations among secondaries add additional craters to the sequence in the Copernican System that cannot be dated by relations with mare materials (Kepler and Copernicus lie outside the mapped area):

Aristarchus (very fresh secondaries superposed on all units)
 Kepler (secondaries superposed on Pytheas)
 Pytheas (superposed on Copernicus secondaries)
 Copernicus
 Diophantus

MARE AGES ON BASIS OF SMALL CRATERS

FLOODING OF SMALL CRATERS

On good photographs many small craters (1 to 8 km) with subdued yet distinct rims appear flooded by mare material that spared the craters' interiors (fig. 9). Some craters are flooded nearly to the brim and look like deep rimless pits. According to the criteria of Trask (1970) the craters are Eratosthenian; craters of this size would be more subdued if Imbrian and would be sharper and brighter if Copernican. The encroachment by the mare on Eratosthenian craters together with an apparently "normal" population of superposed Copernican craters shows that the mare deposits are Eratosthenian.

MORPHOLOGY OF SMALL SUPERPOSED CRATERS

The method of Soderblom and Lebofsky (1972) has been applied to small craters here and elsewhere to determine the relative ages of the underlying surfaces (Boyce and Dial, 1973, 1975; Boyce and others, 1975; Boyce, 1976; Chapter B of this series). Relative ages are expressed as the largest diameter of craters (D_L ,

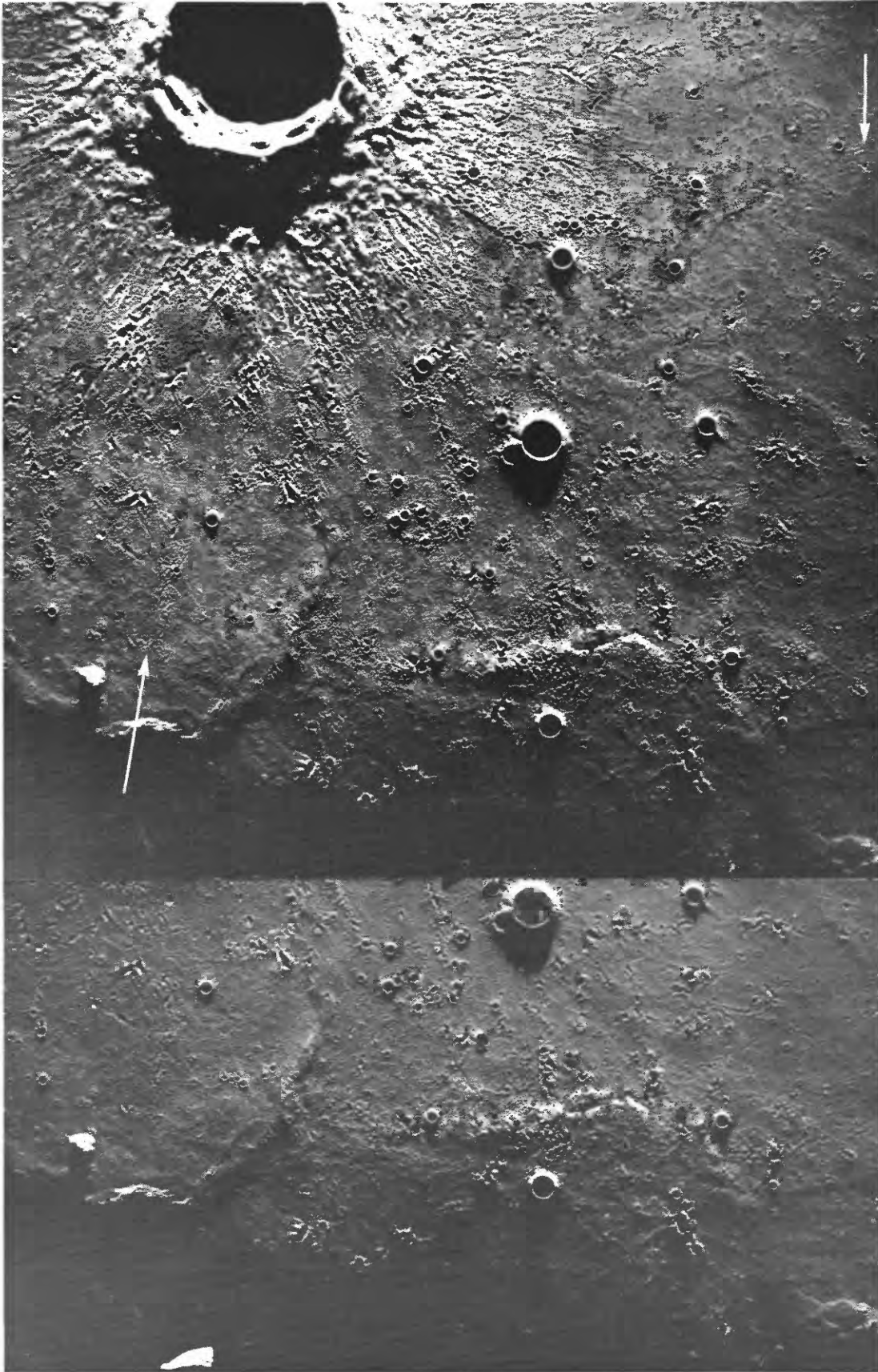


FIGURE 8.—Stratigraphic relations between oldest Eratosthenian mare material and secondary crater of Timocharis (large crater, 34 km diameter) and Eratosthenes. The mare unit, with northeast-trending flow texture, truncates Timocharis secondaries (upper arrow). Timocharis secondaries may be superposed on Eratosthenes secondaries (lower arrow). Stereopair, parts of Apollo 15 mapping-camera frames 0600 (right) and 0602; sun illumination from right (east) 2° above horizontal at center of right frame.

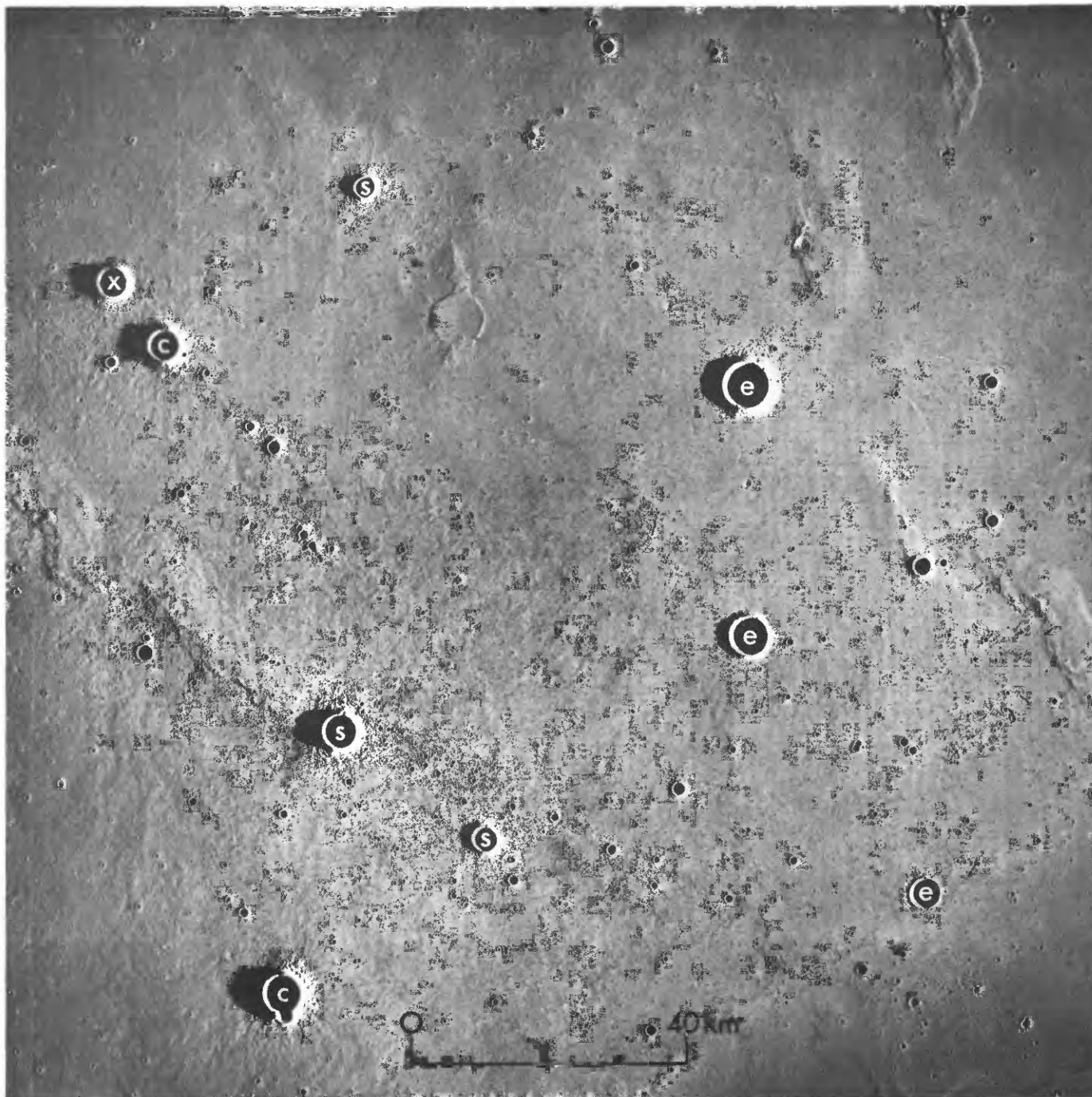


FIGURE 9.—Area in northern Oceanus Procellarum covered by approximately the eastern two-thirds of figure 2A. Ejecta of some of the largest craters are embayed by mare material (e), some are superposed on mare material (s, c) and one crater is partly embayed and partly superposed (x). The unit which crater x overlies is red mare material of Imbrian age; the embaying unit everywhere is blue Eratosthenian mare material. The craters superposed on the blue unit are probably Copernican in age (c). Apollo 15 mapping-camera frame 2489; sun illumination from right (east) 4° above horizontal.

meters) that are eroded to an interior slope of one degree by the net accumulated flux of small impacts. The units mapped here are closely consistent with ages based on the D_L values (table 1). A few individual measurements within a unit disagree with the average

for the unit. Some of these measured points are so close to a mapped contact that the disagreement is probably one of exact location; Boyce and his coworkers plotted their data points along a standard grid, not at the craters measured. Other anomalous values seem to be

TABLE 1.— D_L values of mare material units (Boyce and others, 1975) in the areas mapped in figures 2 and 3

[A few obviously anomalous measurements have been excluded. The uncertainty ranges given by Boyce and others (1975) for each measurement average plus or minus 35 and all but a few range between 20 and 50]

Mare material unit	D_L	Number of points	Average D_L
Youngest Eratosthenian	140–195	12	165
Intermediate Eratosthenian	170–215	13	200
Oldest Eratosthenian	210–245	21	220
Intermediate-color Imbrian	255	1	Small sample
Younger red Imbrian	240–260	9	250
Older red Imbrian	270–385	16	310
Dark, red mantling material	360	1	Small sample

measured on islands of old surfaces too small to map, on secondary impact craters to which the Soderblom-Lebofsky-Boyce method may not apply exactly, or on craters whose ejecta is flooded by a thin unit and whose unflooded interior slopes tell the age of an older buried unit (fig. 9). A few additional anomalies remain, but the match is so close that I am convinced of the validity in this region of the crater-morphology technique of determining relative ages.

Schaber (1973) reported D_L values of the three Eratosthenian units as 235 ± 20 , 175 ± 5 , and 160 ± 5 meters (his phases I, II, and III). Schaber and others (1976) proposed that each of these phases represents a rapid and extremely voluminous eruption. The wider range of D_L values in table 1, however, suggests that each unit consists of many discrete flows erupted over a long time.

OTHER PROPERTIES

COLOR

Color as displayed by the color-difference photographs taken by Whitaker (in Kuiper, 1965; Whitaker, 1966, 1972a, b) clearly correlates with mare units in this region (fig. 10). There is a progression from relatively reddish to relatively bluish with decreasing age, except for the youngest Eratosthenian unit, which is slightly more reddish than the next oldest (Schaber and others, 1975). The Imbrian unit of intermediate color apparently fits the sequence on the basis of superposition relations and one D_L value. Generally the Imbrian units are reddish and the Eratosthenian bluish, although small patches apparently of youngest Imbrian age in the Aristarchus-Harbinger area are bluish (Zisk and others, 1977).

Even where not correlative with age in other areas, color is useful in locating contacts and particularly in distinguishing between heavily cratered mare units and secondary crater fields. Except in the densest secondary fields, continuous color patterns characteristic of mare contacts continue across the more-ragged patterns characteristic of secondary fields.

The lava flows that flood the small Eratosthenian craters west of the Aristarchus plateau (fig. 9) are strongly blue, whereas adjacent surfaces upon which similar Eratosthenian craters are superposed are red; hence, thin flows are capable of masking underlying colors and imparting their own colors to the soil (which is the material detected by the photograph). Large primary and secondary craters, however, can excavate the underlying material and spread it as a halo of different color upon the near-surface lava or soil.

RADAR

Schaber and others (1975) have investigated the correlation between diffuse echoes of Earth-based radar transmissions at 3.8- and 70-cm wavelengths with geologic units in Mare Imbrium. They find that the youngest Eratosthenian flows have the weakest depolarized echoes at the 70-cm wavelength. Some of the intermediate Eratosthenian unit also has weak echoes, notably the tongue southwest of Lambert (fig. 3B), and this could be part of the youngest Eratosthenian unit. West of 40° longitude (fig. 2A), there is a clear distinction of 3.8-cm echoes between the dark, reddish mantle and mare materials (Zisk and others, 1977).

REFLECTIVITY

The property of reflectivity was not used as a prime mapping criterion in the area. For mare units, it seems to correlate with color: blue units are dark, red units bright. Therefore the progression here is light to dark. The reddish mantle, however, is very dark, apparently because of its content of devitrified glass (Zisk and others, 1977). These interrelations are explored in the discussion of southern Oceanus Procellarum.

CORRELATIONS WITH TIME-STRATIGRAPHIC UNITS

Traditionally, rayed craters have been assigned to the Copernican System and unrayed craters superposed on mare materials to the Eratosthenian System. More exact definitions of the Copernican-Eratosthenian boundary have never been made. The relations younger than Eratosthenes and older than Copernicus established here conflict with previous assignments based on this scheme (table 2). The bright craters Timocharis and Euler are older than the rayless craters Diophantus and Delisle. The nature of the ejecta or of the materials impacted by the ejecta presumably accounts for the discrepancy.

In this report three mare units have been dated as Eratosthenian and three as Imbrian, consistent with traditional assignments, although previous mapping

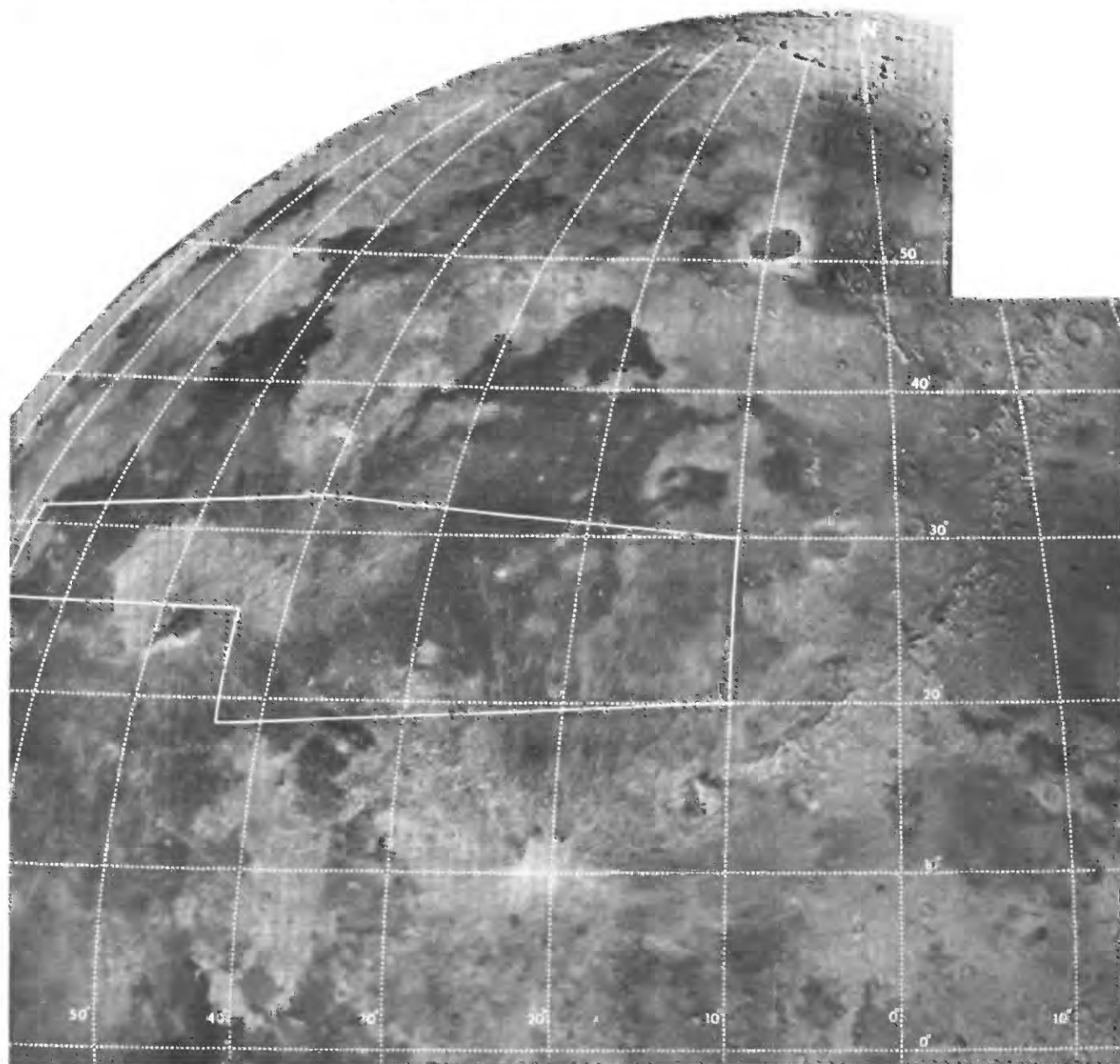


FIGURE 10.—Area mapped in figures 2 and 3 (outlined) showing color differences between wavelengths of 0.31 to 0.40 μm on one hand and 0.73 to 0.90 μm on the other. Dark is blue, light is red. Courtesy of E. A. Whitaker (Whitaker, 1966, 1972b).

has differed in detail (Wilhelms and McCauley, 1971; Schaber, 1973). The stratigraphic relations among craters and the correlations with D_L values both allow and require us to re-examine the suitability of these assignments, particularly with respect to Timocharis and Euler, and Diophantus and Delisle.

The change that would least disrupt assignments over the whole Moon while removing inconsistencies here is to reassign Timocharis and Euler to the Eratosthenian System. Age assignments of mare units

in this area can then remain unchanged, whereas if Timocharis and Euler remained Copernican, the Eratosthenian maria here and probably elsewhere on the Moon would become either Imbrian or Copernican as would most craters.

If the desirability of reassigning Timocharis and Euler to the Eratosthenian to preserve the importance of that system is acknowledged, the definition of the Imbrian-Eratosthenian and Eratosthenian-Copernican boundaries can be narrowed. Informally the Imbrian-

TABLE 2.—Crater age assignments in the area (figs. 2 and 3)

[W/M = Wilhelms and McCauley, 1971]

Crater	Previous assignment	Reference	Recommended assignment
Aristarchus	Copernican	Moore, 1965; W/M	Copernican.
Kepler	Copernican	Hackman, 1962; W/M	Copernican.
Fytheas	Copernican	Carr, 1965; W/M	Copernican.
Copernicus	Copernican	Shoemaker and Hackman, 1962; W/M.	Copernican.
Diophantus	Imbrian ¹	Moore, 1965	Eratosthenian.
	Eratosthenian	W/M	
Delisle	Imbrian ¹	Moore, 1965	Eratosthenian.
	Eratosthenian	W/M	
Euler	Copernican	Carr, 1965; W/M	Eratosthenian.
Timocharis	Copernican	Carr, 1965; W/M	Eratosthenian.
Eratosthenes	Eratosthenian	Shoemaker and Hackman, 1962; W/M.	Eratosthenian.
Lambert	Eratosthenian	Carr, 1965; W/M	Eratosthenian.

¹Moore (1965) designated the materials of Diophantus and Delisle as the Diophantus Formation, meaning older than some mare materials but younger than others.

Eratosthenian boundary has been regarded as the top of the mare material in roughly the eastern third of figure 3B that is overlain by secondary craters of the crater Eratosthenes and overlies materials of the Imbrian crater Archimedes (Wilhelms, 1970). This mare material, mapped here as red Imbrian of both ages (map symbols Imr_1 and Imr_2), includes D_L values 250 to 360. Eratosthenes is overlain by mare material that has to be considered Eratosthenian (if not Copernican), which has D_L values of 210 and 230 (oldest Eratosthenian unit, southeast of Lambert, fig. 6). Other large stretches of the same mare unit also have these D_L values, and only three measurements are larger than 230. Accordingly, I propose that mare units with D_L values of 230 and smaller be considered Eratosthenian, units 250 and larger Imbrian, and units with intermediate values be assigned according to the weight of other evidence. All mare units which have been dated radiometrically are Imbrian in this scheme, except that sampled by Apollo 12 (D_L 210 ± 20 ; Boyce, 1976). Craters in the intervening range such as Lambert are best retained as Eratosthenian unless proved otherwise.

If the maria here are Eratosthenian, the Eratosthenian-Copernican boundary lies above the youngest Eratosthenian unit and has D_L values smaller than 140. No lunar maria are known to have smaller D_L values. Unrayed craters younger than the youngest Eratosthenian unit, such as Diophantus, may be retained as Eratosthenian pending more study of superposed craters. Thus Copernicus is the oldest large Copernican crater in the vicinity. Assignments of moderately bright craters elsewhere on the Moon older than Copernicus, such as Langrenus and Theophilus, depend on determinations of D_L and crater size-frequency values (Neukum and König, 1976).

Approximate absolute ages have been assigned to D_L values by Boyce (1976) by calibration with ages deter-

mined radiometrically on returned samples. Boyce estimates the ages (in billions of years) between D_L 140 and 190 to be 2.6 ± 0.3 , between 211 and 240 to be 3.2 ± 0.1 , and between 241 and 260 to be 3.4 ± 0.1 . Thus the Imbrian-Eratosthenian boundary proposed here of between D_L 230 and 250 would be about 3.3 ± 0.1 b.y., and the Eratosthenian-Copernican boundary of about D_L 140 or less would be about 2.3 ± 0.1 b.y. or less.

APENNINUS-HAEMUS REGION

TERRA MATERIALS—IMBRIUM BASIN

The terra units of the north-central near side (fig. 11) are almost entirely parts of the Imbrium multi-ringed circular basin and its flanks. The area overflowed by Apollos 15 and 17 includes a radial sample of the basin from a point on the Apennine bench (informal name by Hackman, 1964, 1966) within the main basin rim, over that rim (Montes Apenninus), and through a series of transitions on the Apennine flank and Montes Haemus to the western edge of Mare Tranquillitatis. The impact origin of the basin and the general nature of basin materials were established by early work (Gilbert, 1893; Baldwin, 1949, 1963; Shoemaker and Hackman, 1962; Hartmann and Kuiper, 1962; Hackman, 1964, 1966). Remaining questions about emplacement of the materials are considered here on the basis of the stereoscopic photographs and comparison with the better exposed Orientale basin. Analogs pertinent to Imbrium are also displayed by the large crater Theophilus discussed under the heading "Northern Nectaris Basin Rim."

The current general picture of emplacement of basin materials is as follows. Terrestrial cratering studies indicate that crater rims and presumably basin rims are structurally uplifted, partly outthrust, and covered with ejecta in a stratigraphic order that is inverted from the original order in the target materials (Shoemaker, 1959; Roberts, 1966; Gault and others, 1968; Moore, 1971, 1976; Gault, 1974). The ejecta travels outward from the basin rim in a conical curtain, depositing materials closest to the rim first and distal materials last (Shoemaker, 1962; Oberbeck, 1975; Oberbeck and others, 1974, 1975). The close-in ejecta is also the last to leave the cavity, hence deposition occurs in reverse order from excavation. The close-in ejecta travels relatively slowly along ballistic trajectories (Oberbeck, 1975; Oberbeck and others, 1974, 1975; Morrison and Oberbeck, 1975), by gliding on the surface (Chao, 1974, 1977), and by flowing (Moore and others, 1974). The outer materials impact after long ballistic flight with high velocities, producing secondary craters much larger than the fragments of impacting ejecta. Thus there is a transition outward

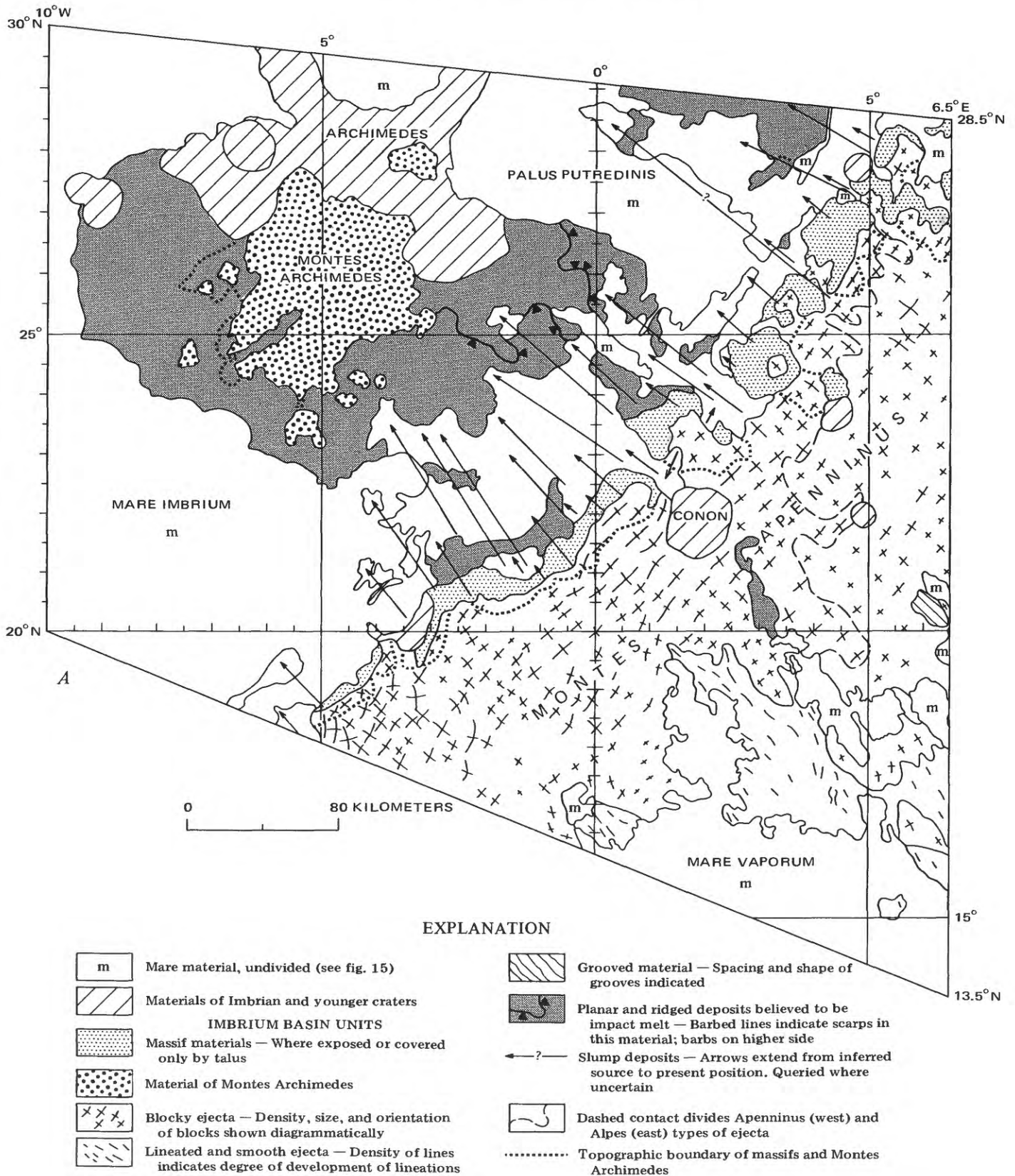
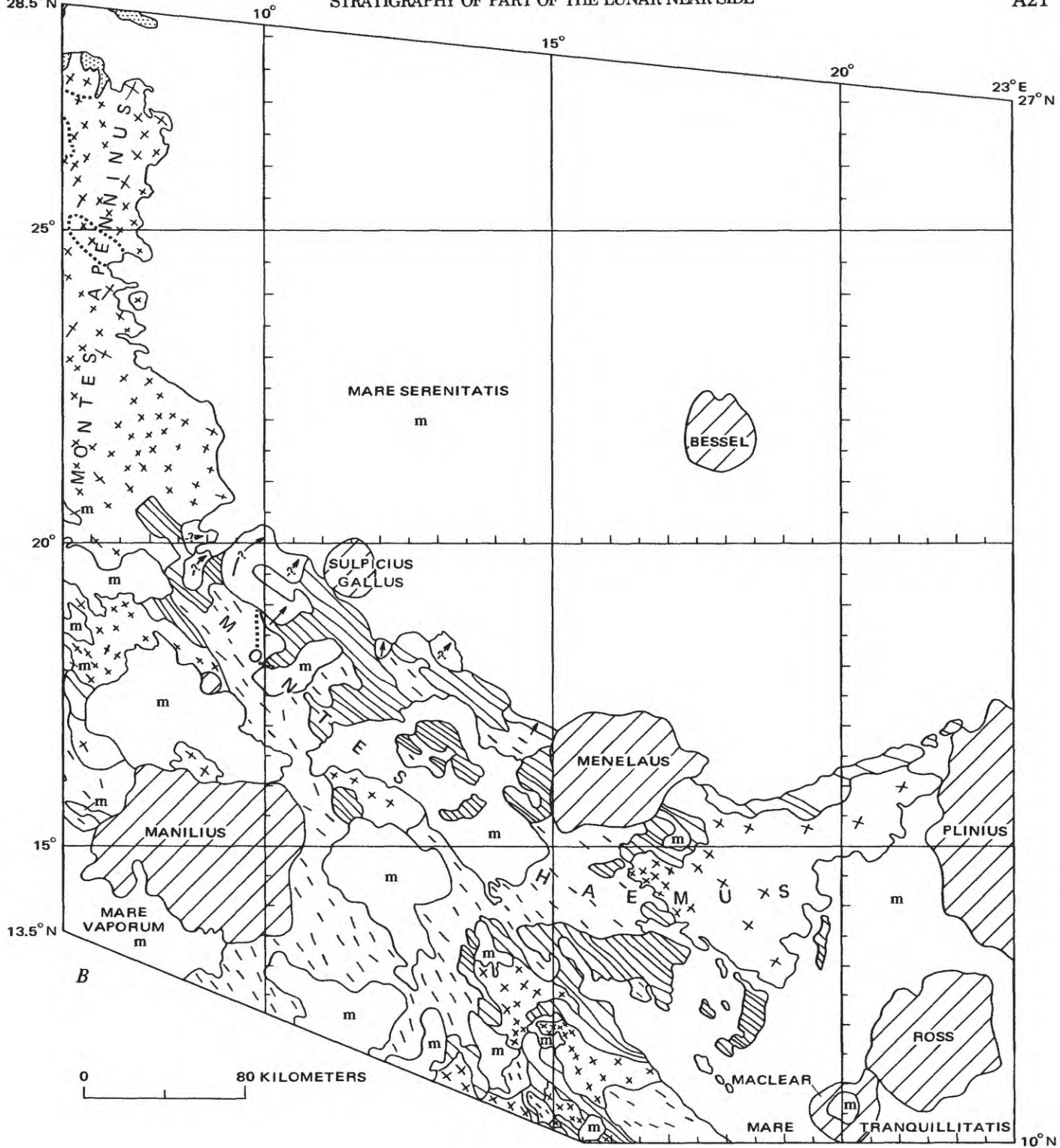


FIGURE 11.—Geologic map of the terra materials in the Apenninus-Haemus region. The Apennine Bench is the terra south of Archimedes including Montes Archimedes. Photographic data sources: Apollo 15 mapping-camera frames 409-425, 580-597, 988-1004, 1129-1146, 1669-1687, 1809-1829, 2143-2170, 2287-2315, and 2696-2721; Apollo 17 mapping-camera frames

28.5°N 6.5°E

STRATIGRAPHY OF PART OF THE LUNAR NEAR SIDE

A21



804-813, 1229-1241, 1510-1522, 1813-1831, 2100-2115, 2262-2279, 2697-2716, and 2882-2909; Lunar Orbiter IV high-resolution frames 85, 90, 97, 102, and 109 supplementary in southeastern third of area where Apollo photographs were taken at sun illuminations higher than 45° above horizontal.

in the resulting deposits from predominantly primary ejecta to predominantly local material excavated by the secondaries. Many relations are explained by the fact that the inner materials override the outer materials, even though deposited earlier, because their momentum carries them outward behind the advancing curtain of ejecta.

The principal remaining problems may be grouped in two categories: (1) the origin of basin rings, particularly the question of which ring best approximates the rim crest and related questions about depth and volume of the excavation and ejecta; and (2) the exact nature of the trajectories (surface or ballistic) and the related question of the proportions of secondary and primary ejecta in the basin deposits at any point. Ring origin and rim-crest location are discussed briefly in the sections on "Massif Material," "Material of Montes Archimedes," "Blocky Ejecta," and "Slump Deposits," and in the later section on "Theophilus," but they are not major themes of this paper. The radial sample of Imbrium is favorable, however, for consideration of the emplacement processes including the primary-secondary controversy and is a recurring subject in the

paper. Because of the uncertainties, the neutral descriptive term "continuous deposits" (Oberbeck and others, 1974; Oberbeck, 1975) is preferable to "primary ejecta" even in regions like the Apennine flank where exposed secondary craters are scarce and primary ejecta must constitute a large proportion of the blocky ejecta and lineated deposits.

Further controversy centers on the proportions of solid, melted, and gaseous material in the deposits. This and earlier studies (Moore and others, 1974) have identified impact melt on basin flanks, but much ejecta was probably clastic; thus the terms "debris surge" (Morrison and Oberbeck, 1975) or "debris flows" (Moore and others, 1974) are appropriate. These terms embrace primary and secondary ejecta and mixtures of the two. The commonly used term "base surge" (for example, Lindsay, 1976) is less desirable because it implies gas transport, a process not yet shown to be important in emplacing lunar ejecta deposits.

MASSIF MATERIAL

The Apennine front is characterized by rugged massive mountains, the Moon's largest (fig. 12). They have

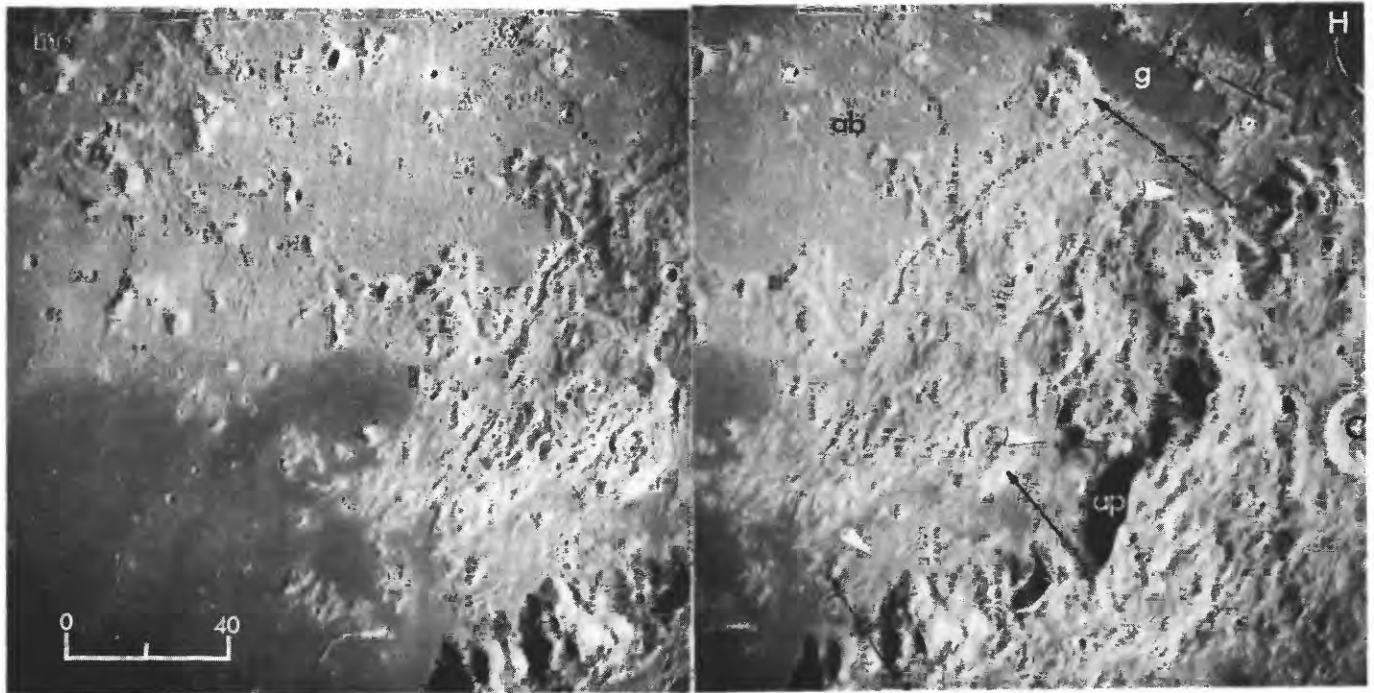


FIGURE 12.—Stereoscopic photographs of central part of area mapped in figure 11A including steep front of Montes Apenninus massifs (ap), smooth material of Apennine Bench Formation (ab), part of material of Montes Archimedes (ma), head end of Rima Hadley (H), and west half of crater Conon (C). Apenninus type of basin ejecta, with basin-concentric structure, covers Apennine flank southeast of Apennine massifs. Black arrows show matching terrain of Apennine front and slump masses derived therefrom. Black cross shows intersection of a slump mass parallel to mountain front and a later mass elongate perpendicular to front. White arrowheads show probable Imbrium impact melt with fissures and flow ridges that was emplaced in gap between slumps and front. Apennine Bench Formation apparently subsided into basin-radial depression north of letters ab. Graben (g) apparently cuts mare as well as slump material and indicates basinward movement of Apennine bench long after slumping ceased. Apollo 17 mapping-camera frames 2709 (right) and 2711; sun illumination from right 32° above horizontal in center of right frame; 30° in left.

steep, relatively smooth slopes that are bright at high sun illumination. Their stratified appearance as reported by the Apollo 15 astronauts is probably a lighting artifact (Swann and others, 1972; Howard and Larsen, 1972; Wolfe and Bailey, 1972). Their massive structure indicates that they are parts of the rim of the Imbrium crater of excavation (Baldwin, 1963; Hodges and Wilhelms, 1976; Wilhelms and others, 1977). The amount of upthrust or outthrust pre-Imbrian material relative to basin ejecta in the massifs is uncertain (Carr and others, 1971). The Apollo stereo photographs of the tops of most massifs show textures like those of the adjacent ejecta (figs. 11, 12, 13), but the thickness of ejecta is not known; it may amount to the entire height of the massifs (Moore and others, 1974).

MATERIAL OF MONTES ARCHIMEDES

Montes Archimedes (fig. 12) is a chaotically structured elevated region south of the crater Archimedes. Bright, smooth-sloped peaks protrude above jumbled material, and textural elements tend to parallel the Apennine front. The origin of Montes Archimedes is tied to the question of original size of multi-ringed impact basins. For example, Head (1977) proposed that it is part of the rim crest of the Imbrium crater of excavation, modified by slumping. Thus Montes Apenninus would be external to the original crater, uplifted by outward-directed stresses, and the steep frontal scarp would be formed by faulting as Montes Archimedes and the adjacent shelf moved toward the basin center. The alternative preferred here is that the Apennines, a far larger structure than Montes Archimedes, approximate the main crater rim. Montes Archimedes would thus have been formed inside the crater either as a subsidiary crater rim nested inside the main excavated cavity (Hodges and Wilhelms, 1976; Wilhelms and others, 1977) or as a relatively surficial slump from the Apennines.

BLOCKY EJECTA

The most extensive unit is blocky ejecta from the Imbrium basin. It dominates the southeast Apennine slope (figs. 12, 13), where it is coarse, and also occurs in Montes Haemus. Originally it was named the hummocky member of the Fra Mauro Formation (Hackman, 1964, 1966). Later it was divided into the Alpes Formation (Page, 1970; Wilhelms and McCauley, 1971) and material of Montes Apenninus (Wilhelms and McCauley, 1971), depending on whether its blocks were roughly equidimensional and widely spaced (Alpes) or elongate subparallel with the Apennine crest and closely spaced. The Alpes Formation was considered either ejecta or fractured bedrock, and the

material of Montes Apenninus as bedrock cut by closely spaced imbricate faults. On figure 11, the variations in orientation, spacing, and size of the blocky ejecta are indicated diagrammatically by the cross symbols. The concentric, more massive Apenninus type dominates in the southwest Apennines (fig. 11A), and the knobby Alpes type dominates east of roughly 4° to 5° east longitude.

The mode of emplacement of the blocky ejecta is still not entirely certain. The Apenninus facies apparently consists either of ejecta or of outthrust blocks covered by ejecta, for it grades outward into deposits that clearly have flowed (figs. 11, 13). In either case, its coarse structure and a lack of secondary craters produced by its impact indicate that it was emplaced in short, slow ballistic trajectories or entirely on the surface, in accord with the general picture of emplacement of near-rim primary deposits. Material in a comparable position at Orientale has textures indicative of deposition and not of structural deformation (fig. 14). The Alpes facies seems to be a mix of detached blocks and finer material and so is probably entirely depositional. Its more chaotic structure may indicate a longer ballistic flight and a different source than for the Apenninus facies. If lunar basins consist of nested craters, ejecta could leave the inner crater(s) at higher angles than from the outer and fall back upon the outer crater's ejecta (Oberbeck, 1975). The Alpes might represent the inner ejecta and the Apenninus the outer crater's ejecta, a relation suggested by McCauley (1977) for similar materials at Orientale (although he suggests sources closer to the basin center).

Some concentric texture in Montes Apenninus seems to have formed by deceleration of ground-flowing deposits (fig. 13, t) as is common at Orientale (fig. 14, t) (McCauley, 1968; Hodges, 1972; Moore and others, 1974; Scott and others, 1977; see also fig. 29, p). Such piled-up ejecta commonly resembles sand dunes and has been called "deceleration dunes" (McCauley, 1968). Similar small, bright, blocky hills and intervening deposits in Montes Haemus (fig. 11B) lie "downstream" from craters and other elevations which seem to have been overridden by deposits moving along the surface (lat 12° N., long 15° E., and lat 14.5° N., long 19° E., south of Auwers). However, these blocks could conceivably have been plucked from the upstream elevations.

LINEATED AND SMOOTH EJECTA

Other ejecta in the region has few or no blocks. Such ejecta, where lineated subradially to the basin, has been called the Fra Mauro Formation (Wilhelms and McCauley, 1971). Other material here interpreted as ejecta forms planar or wavy surfaces (mapped in fig. 11 by an absence or low density of dashes).

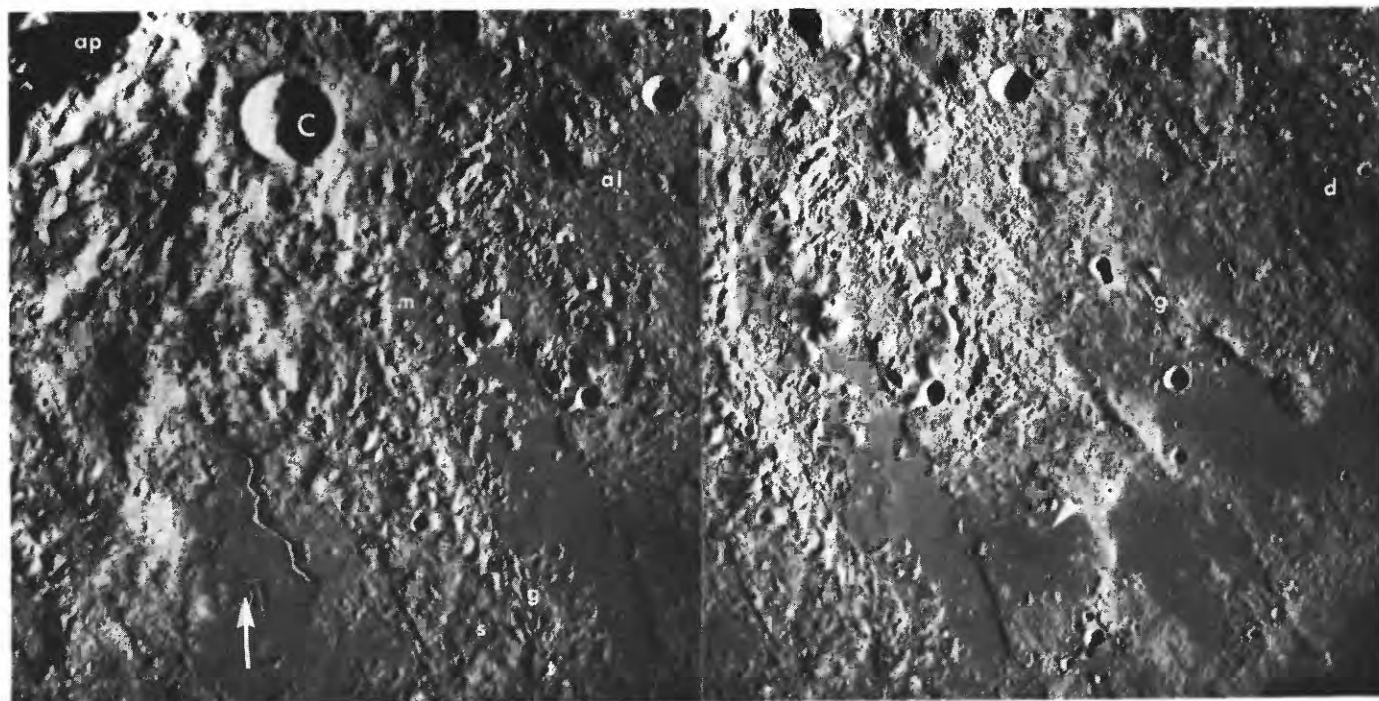


FIGURE 13.—Varieties of ejecta and mare features on southeast-sloping flank of Montes Apenninus. Blocks alined upper right to lower left such as those between mountain front (ap) and crater Conon (C) are part of the Apenninus facies. More widely spaced knobs (al) are part of the Alpes facies (Alpes Formation); here they are alined radially away from basin. At bottom of photographs, knobs seem to be covered by a smooth facies (s). Grooves (g) probably were formed by surface flow, and transverse ridges (t) probably from deceleration of flow. Mantle at (m) contains narrow fissures that suggest contraction of cooling material; this may be impact melt, as may other smooth ejecta (s). Narrow transverse fissures (f) in other ejecta could also be contraction cracks. Dark mantling material (d), D-caldera (arrowhead), and subsidence features (arrow) like those in Apennine Bench Formation (fig. 12) are post-Imbrium, mare-related features. Same scale as figure 12. Parts of Apollo 17 mapping-camera frames 1821 (right) and 1823; sun illumination from right (east) 13° above horizontal in center of right frame, 10° in left.

The lineated ejecta shows clear evidence of flow generally away from the basin (shown by orientation of dashes on fig. 11). Some lineations curve around obstacles. Most lineations in this area are narrow, but some are distinct grooves (fig. 13, g) as at Orientale (fig. 14, g) (Moore and others, 1974, figs. 5 and 7). The lineated and smooth ejecta appear to grade from blocky or other coarsely structured ejecta at both basins. The gradation could reflect a finer grain size or greater melt content in the outer ejecta (Moore and others, 1974) or a greater lateral velocity component during emplacement.

GROOVED MATERIAL

Much of the high terrain beyond about 150 km from the Apennine crest is grooved and streamlined.

Grooves, on the average about 2 km apart, are radial to the basin and are straight or gently curved. Mountains and slopes facing the basin are the most commonly grooved features, but some slopes facing away from the basin are also grooved. Reflectivity is mostly high, although some occurrences are covered by dark material (mapped in fig. 15). Ejecta is banked up against both sides of some of the grooved hills.

Evidence in the area is insufficient to preclude either an erosional or a depositional origin of the grooves, but similar occurrences on pre-Orientele eminences are continuations of flow features within the adjacent ejecta deposits (fig. 14) and purely erosional grooves this close to the basin seem rare at Orientale.

Most eminences in the Apennine-Haemus region lie along continuations of rings of the pre-Imbrian Serenitatis basin (Wilhelms and McCauley, 1971) and



FIGURE 14.—Area on flank of Orientale basin at same position relative to basin rim, similar azimuth (east-southeast), similar scale, and similar geology as the Imbrium area in figure 13. Crater Eichstädt (E) 50 km diameter. Topographic basin rim of Orientale is Montes Cordillera (co). Centrally oriented ejecta near basin rim and Eichstädt grades outward into smoother, radially lineated ejecta (s) with occasional deep flow grooves (g). Transverse ridges of ejecta (t) are piled up where ejecta flow encountered obstacles. Concentric structure of inner ejecta may have a similar deceleration origin or may result from low original ejection velocities and trajectories. Narrow transverse fissures (f) similar to those of the Imbrium area are also present, but their significance is uncertain; they may indicate shrinkage of hot impact-melted material in ejecta. Part of Lunar Orbiter IV frame 173-H; sun illumination from right (east) 15° above horizontal.

presumably are massifs of that basin, but some are Imbrium basin secondaries emplaced only momentarily before being overridden by a debris surge (Oberbeck, 1975; Wilhelms, 1976). Some occurrences are not strongly grooved but consist of single or aligned knobs ("volcanic domes," Morris and Wilhelms, 1967). These knobby features may also have been overridden and are included in the grooved unit (fig. 11). The greater contrast in albedo and texture between ejecta deposits and the eminences relative to the Orientale analogs may be a result of erosion of the Imbrium ejecta from steep slopes.

POSSIBLE IMPACT MELT

Three types of terrain in the area may be formed by material that was melted or partly melted by energy of

the impact that formed the Imbrium basin. The first is the lineated and smooth ejecta discussed above. Second, cracks in some wavy surfaces suggest origin as shrinkage of molten material (fig. 13, m). Material in comparable positions in the Orientale ejecta ("fissured facies") is interpreted as impact melt by Moore and others (1974).

The third and largest expanse of possible impact melt is the planar or wavy material inside the Apennine scarp and around Montes Archimedes (fig. 12). This terrain was named the Apennine Bench Formation by Hackman (1964, 1966) and interpreted by him and E. M. Shoemaker as impact melt (oral commun., 1963). Subsequently a volcanic origin was proposed (Wilhelms, 1970). Fluid emplacement seems indicated by the smooth surface, irregular fractures roughly radial and concentric to the basin that resemble shrink-

age cracks, and gentle, smooth-walled depressions that suggest subsidence of viscous fluid into underlying cavities (fig. 12, above symbol ab). Volcanism cannot be excluded, but an impact origin is more consistent with current understanding of Orientale (Scott and others, 1977) and the lunar terrae in general. Fractured melt overlies slumps from the Apennine front (fig. 12), in accord with inferences by Dence (1971) that melt in terrestrial craters is emplaced after slumping.

SLUMP DEPOSITS

Much evidence suggests that the hilly material immediately northwest of the Apennine front slumped from the mountains. The mounds and ridges nearest the front roughly parallel the Apennine crest, are most massive opposite the largest concavities, and in general can mentally be fit back into the front in jigsaw puzzle fashion (figs. 11, 12, arrows). Their finer morphology—mostly irregular imbricate structure and a few massif-like hills—also matches that in the Apennines. Lineations radial to the front are probably scour or flow grooves along the direction of movement.

Superposition relations show that the slumps formed episodically. Superposition of the impact melt shows that major slumping occurred within a short time after the basin formed. Near the head of Rima Hadley, a massive, linear slump ridge parallel to the front is transected by a later hummocky tongue of slump material (Carr and others, 1971) perpendicular to the front (fig. 12, black cross). The topography of these intersecting slumps matches “missing” parts of the Apennine crest. The later, radial flow apparently was a fragmental mass that travelled farther than the earlier more coherent slump. Long-continued movement toward the basin center—though probably regional subsidence rather than true slumping—is indicated by grabens parallel to the Apennine front that cut the mare material as well as the slumps (fig. 12, g).

DARK MATERIALS

The regions of Mare Serenitatis mapped here (fig. 15) and to the east (fig. 17) contain typical and long-studied examples of the two major morphologic types of lunar dark material, mare material and dark mantling material. The returned samples are generally assumed to show that mare materials are basaltic lava (overlain by regolith derived from the lava by impacts) and that the dark mantling materials consist of glassy droplets of the same approximate composition as the lava emplaced in “fire fountains” (Heiken and others, 1974). The darkest of both types occur in the border zone of Mare Serenitatis and Mare Tranquillitatis including

the highland rim. The dark border was once thought younger than the brighter center (Carr, 1966; Wilhelms and McCauley, 1971). The dark mantling materials are level (marelike) in places, and this was thought to indicate that they overlay the mare. The dark mare materials were believed younger than the lighter ones on the basis of sparse crater counts and analogy with the better understood relations in the northern Procellarum-southern Imbrium region discussed above, where the younger mare units are indeed the darker. The Apollo photographs show, however, that the lighter mare materials of central Serenitatis abut and embay the border mare materials and hence are younger (Howard and others, 1973). The dark mantling materials are also clearly embayed by mare materials in most places; the level parts of the mantle may overlie old mare material, or they may be thick accumulations of dark mantling materials themselves, as will be discussed.

MARE MATERIALS

Mare units are mapped (fig. 15) in the eastern two-thirds of the area of figure 11 much as in Mare Imbrium and northern Oceanus Procellarum. Most of central Mare Serenitatis is composed of red mare material in which 18 D_L values ranging from 225 to 320 were measured (Boyce and others, 1975). This wide range presumably reflects a complex stratigraphy, but in the absence of strong color boundaries (fig. 16), only two red units (both Imbrian, map symbols Imr_1 and Imr_2) could be tentatively distinguished in this study.

The marginal zone of Mare Serenitatis appears more diverse than the interior. The easternmost unit of the margin in this area is the oldest (older Imbrian blue mare material) and is a continuation of the materials that fill northern Mare Tranquillitatis (basalt of Plinius area of Howard and others, 1973; McCord and others, 1972; Thompson and others, 1973; Johnson and others, 1975). The unit slopes sharply from Tranquillitatis toward Serenitatis (arrows) and is faulted by grabens. This slope presumably results from subsidence of central Mare Serenitatis. Locally faulted blue mare materials west of the unit appear to be younger Imbrian.

The western margin of Serenitatis includes a unit of Eratosthenian blue mare material that was detected on the color difference photographs and indicated by three low D_L values (caption, fig. 15); it was then mapped in detail according to embayments of small Eratosthenian craters. Another marginal unit that could be Eratosthenian (map symbol Elm) is intermediate in color, recalling a unit similar in age and color in northern Oceanus Procellarum.

Mare Vaporum seems to contain the unit of Eratosthenian or Imbrian age and intermediate color and a similarly colored but clearly Eratosthenian unit that embays deposits of the crater Manilius.

Thus the sequence here contains a red-to-blue progression like that in the northern Procellarum-southern Imbrium region, but some young units are not the bluest and extensive blue units occur in the old part of the sequence. As will be discussed in the section on southern Oceanus Procellarum, color and reflectivity correlate in mature mare regoliths, and both depend on composition of the underlying basalt. This explains why the generalization that young lavas are dark could not be correctly extrapolated to the present region— young lavas are dark only if they happen to be blue (titanium rich). Blue old lavas are also dark.

The presence of the old blue materials here and not in the northern Procellarum-southern Imbrium region has been taken as an indication that erupted lunar mare lavas progressed in time from blue in the east to red in the center to blue again in the west (western Oceanus Procellarum contains many young blue lavas) (Soderblom and Lebofsky, 1972; Soderblom and Boyce, 1976). However, there are numerous exceptions to this generalization here and elsewhere including to the east in Sinus Amoris, where very old red materials are exposed (fig. 17).

MARE AND DARK MANTLING MATERIAL IN MONTES HAEMUS

Dark materials were deposited on most of Montes Haemus at levels considerably higher than Maria Serenitatis and Tranquillitatis (fig. 13). The terra along the border of Mare Serenitatis is thickly mantled by a deposit called the Sulpicius Gallus Formation (Carr, 1966) that grades outward to a thinner blanket (fig. 15). Small bright peaks protrude through all but the thickest parts of these deposits. The mantle was probably deposited even on high ground, for some material on steep slopes is streaked with dark as well as bright material (the latter presumably derived from the underlying bedrock). The thick deposits are distinctly reddish (for example, Lucchitta and Schmitt, 1974). Unit Idr north of Menelaus is an arched, faulted deposit (dark member of the Tacquet Formation; Carr, 1966) that was included in the blue mare unit called basalt of the Plinius area (Howard and others, 1973), but is more like the Sulpicius Gallus Formation because it surrounds some bright terra peaks and is reddish (Johnson and others, 1975).

Farther inland are dark "lakes" of Imbrian dark materials arranged in two color belts parallel to Montes Haemus: the belt closer to Mare Serenitatis is red or intermediate in color, the outer belt blue. Most patches

in both belts appear to be as old as the older blue and red mare units along the Serenitatis margin, but the stratigraphic relation between red and blue "lakes" is uncertain. In addition, a few small patches of intermediate or uncertain color and age are mapped as mare, undivided (map unit m), and an elevated, blue, young, probably Eratosthenian patch forms a swell surmounted by the "D-caldera" (fig. 13) (Whitaker, 1972d; El-Baz, 1973).

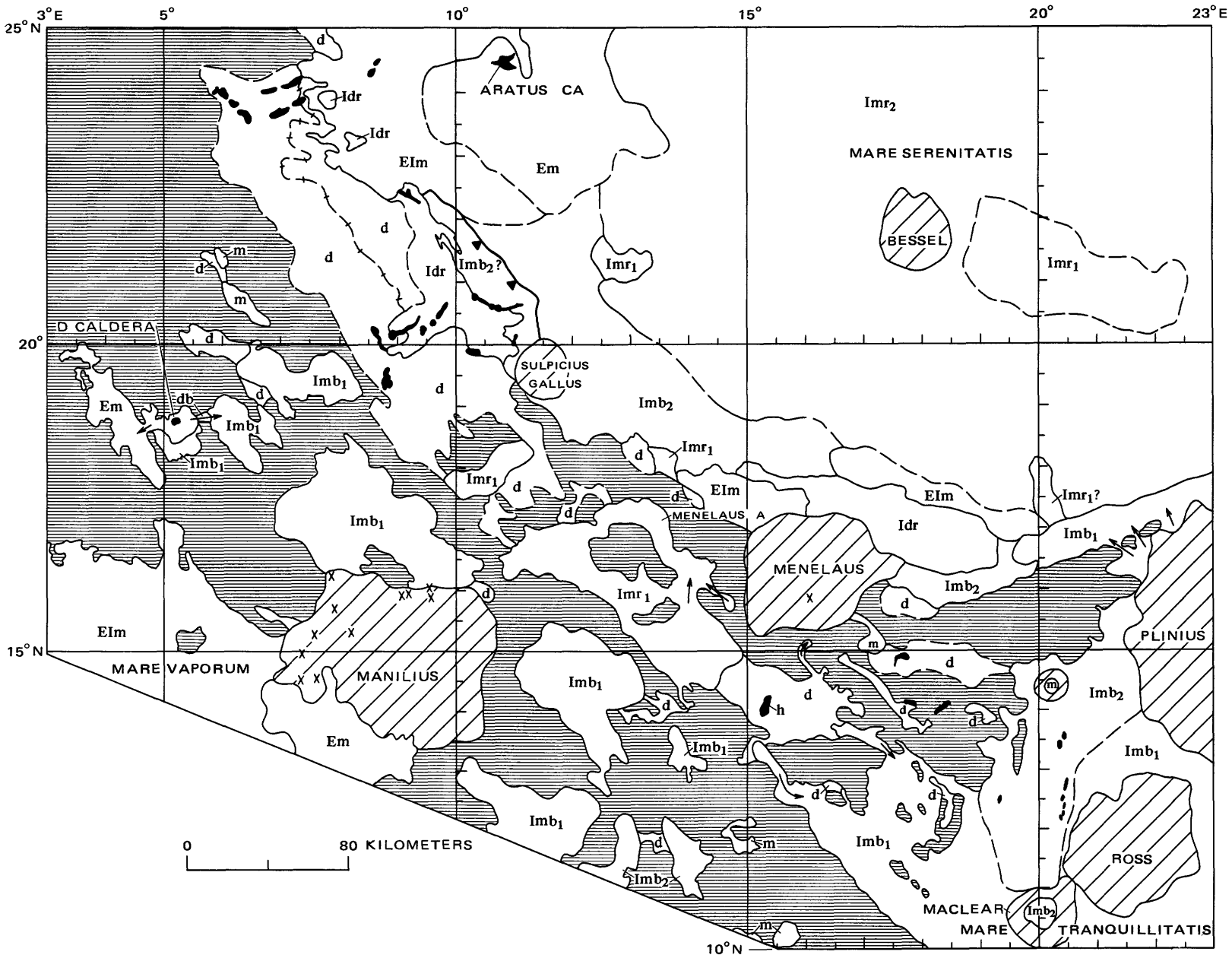
The distinction between mantling and mare materials is unclear in this region. The "lake" materials would normally be mapped as mare materials because of their overall level surfaces, but they thinly cover Imbrium basin materials; in the best low-sun stereoscopic pictures, linear radial structures of Imbrium show through. Most patches have sloping contacts that also reflect the subjacent topography. Thin, probably gradational deposits mantle the adjacent terra. Some of these mantles connect "lakes" and seem to have flowed from one lake to another (arrows in fig. 15). Other dark mantles (mapped as unit d or db) are sufficiently like the adjacent terra, only slightly more bluish, as to suggest that their original color was weakened by mixture with terra material. Thus all of Montes Haemus may have been mantled early in the Imbrian epoch of basaltic volcanism by pyroclastic deposits—"mare materials" being those which accumulated in sufficient thickness or on suitable flat substrate to appear flat.

SOURCES

The region has an unusually large number of irregular craters, rilles, and cones which might have been sources for the dark materials. Aratus CA is an irregular crater in the mare (Greeley, 1973). A dark cone is perched high on the terra (fig. 15, h, lat 14° N., long 15.3° E.). The most common possible sources, especially numerous in the Sulpicius Gallus Formation, are irregular craters that appear too deep on the stereo photographs to be secondary impact craters. The Sulpicius Gallus rilles are likely additional sources for much of that formation (Carr, 1966). Some volcanic depressions could have formed by passive collapse without eruption.

TERRA EAST OF MARE SERENITATIS, WEST OF CRISIUM, AND NORTH OF TRANQUILLITATIS

The origin of the complex terra described here is less clear than that of the Imbrium-dominated Apennine-Haemus region. Imbrium and several pre-Imbrian basins have undoubtedly shaped this region, but their relative contributions are uncertain (Wilhelms and McCauley, 1971; Wilhelms, 1972a, c, 1973; Scott and



EXPLANATION

<p>h</p> <p>Em</p> <p>EIm</p> <p>Imr2</p> <p>Imb2</p> <p>Imr1</p> <p>Imb1</p> <p>Idr</p>	<p>Volcanic hills (h) or depressions</p> <p>Eratosthenian mare material, blue except intermediate color south of Manilius - Three D_L values 160-215, avg. 185</p> <p>Eratosthenian or Imbrian mare material, intermediate or unknown color - Three D_L values, 200-245, avg. 230</p> <p>Imbrian mare material, red, younger - Twelve D_L values 225-270, avg. 250; high albedo</p> <p>Imbrian mare material, blue, younger - Five D_L values 235-265, avg. 260</p> <p>Imbrian mare material, red, older - Six D_L values 285-320, avg. 295</p> <p>Imbrian mare material, blue, older - No D_L values in this area; faulted, dark</p> <p>Dark mantling material, red</p>	<p></p> <p></p> <p></p> <p></p> <p></p> <p></p> <p></p> <p></p>	<p>Dark mantling material, color and age unknown - Line with crosses separates thicker (northeast) and thinner mantles</p> <p>Dark mantling material, blue, age unknown</p> <p>Mare material, mostly blue, age unknown</p> <p>Materials of Imbrian and younger craters</p> <p>Materials of Imbrium basin, undivided (see fig. 11)</p>
		<p></p> <p></p> <p></p> <p></p>	<p>Scarp within geological unit; barb on higher side</p> <p>Dark-haloed crater - Shows that dark material underlies crater ejecta</p> <p>Scarp and possible flow direction</p> <p>Indefinite contact</p>

Figure 15.—Geologic map of dark materials in parts of the Apenninus-Haemus region, Mare Serenitatis, and Mare Tranquillitatis. Based on Apollo 15 mapping-camera frames 398-416, 570-588, 977-995, 1119-1137, 1659-1678, 1800-1819, 2029-2048, 2143-2162, 2287-2305, 2426-2445, 2694-2712; Apollo 17 mapping-camera frames 796-813, 1221-1241, 1502-1522, 1805-1825, 2091-2108, 2252-2271, 2688-2708, 2882-2901; and color-difference photograph reproduced in figure 16.

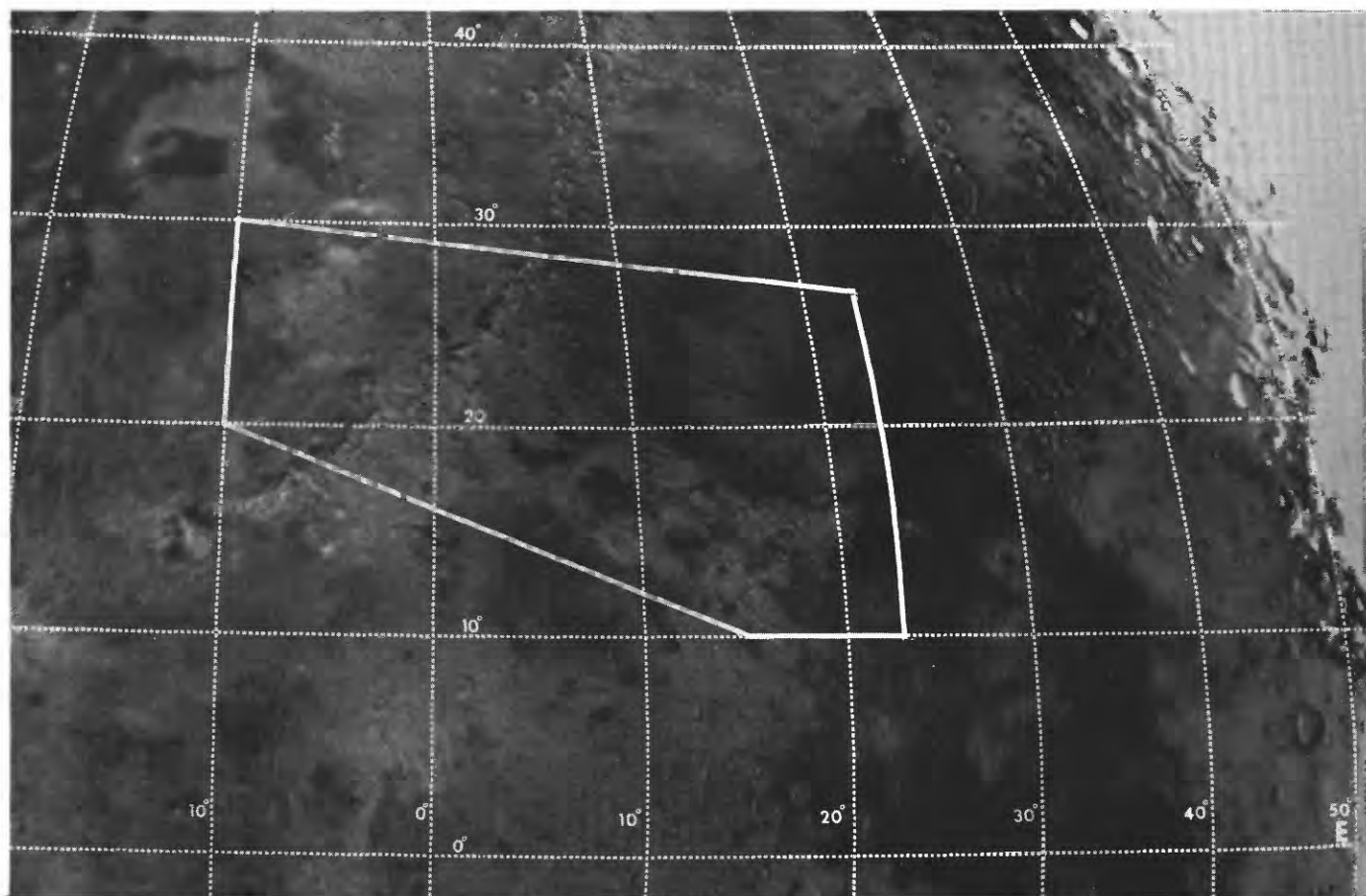


FIGURE 16.—Color-difference photograph of region mapped in figure 11 (outlined). Wavelength pairs $0.31\text{--}0.40\ \mu\text{m}$ and $0.73\text{--}0.90\ \mu\text{m}$. Dark is blue, light is red. Courtesy of E. A. Whitaker (Whitaker, 1966, 1972b).

Pohn, 1972; Scott and others, 1972; Head, 1974a). The dominant northwest-southeast topographic "grain" of the terrane (figs. 17, 18, 19) is radial both to Imbrium (1,200 km to the northwest) and, in places, to the nearby Serenitatis or Crisium basins. This grain and a weaker, roughly northeast set of lineations follow the most common "lunar grid" directions (Strom, 1964; Scott and others, 1975) and have been ascribed to impact rejuvenation of endogenic structures (Scott and Pohn, 1972; Scott and others, 1972; Head, 1974a). After considering the pre-Imbrium basins, I conclude that Imbrium ejecta has played a major role in shaping the terrane and that endogenic interpretations are unnecessary. This conclusion relies less on direct observations here, which remain ambiguous, than on observations of the informative Orientale analog and of Imbrium features described elsewhere in this report.

The dark nonterra materials are not discussed in detail because they are similar to those described above or have been treated extensively in the literature. Novel features in the older part of the sequence include a heavily cratered red unit (fig. 17, symbol Imr_0) in

Sinus Amoris and the dark, blue, probably pyroclastic mantling deposit of the Apollo 17 site (Scott and Pohn, 1972; Scott and others, 1972; Hinners, 1973; Lucchitta, 1973; Pieters and others, 1973; Thompson and others, 1973; Muehlberger and others, 1973; Adams and others, 1974; Head, 1974b; Lucchitta and Sanchez, 1975; Wolfe and others, 1975). In addition, reddish dark mantling materials were found in this study on the Crisium basin rim just east of the mapped area at the latitude of Macrobius. A red Eratosthenian mare unit apparently is also present (fig. 17, symbol Em). Steplike distribution of patches of mare material connected by probable flows starting at elevations substantially above that of the predominant mare level was noted in the "lakes" peripheral to Crisium (Wilhelms, 1973) and at either side of Sinus Amoris (fig. 17, arrows; fig. 19, m). A line of small dark volcanic cones also occurs at a high elevation in the crater Tisserand (fig. 19). The Apollo 17 mission returned excellent photographs of other small volcanic features (Scott, 1973a; Bryan and Adams, 1973; Young and others, 1973b) and of mare ridges and scarps (Hodges,

1973; Howard and Muehlberger, 1973; Scott, 1973b; Young and others, 1973b; Muehlberger, 1974; Lucchitta, 1976). However, Mare Tranquillitatis south of Dawes, a diverse area that includes a large sinuous rille, disc-shaped filled craters or domes, flow lobes, large mare ridges, orthogonal faults in different units, and degraded terra islands, was not well photographed.

PRE-IMBRIAN MATERIALS

The pre-Imbrium basins most likely to contribute to the topography and lithology of the region are Serenitatis, Crisium, and Tranquillitatis (Stuart-Alexander and Howard, 1970; Wilhelms and McCauley, 1971; Wilhelms, 1972a, 1973; Short and Forman, 1972; Scott and Pohn, 1972; Head, 1974a). The Tranquillitatis basin is very obscure but may have contributed to the gross form of the terra. The massifs around the Apollo 17 landing site (figs. 17A, 18) are part of the most conspicuous ring on the southeast side of the Serenitatis basin, which may be double (Scott, 1972c, 1974; Reed and Wolfe, 1975; Wolfe and Reed, 1976). Groups of irregular, overlapping craters north of the area mapped here are aligned radially to the southern Serenitatis basin and are probably its secondary impact craters (Wilhelms, 1976). Crisium basin massifs and radial lineations (of possible non-Crisium origin) occur near the eastern map boundary (figs. 17B, 19), and hummocky terrain west of Proclus (fig. 19) that resembles the Alpes Formation of Imbrium may be ejecta of Crisium. Otherwise, few features attributable to Crisium have been identified in spite of the proximity of the area to this large and relatively youthful-appearing basin. Possible reasons are that Crisium ejecta was ejected preferentially in other directions or that it is covered here by Serenitatis ejecta. This younger age of Serenitatis, though contrary to intuition because of its degraded appearance, is supported by superposition relations outside the mapped area. Its "old" appearance probably results from modification by Imbrium ejecta.

POSSIBLE IMBRIUM EFFECTS

Five general types of small-scale topographic elements oriented northwest-southeast are superposed on probable pre-Imbrian terrain: small, irregular pits (p), lineations (l), terra mantling material (t), pits intermixed with, or on the Imbrium side of, lineations (pl), and lineations and a thin mantle (lt) (figs. 17, 18, 19). These features are best interpreted by comparison with the more continuous exterior features of the Orientale basin. Orientale is about three-fourths the size of Imbrium, so a comparison 900 km from the center

of Orientale was selected (fig. 20). Small pitlike secondary craters (p) and lineations (l, pl) score the pre-Orientale terrane. Lineations on the southeast side of secondary pits (pl) apparently are partly the coalescent ejecta of the pits and partly flow features in continuity with thick masses of continuous ejecta farther west toward the basin (figs. 26, 29). Isolated lineations (l) far from the basin are likely to be secondary ejecta and gouges, but origin as flow grooves of continuous ejecta is also possible. If the Orientale lineations were more degraded or poorly photographed, they might be interpreted as faults. Thus regional context is essential in interpretations of landforms. By analogy with the Orientale scene, the pits east of Mare Serenitatis are interpreted as Imbrium secondary craters, and the lineations as textures of either primary or secondary ejecta.

The mantles on the pre-Imbrian terrane (units t and lt) are also probably of Imbrium origin, as are mantling and plains deposits that are sufficiently thick to obscure the pre-Imbrian topography and that appear clearly to be of Imbrian age (units It, Itl, and Ip). Orientale is surrounded at a similar distance by mantles and plains in comparable amounts that are gradational with secondary crater ejecta and with the continuous ejecta on the basin flanks (fig. 20, same symbols). The covered terrane consists either of pre-basin crater rims or of secondary craters of Orientale itself (fig. 20, c; compare figs. 26 and 29, c). Continuous and secondary basin ejecta may appear quite similar, and the former may flow outward past secondary craters (figs. 20, 26, 29). The Imbrium origin of the features east of Mare Serenitatis presumably would be more apparent if the zone between there and the Apenninus-Haemus region were still exposed like its Orientale counterpart (fig. 20).

INTERNAL VERSUS BASIN ORIGIN OF STRUCTURES

Not only fine lineations but also major terra blocks and mare-terra "shorelines" formed by steep scarps are oriented northwest-southeast (figs. 17, 18, 19). Endogenic interpretations were based on the assumption that these gross structures were too large and too "squared off" to have been produced by ejecta. Moreover, this trend is parallel to the Cauchy rille and scarp south of the area, which cut the mare so are presumably endogenic though perhaps impact initiated (Wilhelms, 1972a). Yet structures of considerable magnitude appear to have been formed around Orientale by accumulations of primary and secondary ejecta (fig. 20, X). Hence the large structures of the terra discussed here could be tongues of ejecta from Imbrium either alone or superposed on radial ejecta of Serenitatis.

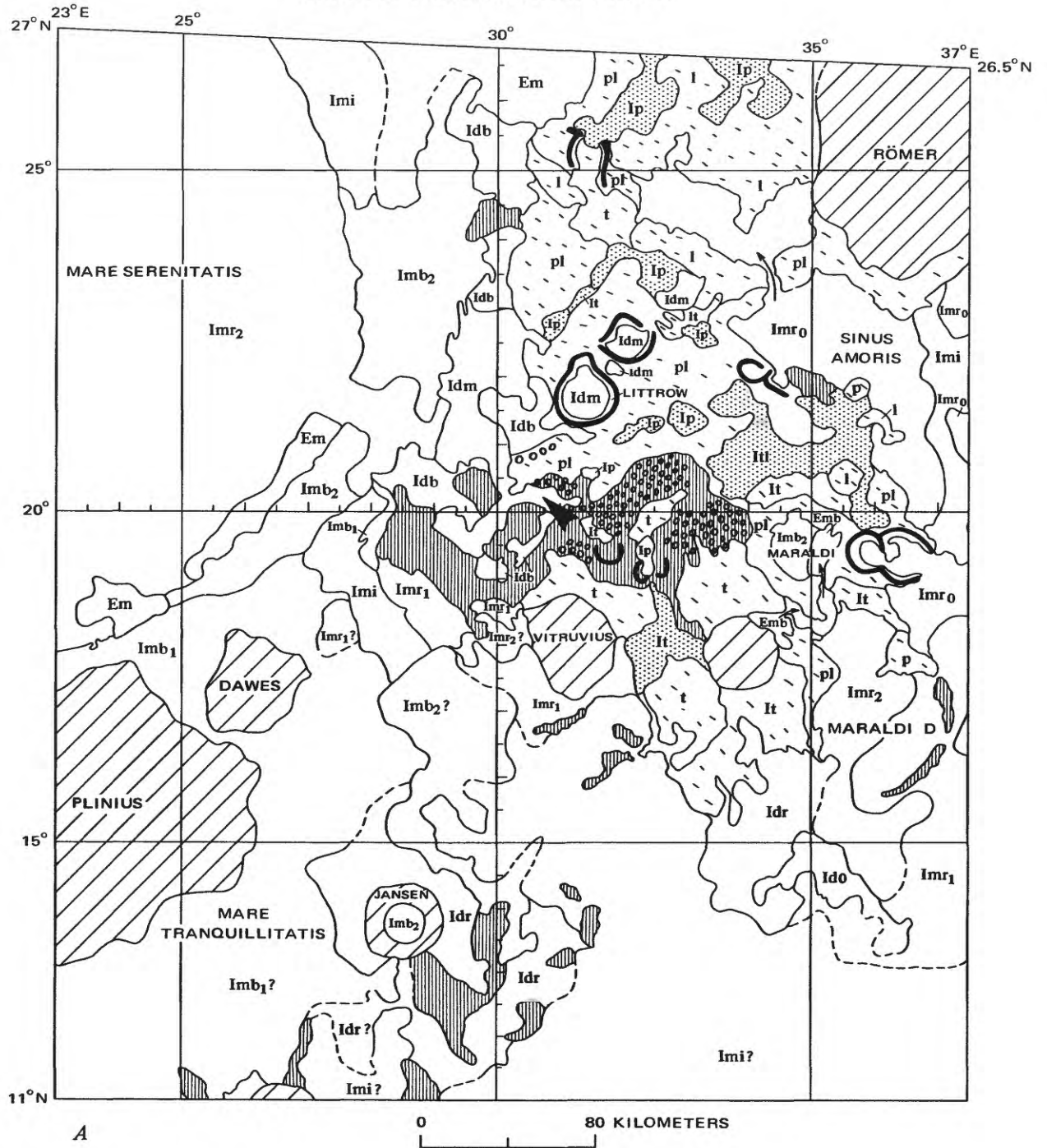
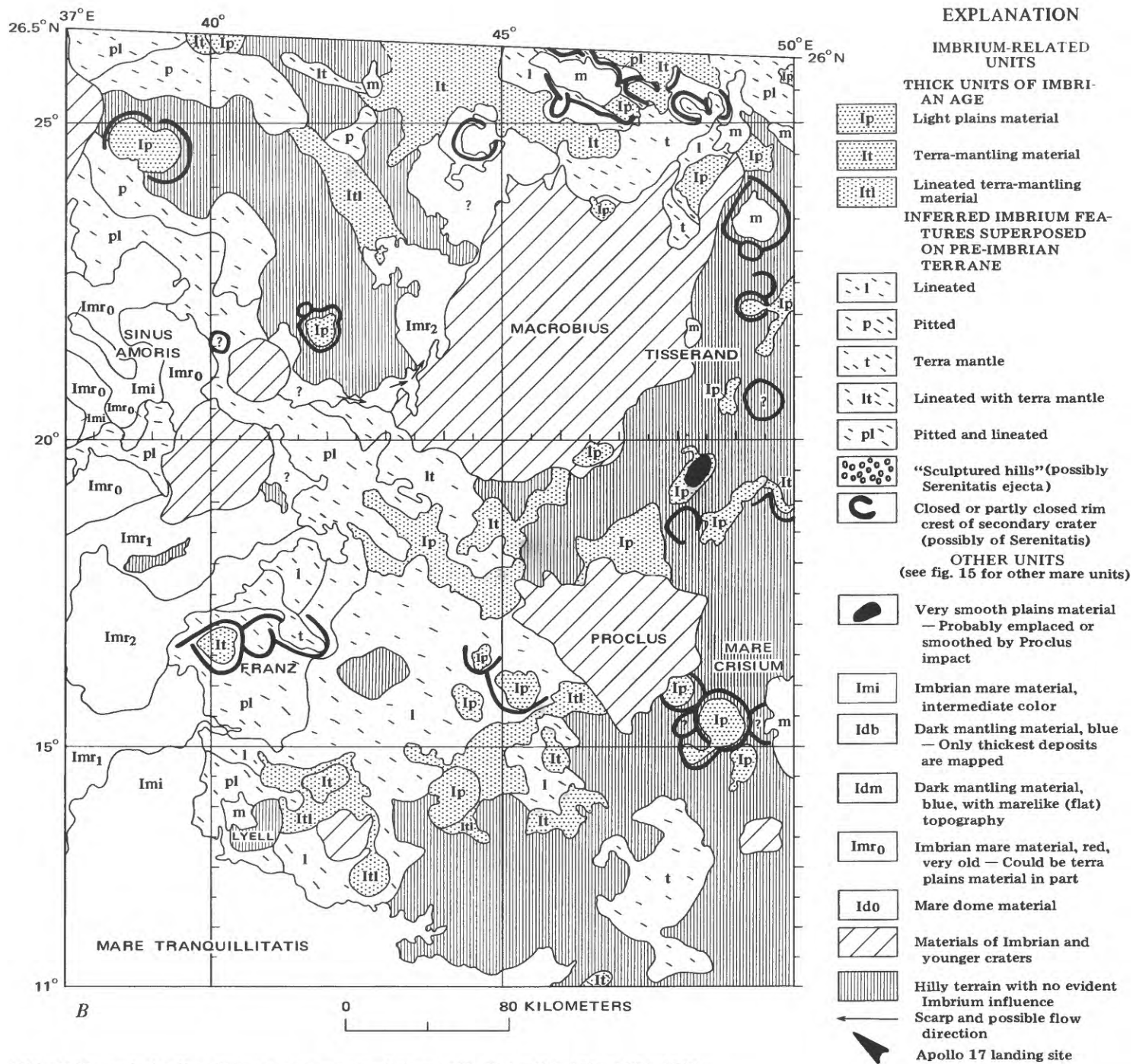


FIGURE 17.—Geologic map of the eastern Serenitatis, western Crisium, and northern Tranquillitatis region. Based mostly on Apollo 15 mapping-camera frames 383-400,



2278–2287, and Apollo 17 mapping-camera frames 289–314, 432–453, 1484–1506, 2671–2692; Lunar Orbiter IV frame H-78 was supplementary.

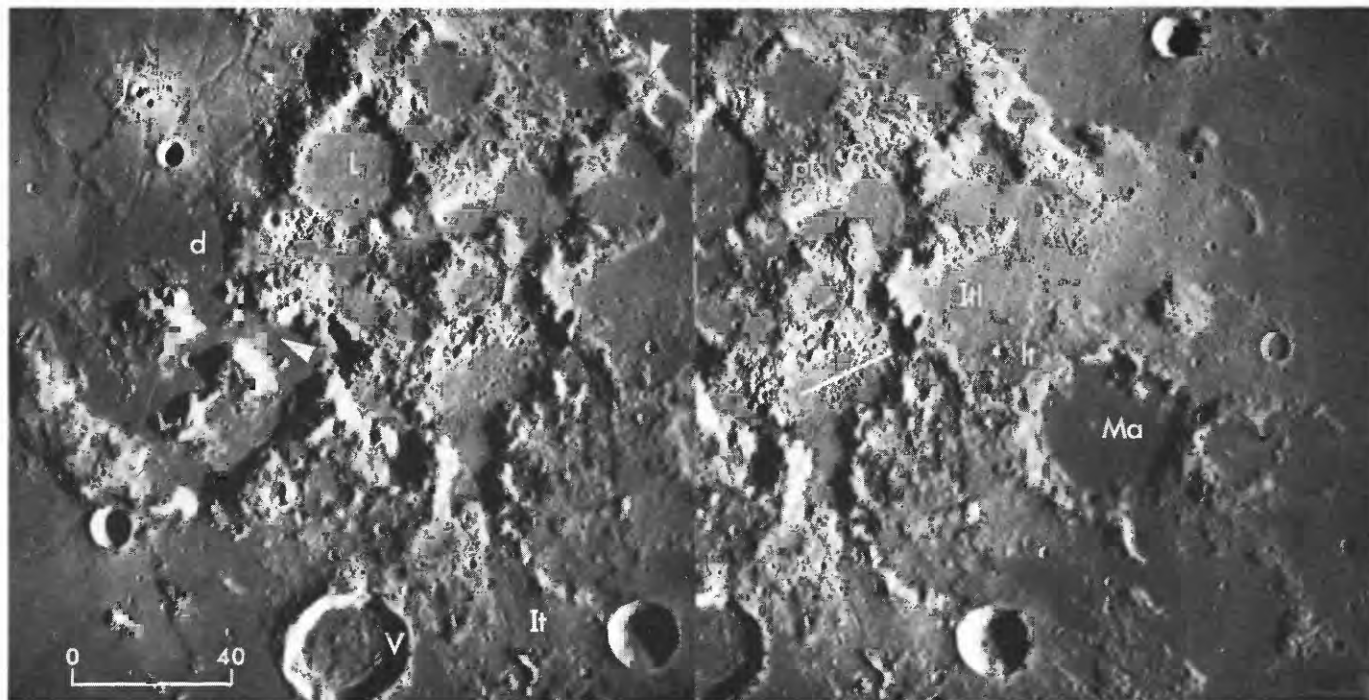


FIGURE 18.—Stereoscopic photographs showing east-central (right-central) part of area covered by figure 17A. Arrowhead indicates Apollo 17 landing site; d, dark mantling material. Labelled craters are Vitruvius (V), Maraldi (Ma), and Littrow (L). Serenitatis massifs surround Apollo 17 site; smaller hills in remainder of picture have been termed "sculptured hills." Rugged, ragged elevation between Vitruvius and arrow with shaft at top of picture ("Vitruvius front," Head, 1974a) may be a Serenitatis basin ring. Typical occurrences of mapped units (fig. 17) are shown by geologic symbols. Hilly, pitted, and lineated terrain (pl) on rim of Littrow and adjacent terrain; thick lineated mantle (Itl) grades to thinner mantle with lineations on rim of crater Maraldi (It). Structure (white line) transverse to Imbrium radials helps give region an orthogonal pattern. Parts of Apollo 17 mapping-camera frames 444 (right) and 446; sun elevation 18° in center of right frame, 14° in left. North at top.

Coarse and fine lineations not radial to Imbrium, Serenitatis, or Crisium also bound many of the small knoblike mounds called "sculptured hills" or "corn-on-the-cob" in Apollo mission terminology (fig. 18; Lunar Sample Preliminary Examination Team, 1973). Major scarps of the roughly northeast-southwest trend seem too irregular to be endogenic and are probably parts of pre-Imbrian concentric basin structure like the "Vitruvius front" (fig. 18; Head, 1974a). The small hills could be Imbrium or Serenitatis ejecta blocked by obstacles, as is common around Orientale (fig. 29). An origin as an inner knobby facies of Serenitatis ejecta comparable to the Alpes Formation of Imbrium is also consistent with the morphology and distribution of the small hills (Head, 1974a).

CRATERS

Stereoscopic study and comparison with the periphery of the Orientale basin have drastically revised previous interpretations of the larger, degraded craters in this area. Most were previously believed to be primary impact craters of pre-Imbrian age (Wilhelms and McCauley, 1971; Scott and Pohn, 1972), and their sub-

dued topography and irregular outlines were ascribed to burial and deformation by the nearby pre-Imbrian basins. Origin by secondary impact of Imbrium and perhaps Serenitatis basin ejecta now seems more likely. This conclusion is far from obvious and must be supported by the Orientale analog, where nearly identical craters of almost certain secondary impact origin occur (figs. 20, 26, and 29; discussed further in later sections). Morphologies of the Orientale secondaries differ greatly because of different degrees of modification by lineated and planar primary and secondary ejecta, but the craters are contemporaneous (Wilhelms, 1976). This wide morphological range around a given basin shows that secondaries of different basins may also resemble one another.

The recognition of craters as secondary of course reduces the number formerly identified as primary and leads to revised estimates of impact flux (Oberbeck and Morrison, 1976; Wilhelms, 1976). Among the craters covered by figures 18 and 19, the only visible craters of any size likely to be primary impact craters older than Imbrium but younger than the local pre-Imbrian basins are Maraldi, which is deep, terraced, and rug-

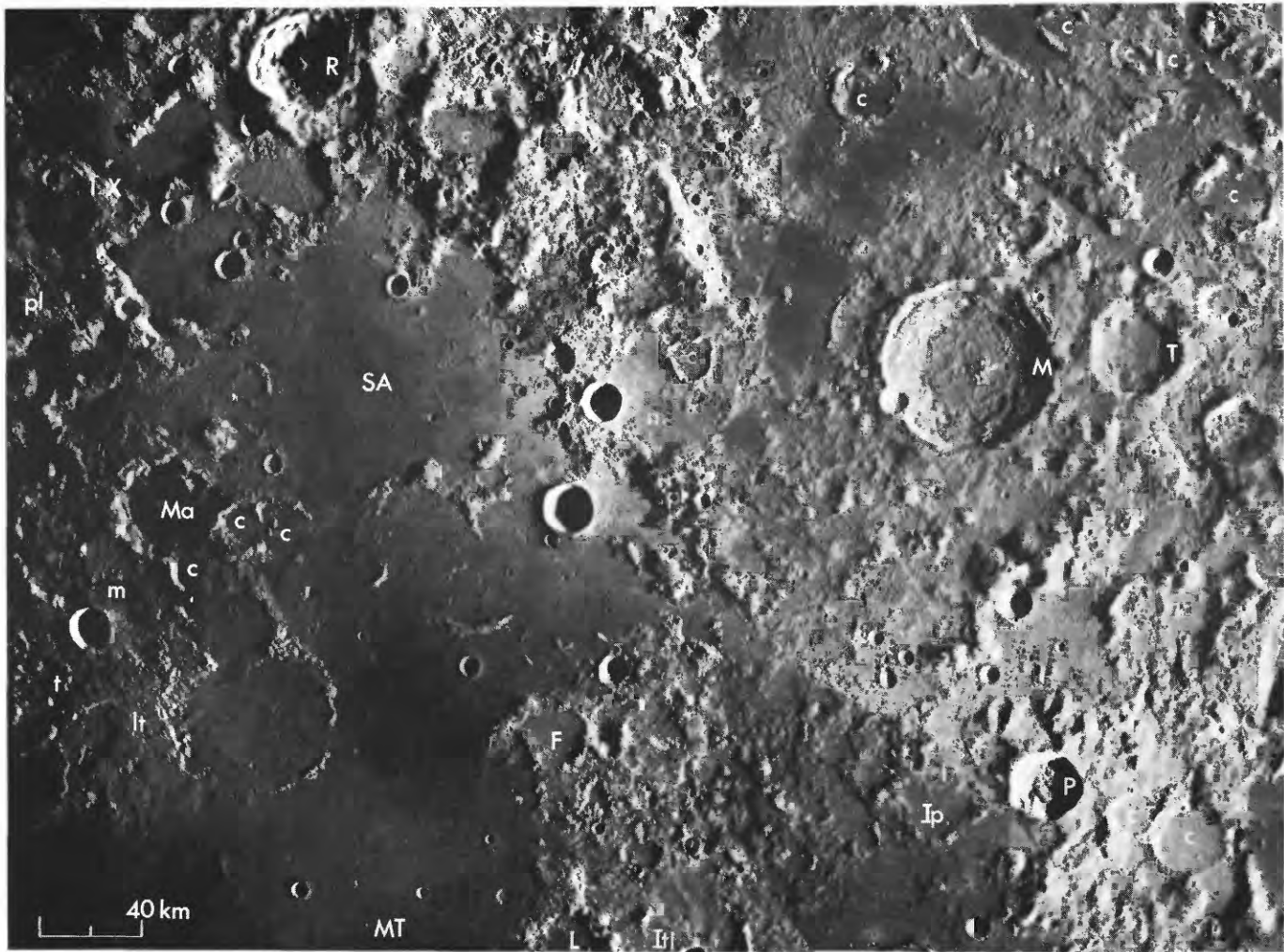


FIGURE 19.—Labelled craters are Maraldi (Ma, compare fig. 18), Römer (R), Macrobius (M), Tisserand (T), Proclus (P), Franz (F), and Lyell (L). Large maria are Mare Tranquillitatis (MT) and Sinus Amoris (SA); cluster of mare domes is near scale bar; mare patches at high elevations, m; secondary impact crater of Imbrium or Serenitatis basin, c. Other letter symbols refer to typical occurrences of geologic units or features (compare figs. 17, 18, 20). Large scarps (X) could be Imbrium basin ejecta (compare fig. 20, X). Uncontrolled mosaic of Apollo 17 mapping-camera frames 295 (right) and 302; sun illumination from right (east), varies from 20° above horizontal at right edge to 6° at left.

ged, and perhaps Tisserand, whose depth is intermediate between depths typical of primary and secondary craters.

TARUNTIUS REGION

The stereoscopic Apollo mapping photographs and the reinterpretations of terra units forced by the Apollo 16 results are the impetus for reinterpretations in the Taruntius region east of Mare Tranquillitatis previously mapped by the author (Wilhelms, 1972a; Wilhelms and McCauley, 1971). Many of the morphological forms and albedo variations in the region were previously ascribed to volcanic rocks of different com-

positions and ages. Because of the high sun illumination of the Apollo photographs, reinterpretations are not attempted west of long 39°E. and are partly dependent in the rest of the region on the observations made of the better photographed terra north of Mare Tranquillitatis discussed above.

TERRA UNITS

On an earlier large-scale map (Wilhelms, 1972a) eight geologic units were mapped to express the diverse topography and albedo of the noncrater part of the terra. Internal origin was the favored interpretation for four units and was considered possible for the

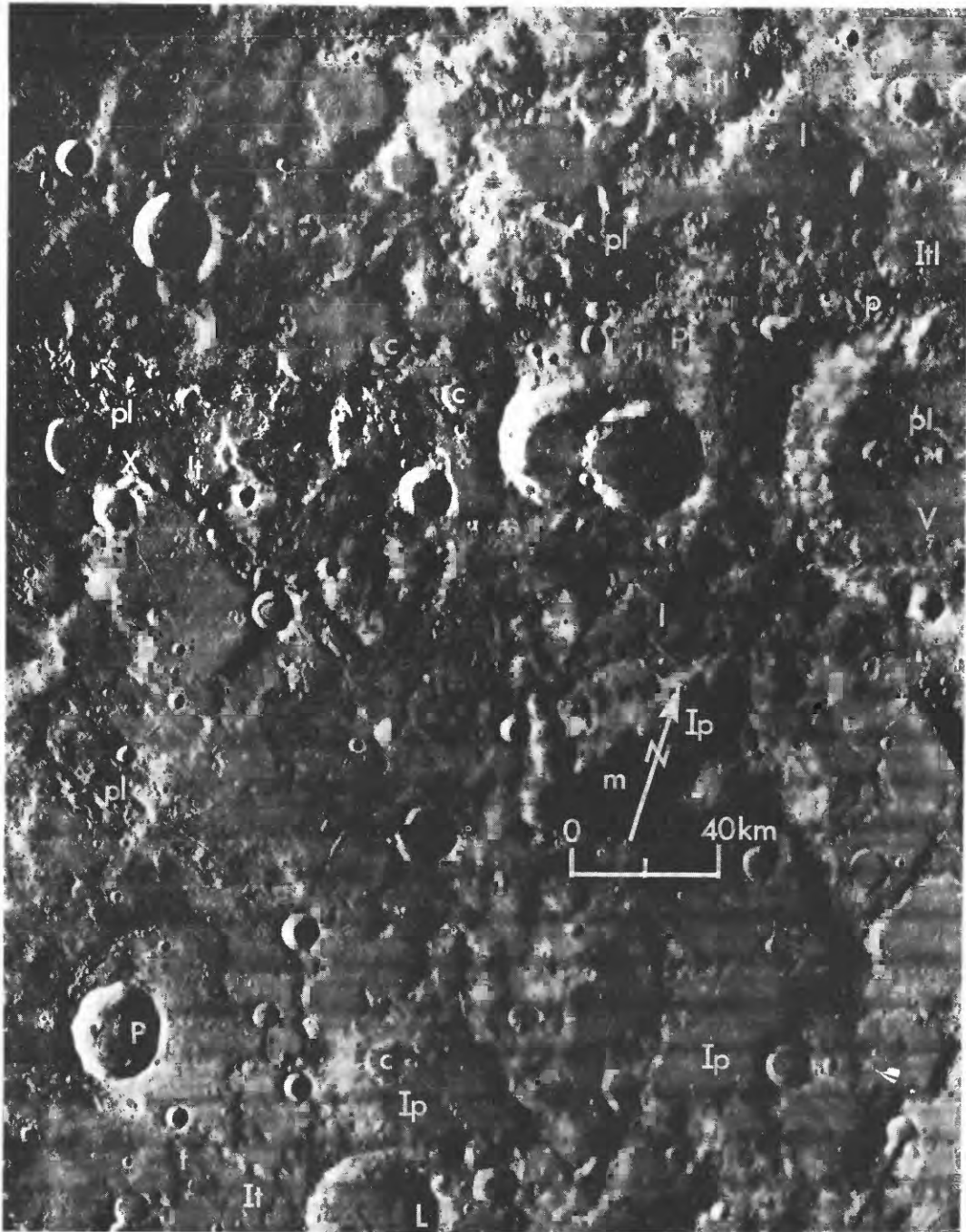


FIGURE 20.—Area 900 km east-southeast of Orientale basin center. Labelled craters are Vieta (V), Piazzis C (P), and Lacroix (L); the latter two are also on figure 26. Geologic symbols 1, p, t, lt, pl, Ip, It, and Itl have same meaning as in Imbrium-influenced area west of Mare Serenitatis (figs. 17, 18, 19). The pitted and lineated terrain (pl) north of Piazzis C is part of the continuous Orientale ejecta, whereas the other, similar occurrences and the pitted (p) and lineated (l) terrain are cut off from the continuous ejecta and could be secondary in origin. Similar uncertainties between continuous ejecta or secondary origin pertain to the thin terra mantling deposits (t, lt) and the other deposits (Ip, It, Itl), but all are clearly of Orientale origin. Unit c, Orientale secondary craters partly covered by above units. Unit m, mare material. High scarp at (X) apparently is formed entirely of ejecta. Part of Lunar Orbiter IV frame 160-H, sun illumination from right (east) 17° above horizontal.

others. In the remapping (fig. 21), six units are employed that reflect new evaluations of the landforms.

Lineations radial to the Imbrium basin pervade the center of the area. Dense lineations are observed, even

on high-sun photographs (fig. 22), in mantling deposits (unit Itl) and in hilly terrain southeast of numerous irregular pits (unit pl). The radial lineations resemble those north of Mare Tranquillitatis and elsewhere at similar distances from Imbrium, which is centered 1,950 km to the northwest. Hence it is inferred that the mantling deposits are secondary or primary Imbrium basin ejecta and that the lineated and pitted deposits are Imbrium secondaries and their ejecta which are superposed on pre-Imbrian materials (probably of the Nectaris and Crisium basins). The patch of lineated material that seems to embay the crater Taruntius M could be a tongue of Imbrium deposits.

Volcanic or tectonic interpretations are also unnecessary for the irregular craters. Secchi and Taruntius L, for example, previously considered endogenic and pre-Imbrian because of their shape and degradation (Wilhelms, 1972a), in fact resemble other large Imbrium secondary craters at comparable distances from the basin.

LOW ALBEDO OF SOME TERRA UNITS

In the Taruntius region and adjacent areas, the dichotomy between mare and terra that is distinct on

most of the Moon is blurred. Previous mapping vacillated between mare and terra-mantling designations for units having properties intermediate between typical wavy, textured, red, high-albedo terra material and flat, smooth, blue, dark mare material (compare the maps by Wilhelms, 1972a, and Wilhelms and McCauley, 1971). The proposed relation to Imbrium of the lineations and pits in the units with intermediate properties shows them to be of terra affinity. Thus the darkening is probably due to mantling by materials of mare affinity. The stereoscopic photographs (fig. 22) support the telescopically observed relation (Wilhelms, 1972a) that the flattest areas are the darkest and the rugged areas bright. This relation is consistent with superposition of a mantle upon the whole terra followed by shedding from slopes, as observed more clearly in Montes Haemus.

This hypothesis is supported by stereoscopic observations of dark materials that are blue on the color-difference photographs (fig. 16). Blue spots and streaks appear superposed on an otherwise red background, which includes both the main mare material and the dark and light terra materials. The blue materials appear to have flowed from Mare Tranquillitatis to Mare Fecunditatis across the intervening isthmus of terra

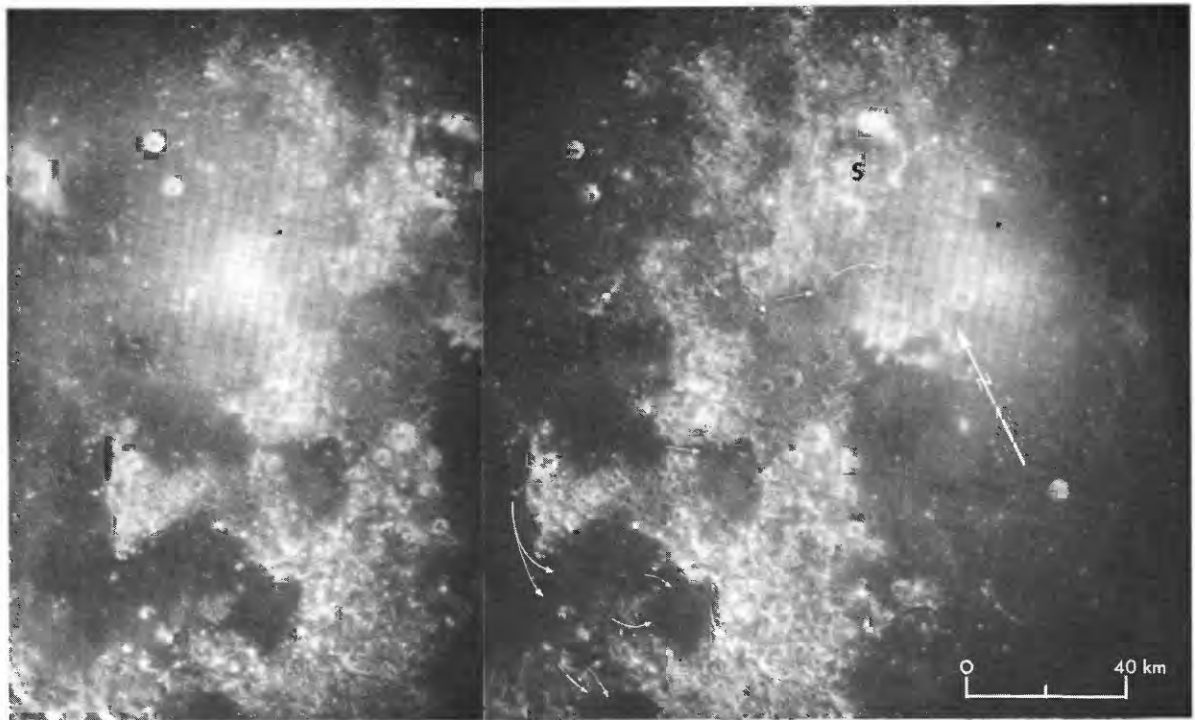


FIGURE 22.—Stereoscopic photographs showing southwestern corner of area of figure 21; S, crater Secchi. Arrows representing inferred flow directions of blue materials same as on figure 21. Parts of Apollo 15 mapping-camera frames 2409 (right) and 2411 (partial); sun illumination from right (east) 72° above horizontal in center right frame (that is, 18° from 0° phase angle).

(arrows, figs. 21, 22). Tranquillitatis is obviously higher than Fecunditatis; Defense Mapping Agency topographic orthophoto map LTO 61C4 shows a difference of about 200 m. The descent of the blue material occurs in a series of steps and cascades. In places it forms smooth surfaces that probably represent deep pools, while elsewhere it only thinly mantles the terra material, darkening it but leaving the various textures including rims of superposed craters still visible.

NORTHERN NECTARIS BASIN RIM

The overall terra topography north of Mare Nectaris is that of the pre-Imbrian Nectaris basin rim, but origins of the smaller features including diverse craters, irregular pits, and hills (figs. 23, 24) are less obvious. Most were previously believed to be volcanic (Elston, 1972; Wilhelms and McCauley, 1971) but are here interpreted as products of the impact of Imbrium basin ejecta. Non-Imbrium features include parts of the Nectaris basin and relatively few large primary impact craters. Stereoscopic photographs of the large (100 km) crater Theophilus (fig. 25) provide a guide to the Imbrium interpretations, as do further references to the Orientale analog (fig. 26). Mare and dark mantling materials are inadequately photographed, so are not discussed.

THEOPHILUS

Lunar impact craters and basins constitute a continuum of impact features that increase in complexity with increasing size (Gilbert, 1893; Baldwin, 1949, 1963; Stuart-Alexander and Howard, 1970; Hartmann and Wood, 1971; Hartmann, 1972; Howard, 1974; Hodges and Wilhelms, 1976). Therefore the generally accepted interpretations of crater features can be applied, with caution, to analogous but more complex and puzzling features of basins. The high, rugged central peak of Theophilus (fig. 25, A) probably formed by instantaneous rebound after impact in response to excavation of the crater, a mechanism advocated by many workers (for example, Baldwin, 1963; Milton and Roddy, 1972). The inner rings of basins may form in a similar fashion, enhanced in layered target materials (Hodges and Wilhelms, 1976; Wilhelms and others, 1977), although the origin of basin rings is problematical. Rolling plains (B) and hummocky material (C) on the crater floor are believed to consist mostly of impact melt because of their general resemblance to floor materials of the younger crater Tycho that preserve textures indicative of melt origin. The presence of abundant impact melt on floors of large craters supports interpretations of hummocky and planar material in Orientale as melt (Moore and others, 1974;

Head, 1974c; McCauley, 1977; Scott and others, 1977) and by extension, a similar interpretation of the Apennine Bench Formation advanced earlier in this paper. The wall terraces of large craters (D) indicate enlargement of the crater rim immediately after cratering. Hummocky parts of the Theophilus crater wall (E) are readily explained as slump features and are probably analogous to chaotic slumps identified along the Apennine front.

The Theophilus crater rim also resembles the Imbrium basin rim. Like the Apennine massifs, the immediate rim crest (fig. 25, F) is sharply uplifted, appears smooth at fine scale, and has a high albedo. The inner part of the rim flank is a massive, hummocky raised ring that terminates at an abrupt escarpment (G) at about 25 km or one-half a crater radius from the rim. Montes Apenninus has a similar distinct outer dropoff, although the raised montes is proportionally narrower—125 km wide as compared with a distance of 600 km from the basin center.

At the base of the escarpment (G) are pools of material apparently emplaced in a fluidlike state (H, I). The contacts of some pools are sharp, whereas others are gradational as if a widespread sheet of fluid covered the hummocky (presumably mostly clastic) ejecta (J) and pooled in depressions. These relations accord with studies of fresher lunar craters which indicate the plains-forming material is impact melt that flowed into place after deposition of the clastic ejecta (Howard and Wilshire, 1975). Cracked material interpreted as impact melt was noted on the Orientale (Moore and others, 1974) and Apennine flanks, but the abundance of these pools at Theophilus and other craters suggests that more may be present around the much larger basins than can be identified by cracks or other textures (Moore and others, 1974).

Outside the massive rim flank and the pools of impact melt are continuous deposits, secondary impact craters, and discontinuous deposits. Clearly these are formed by ejecta from the crater, but as noted their exact means of emplacement is controversial. The morphology of the ridged ejecta closest to the crater (K) could result from flow of primary ejecta along the surface. Close to it, however, the ridges form a herringbone pattern (L), demonstrated by laboratory experiments to result from the intersection of ejecta blankets of secondary craters that formed close together and nearly simultaneously (Oberbeck and Morrison, 1974). Closely spaced secondary craters with well-developed herringbone texture are evident farther out (M). Crater interference also produced blocklike rim intersections in places (N). Planar deposits that are gradational with the herringbone and that therefore probably consist of additional secondary crater

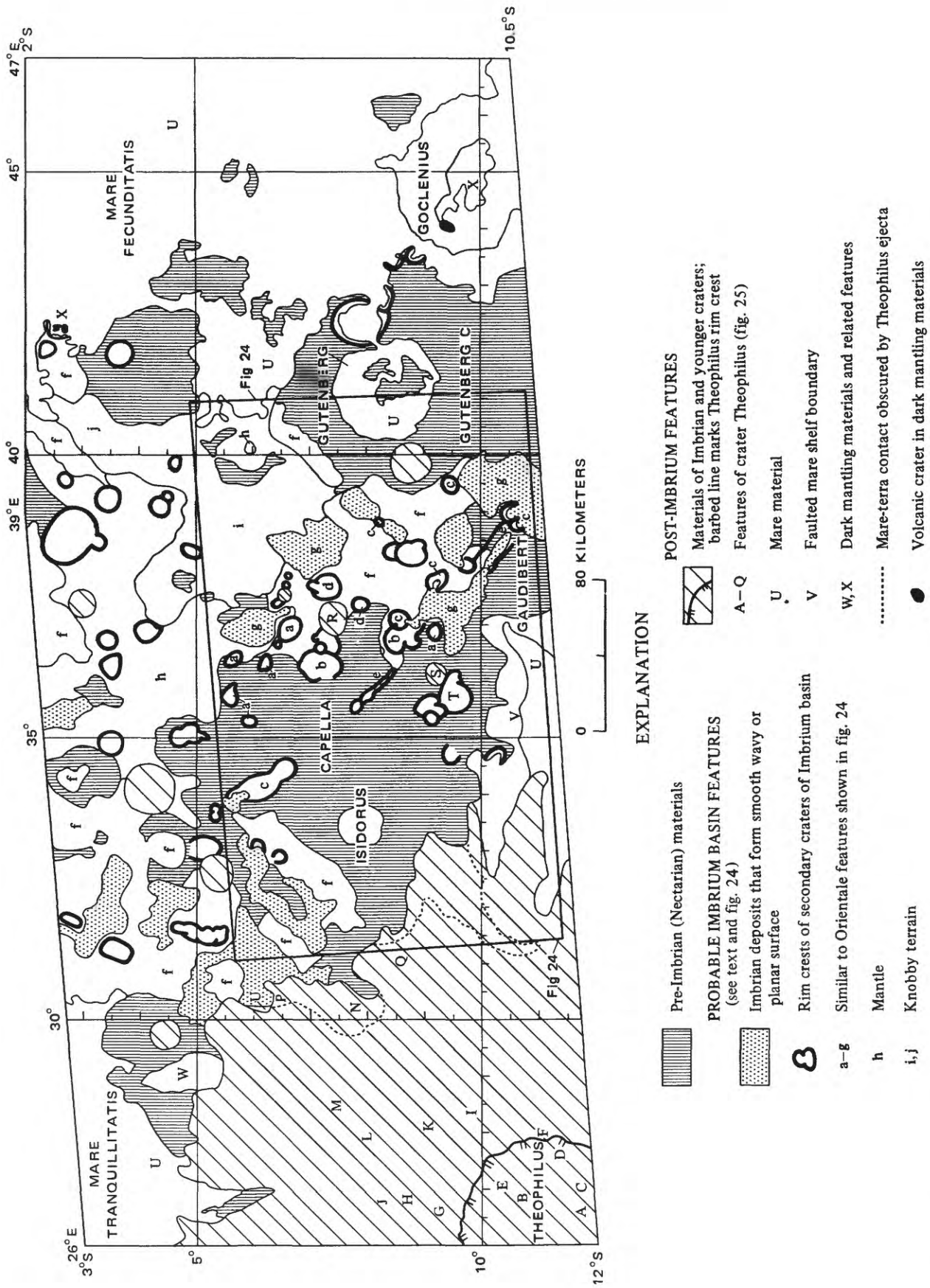


FIGURE 23.—Geologic map of the part of the northern Nectaris basin rim covered by vertical mapping photographs taken by Apollo 16. Principal sources of data: Apollo 16 mapping-camera frames 138-154, 416-433, 952-968, 1243-1258, 1636-1651, 1933-1946, 2156-2172, 2773-2787, 2930-2945. Lunar Orbiter IV high-resolution frames 72 and 77 supplemented the Apollo coverage.

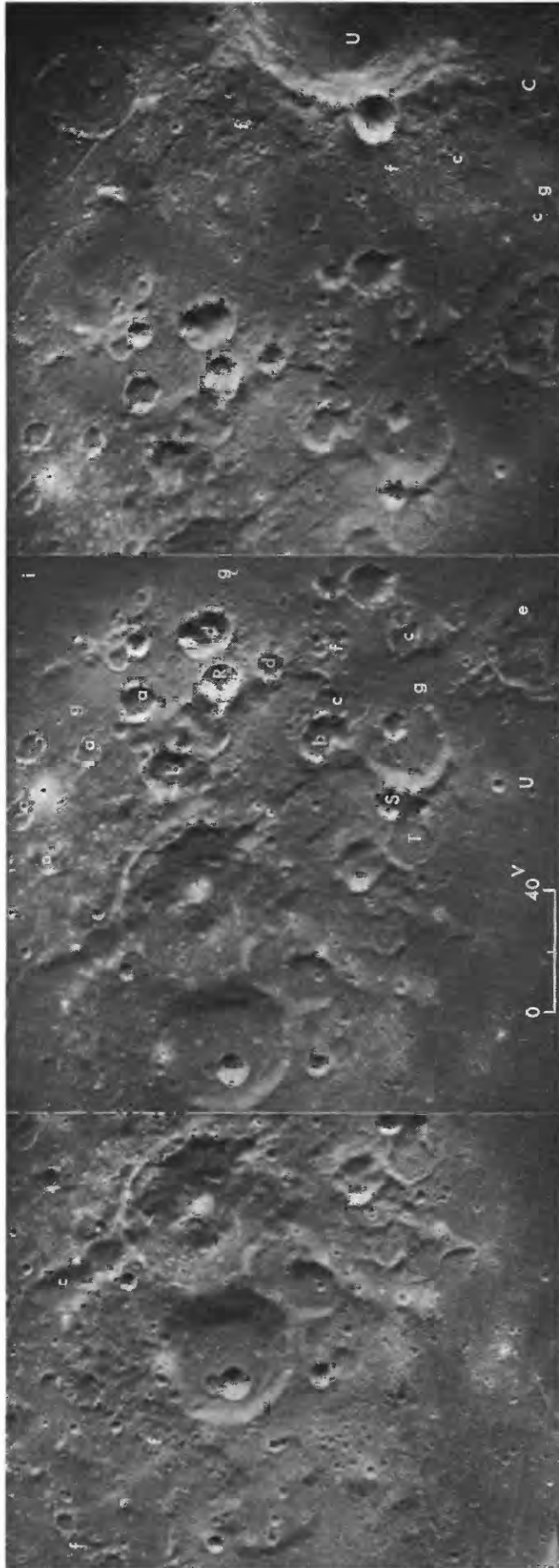


FIGURE 24.—Stereopairs of area outlined in figure 23. The large craters in the left two frames are Isidorus (left) and Capella (with central peak); part of mare-filled crater Gutenberg at right-hand edge (letter U in its mare fill). Letters designating features are the same as in figures 23 and 25: a through g have analogs in figure 26. Apollo 16 mapping-camera frames 422, 424, 426 (partial), right to left. Sun illumination from right (east) 37° above horizon in center.



FIGURE 25.—Stereopairs showing features of crater Theophilus. To right (east) of Theophilus is crater Mädler, 28 km diameter. Apollo 16 mapping-camera frames 427 (partial), 429, and 431 (partial), right to left. Sun illumination from right (east) 30° above horizon.

- | | |
|---|---|
| A. Central peak | J. Smooth ejecta, probably a coating of impact melt like (H) on clastic ejecta |
| B. Plains on crater floor | K. Radially ridged ejecta |
| C. Hummocky material on crater floor | L. Herringbone pattern of secondary craters |
| D. Wall terraces | M. Group of sharper secondaries with herringbone |
| E. Hummocky wall material | N. Closely clustered secondaries with rugged rim intersections |
| F. Raised crater rim crest | P. Thin mantle of material on mare surface |
| G. Massive hummocky crater rim one-half crater-radius wide | Q. Material similar to P but thick and bright enough to obscure nature of underlying unit |
| H. Pool of plains material (probably impact melt) at bottom of slope of (G) | |
| I. Another pool of probable impact melt, less cratered than (H) | |

ejecta are also present in this outer regime (P, Q). Hence there is clearly a general transition from predominantly primary ejecta deposits on the inner rim flank (G) to predominantly secondary deposits at the edge of the continuous Theophilus deposits (L-Q), but the exact point of transition is not known.

ORIENTALE ANALOGS

Many Orientale features in a comparison area 1,200 km from the basin center (fig. 26), proportional to the 1,800 km of the discussion area from the larger Imbrium, resemble outer Theophilus features and landforms superposed on the Nectaris rim. Just as sharply defined satellitic craters appear at about one crater diameter (100 km) from the rim crest of Theophilus (fig. 25, M), concentrations of conspicuous craters appear at about one basin diameter (930 km) from the topographic basin of Orientale (Montes Cordillera). Some Orientale satellitic craters are readily identified as secondary by their moderately shallow depths and irregular outlines (fig. 26; a), like typical Theophilus secondaries. Others are morphologically diverse and have been interpreted as primary impact craters of different ages (for example, Karlstrom, 1974). The diversity can be explained, however, by mutual interaction (Oberbeck and Morrison, 1974) and differential burial of secondary impact craters that formed nearly simultaneously (Wilhelms, 1976). For example, rims have interacted to produce linear septa between the craters (fig. 26, b). Similar interactions occur at Theophilus but are harder to detect because of the smaller scale (fig. 25, N). At Orientale the typical craters are converted into flat-floored craters through burial by deposits from the basin and from other secondaries (fig. 26, c); craters that are located in depressions or are otherwise susceptible to burial are more deeply filled than others. Coalescing craters form linear valleys (fig. 26, e) or small, diverse clusters (f). Very sharp craters that resemble primary impact craters could also be secondary to Orientale (fig. 26, d), perhaps formed by fragments that were ejected at high angles and impacted late, as proposed for craters at Tycho (Shoemaker and others, 1968). A random distribution of such high-angle impacts may explain the difference in crater density of two impact-melt pools at Theophilus (fig. 25, H, I).

Orientale and Theophilus deposits are also similar. Ejecta ridges splay outward from the secondary craters of both, although the ridges are more linear at Orientale than the V-shaped herringbone of Theophilus. Smooth deposits at the distal ends of the secondaries are also probably secondary crater ejecta, local mate-

rial excavated by secondary impact of basin ejecta and redistributed in debris clouds (Oberbeck and others, 1974, 1975). Previously the extensive outer plains around Orientale (for example, fig. 26, g) and Imbrium were interpreted as volcanic, but the smaller analogous plains at Theophilus (fig. 25, P, Q) are unlikely to be coincidental mantles of post-Theophilus volcanic materials.

SECONDARY IMPACT CRATERS OF IMBRIUM

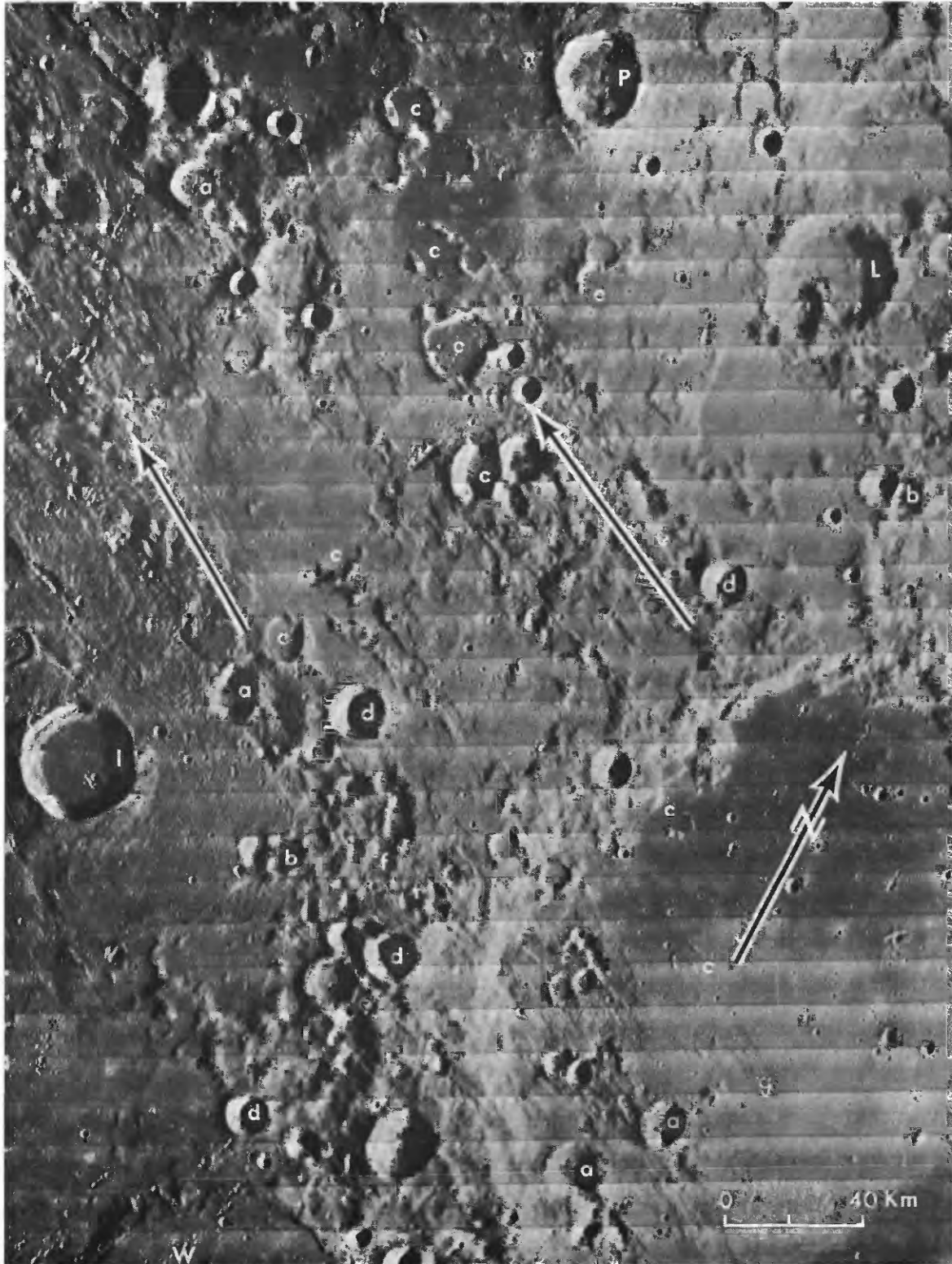
Central to the Imbrium study in this area is a group of diverse craters mostly between 10 and 18 km in diameter (figs. 23, 24). Their rim crests are subcircular or irregular in plan and range from subdued to sharp in profile. Some appear so sharp that the pre-Apollo 16 investigators thought that they were probably not Imbrium basin secondaries, although this possibility was recognized (Elston, 1972). Eggleton's (in Ulrich and others, 1980) interpretation that the diverse craters are Imbrium secondaries is supported by their similar sizes and shapes, their compound elliptical elements, and Imbrium-radial orientation of the compound craters, crater clusters, and accompanying lineations.

Although the overall appearance of the craters is similar enough to suggest a genetic relation, individual craters vary considerably in detailed morphology, and so the relation would not be suspected without the Theophilus and Orientale analogs. Some have typical secondary-crater morphology (figs. 23 and 24, a) as at Orientale (fig. 26, a), but morphologic variability of others led to interpretations as endogenic or primary-impact craters of different ages. Especially misleading was the interaction between crater rims (b) and the filling by deposits (c). Even sharp, deep, unfilled craters (d) once considered young primaries are now thought secondary because of their compound nature and associated Imbrium-radial lineations, although this origin is not certain either here or at Orientale (fig. 26, d). Linear valleys that resemble grabens can be formed by overlapping secondary craters (e).

Hills once considered volcanic can also be explained by secondary-impact mechanisms. The large compound crater (b) on the east wall of Capella (northwest of the post-Imbrium crater "R") has a rugged moundlike floor that may be formed by interaction of simultaneous craters, or perhaps by landslide of material from the Capella rim flank. Clustered craters or irregular pits of widely diverse morphology (f) are also probably secondary to Imbrium. These and the associated mounds and deposits were once interpreted as endogenic because of their morphologic complexity (Elston, 1972; Wilhelms and McCauley, 1971), but similar, better observed features at Orientale (fig. 26, b, f) were produced

by rim interactions. Intercrater septa are radial to Imbrium on the northwest flanks of Isidorus and Gutenberg (fig. 24, f). During nearly simultaneous impact of closely spaced, small projectiles, ejecta of the youngest

crater would have buried older craters and collected in depressions, accounting for the seeming inconsistency that secondary craters can be flooded by their own deposits.



DEPOSITS

Deposits of Imbrian age occur on much of the northern Nectaris rim. The northern part of the mapped area, consisting of plateaus, low hills, and depressions, is heavily to lightly mantled (fig. 23, h). Plains deposits appear transitional with the mantles (figs. 23, 24). A few have sharp contacts and are flat and smooth (fig. 24, g, at top center). In contrast, little or no mantle is observed on rugged terrain including the steepest massifs, a few crater rims, the vicinity of the craters Isidorus and Capella, and the terrain east of about 40.5°E. longitude (the farthest from Imbrium). The deposits are probably local materials that have been excavated and ejected from secondary impact craters as in the outer regime of Theophilus (fig. 25, P, Q) and Orientale (fig. 26, g). Abundant primary ejecta is unlikely to have reached this far from Imbrium by ground flow, because the Nectaris rim would have intercepted it. Therefore the deposits are probably ejecta from the secondaries or, perhaps, primary ejecta that arrived in comminuted form along ballistic trajectories (Chao and others, 1975). Imbrium deposits are treated more fully in the discussion of the region to the west.

A peculiar knobby or hummocky terrain (fig. 23, i, j) is also mantled in places (i) though it appears relatively fresh in a trough cut in the Nectaris basin rim (j). This knobby unit resembles the Alpes Formation of Imbrium and may be the equivalent Nectaris basin ejecta or Imbrium secondary ejecta blocked by the trough as observed at Orientale.

POST-IMBRIUM FEATURES

Post-Imbrium primary impact craters in the area, besides Theophilus, provide some information useful in interpreting crater landforms. The small primary impact crater Capella A (fig. 24, R) has a compound outline apparently due to collapse of part of its rim. The primary origin (and Copernican age) of Capella A is demonstrated by the line of small sharp secondaries to the southwest. Another presumed primary, Capella J

(S), was influenced by the pre-existing terrain; the wall of Capella J that formed against the large horseshoe-shaped crater is higher than the opposite west wall. When degraded, Capella J will probably look like two mounds—a high one on the horseshoe crater rim and a low one opposite. Thus both Capella A and Capella J mimic forms of secondaries.

The peculiar knobby or hummocky fill of the crater (T) next to Capella J may be ejecta from the neighboring Imbrium secondaries or from Capella J. Alternatively the raised, structured floor may result from crater floor rebound. Rebounded crater floors are common near mare boundaries (Pike, 1971; Schultz, 1976). Cylinderlike uplift may explain the unusual interior of the nearby crater Gaudibert (Brennan, 1975). Uplift along the mare border is also indicated by a small fault between the mare (U) and a higher shelf along the terra (V).

CENTRAL HIGHLANDS

The central location and good telescopic coverage of the tract described here have exposed it to scrutiny since the early days of lunar geologic research (Gilbert, 1893). The western two-thirds, closest to the Imbrium basin, is characterized by "Imbrium sculpture"—grooves and ridges radial to the basin that have been variously attributed to an "outrush of matter" from Imbrium (Gilbert, 1893; also Baldwin, 1949, 1963) or to Imbrium-related faulting or volcanism along faults (Shoemaker, 1963, p. 349; Hartmann, 1963, 1964; Wilhelms, 1970, p. F15; Scott, 1972a). Extensive plains deposits and various small hills or "domes" have been interpreted either as related or as not directly related to Imbrium. Part of the Fra Mauro Formation is in the western part of the area, and in the east is the Apollo 16 landing site, which was selected in the hope of sampling terra volcanic materials of the plains and of a peculiar hilly and furrowed terrane called the Descartes mountains (site selection history by Hinnert, 1972; Muehlberger and others, 1972). The discovery that these units are composed of impact breccias (Lunar Sample Preliminary Examination Team, 1972)

FIGURE 26.—Orientale secondary craters and basin deposits southeast of Orientale basin. North arrow (lower right) is on dark mare, and light plains fill of crater Schickard, about 190 km diameter. Left-hand arrows point to center of Orientale basin, 1,200 km from Schickard, a direction also indicated by obvious linear pattern of the terrain (ejecta deposits). a, typical well-formed secondary craters; partly filled by materials of the projectile or ejecta that flowed from nearer the basin. b, pairs of typical secondaries whose rim intersections are straight septa. Linear ejecta of the secondaries (a, b) has covered other secondaries "downstream" from the basin. c, degraded, irregular secondary craters filled by mare materials and by plains deposits composed of secondary or primary Orientale ejecta. d, four sharp, deep, conical craters that resemble primary impact craters but could be secondaries. e, linear valleys composed of overlapping secondaries. f, cluster of diverse small craters like a–d; all are probably secondaries. g, plains probably composed of ejecta of secondaries (a, f). Probable pre-Orientale primary impact craters are not numerous; besides Schickard they include Inghirami A (I), Lacroix (L), Piazzini C (P), and Wargentini (W). Central part of Lunar Orbiter IV frame 167–H; sun illumination from east (right) 17° above horizontal.

fundamentally altered the course of geologic investigations of the lunar terrae (Howard and others, 1974; Ulrich and others, 1980).

Like the terra east of Serenitatis, this tract lies at distances from Imbrium intermediate between the Apennine-Haemus region, dominated by Imbrium continuous ejecta, and the northern Nectaris basin rim and Taruntius regions, in which Imbrium secondary features are conspicuous. The morphology here, including a progressive change with increasing distance from Imbrium (west to east), is fully consistent with an Imbrium origin for most features, although details of formative processes remain to be clarified—in particular the origin of the Descartes terrane and the relative importance of primary and secondary (locally derived) Imbrium basin ejecta. The role of Orientale basin ejecta in the area is also under debate.

The descriptions and discussions of Imbrium-related features are keyed to the geologic sketch map (fig. 27) and the stereoscopic photographs (fig. 28) by means of 84 numbered localities ("loc."). The discussions progress by topic; the locality numbers progress roughly west to east. Features probably younger than Imbrium are lettered. Some of the lettered features and some of the pre-Imbrian terrain in the east are discussed only in the captions. Again, the Orientale basin (figs. 29, 30) provides essential support for the interpretations; an attempt to decipher the area by detailed scrutiny of its features without reference to Orientale proved unproductive.

GROOVES

The stereoscopic photographs of the area (fig. 28) and Lunar Orbiter photographs of the Orientale periphery (figs. 20, 26, 29) contain abundant evidence that the original ejecta explanation of the Imbrium-radial grooves (Gilbert, 1893) is more nearly correct than the later endogenic explanations. Most of the larger grooves consist of overlapping or coalescent elliptical or irregular craters and their ejecta that were undoubtedly produced by impact of ejecta from ballistic trajectories (fig. 27, heavy lines; figs. 28B, 28C, especially locs. 5, 31; figs. 26 and 29, e, h; fig. 31; Head, 1976). Very few faults were identified even tentatively in the entire mapped area (fig. 28, locs. B, S).

Other grooves are not craterlike or pitlike. At Orientale, many grooves and ridges were produced by flow along the surface of an apparently massive deposit (fig. 29, j, k, m, p, q; Moore and others, 1974). Some long and narrow grooves apparently formed where the deposit was free to flow rapidly (j) and grade to smaller grooves or to dunelike deposits transverse to the direction of flow where it was obstructed (k, p). The flow grooves are commonly deflected by subjacent topography (q).

Thus these grooves are part of the continuous deposit and are not secondary impact craters, although they may contain ejecta of secondary craters that has been caught up in the debris flow.

The distinction between ground-flow and ballistic grooves is harder to make in the Imbrium area than at Orientale because Imbrium is more highly degraded. Moreover, continuous-ejecta flow grooves and secondary impact crater chains commonly are juxtaposed by flow of the continuous deposit past or over the secondary features (fig. 29, r). Short, closely spaced, pit-like grooves radial to Imbrium that resemble secondaries pervade the area between about 10° and 18° east longitude (fig. 28D, locs. 64, 65), including the "furrowed unit" (Milton and Hodges, 1972) or "Smoky Mountain" facies of Descartes terrane (loc. 64) north of the Apollo 16 site. Some lineated high terrain is so far from the Imbrium basin that the grooves are presumed secondary (fig. 28D, loc. 70) as at Orientale (fig. 29, h). In most cases, Imbrium grooves are similar on diverse terrain (fig. 28C, locs. 34, 35, 37), and so their origin cannot be as readily established on the basis of interactions with pre-basin terrain as they can at Orientale. Hence, the distribution of flow grooves in the central highlands is uncertain.

SUBCIRCULAR IMBRIUM SECONDARY CRATERS

In the east and south parts of the central highlands, subcircular craters (fig. 28C, locs. 40, 43; fig. 28D, loc. 77) are more numerous than grooves. The craters resemble the Imbrium secondaries on the northern Nectaris basin rim and southern highlands (Scott, 1972b) but are somewhat more irregular, more highly modified by plains and mantling deposits, and more complexly intermingled with pits, hills, deposits, and other features once interpreted as volcanic (Howard and Masursky, 1968; Wilhelms and McCauley, 1971). As noted above, individual secondary craters in a cluster can vary widely in morphology (figs. 26 and 29, a-f) (Wilhelms, 1976). Younger craters overlap slightly older ones (fig. 28B, loc. 23). Ejecta cones interfere to produce ridges (Oberbeck and Morrison, 1974), and ejecta of the whole group is cast away from the basin, mantling downstream craters (figs. 26 and 29, southwest side of a and b; fig. 28C, locs. 40-43; fig. 28D, locs. 49, 73, 76). Both secondary and primary deposits collect in depressions (fig. 29, c, g, i), and if the depression is or contains a secondary crater, the secondary can be filled and thus look much older than its immediate neighbor (fig. 29, c; fig. 28, locs. 6, 8, 11, 18, 20, 26, 28, 39, 40-43, 46, 48?, 49, 50?, 58, 76). Late-arriving deposits that do not collect in depressions can also modify secondaries (fig. 29, r, s; fig. 28A, locs. 1, 3).

Small pits that may be late Imbrium secondaries appear to modify some larger secondaries (locs. 4, 6, 16?, 18, 49, 74), but few such pits are observed at Orientale. Degradation on slopes has contributed to the diversity among secondaries (locs. 17, 19, 42?, 77).

Intersection of adjacent coeval secondary crater rims can produce unusual landforms. A large hill at loc. 43 (fig. 28C) is typical of highland "domes" interpreted as volcanic (Wilhelms and McCauley, 1971). The craters were considered Imbrian or pre-Imbrian in age and volcanic in origin, and the hills were considered part of the igneous complex, inasmuch as no impact process could be thought up for them. However, an Orientale analog (fig. 30) which also has a laboratory analog (Oberbeck and Morrison, 1974, fig. 18) shows that such features do form by secondary impact (Wilhelms, 1976). Interactions of intersecting craters can also produce central peaks (Oberbeck, 1973). The deep central-peak crater Zöllner (fig. 28D, loc 71) resembles a primary impact crater but may have been produced by interactions of secondary ejecta (Eggleton, in Ulrich and others, 1980), as were other complex details of the Zöllner chain (loc. 72, 73, 74).

Internal origin was once regarded as the obvious explanation of the puzzling Müller complex of craters (fig. 28B, loc. 23) (Howard and Masursky, 1968; Wilhelms and McCauley, 1971). The three largest Müller craters have diameters and depths typical of Imbrium secondaries and are at the proximal end of a pair of Imbrium-radial grooves. The straight chain trending N. 65° W., however, makes such an obtuse angle with the Imbrium radial direction as to suggest a different origin. The chain has earmarks of a secondary chain including parallel lineations, overlap of craters from sharp to subdued, and accompanying smooth deposits. A source to the east-southeast is indicated, but no source of an appropriate age (late Nectarian or early Imbrian judging from morphology) lies in that direction. The chain is overlapped by or coeval with Imbrium-radial grooves, so an Imbrium-secondary origin is possible in spite of the alinement. However, internal origin is supported by alinement with the similar Abulfeda chain outside the area, which also lacks an obvious primary impact source.

OTHER POSSIBLE SECONDARY CRATERS

Many deep, topographically sharp, high-rimmed bright craters are of primary impact origin (for example figs. 27, 28 locs. A, C, R, and possibly L), but others may be secondary to the Orientale basin. This origin is suggested by the orientation of the clusters (F, N) and of the herringbone ejecta (N). Size, shape, freshness, and superposition on Imbrium features are also consis-

tent with Orientale origin although they do not exclude Imbrium origin (E, G, H, J, numerous craters a few kilometers across in the area of fig. 27A). The Orientale basin is centered 2,550 km west of the mapped area, comparable to the distance from Imbrium of similar though more subdued outer secondaries of Imbrium (fig. 24, a, b, d). Catena Davy (K) may be of Orientale origin (Oberbeck and others, 1975), although another possible source in the right direction and distance is the Eratosthenian crater Bullialdus. The larger compound crater Davy G (L) at the end of the chain, however, is too large to be of Bullialdus origin. Alternative origins are secondaries of Orientale and a multiple primary impact caused by tidal breakup mechanisms suggested by Sekiguchi (1970) and Aggarwal and Oberbeck (1974).

Secondary craters of the Imbrian crater Arzachel have played a troublesome role in the region. Howard and Masursky (1968), Carr (1969), and Wilhelms and McCauley (1971) believed that the herringbone ridge in the floor of the crater Alphonsus (M) was endogenic, but the Apollo photographs clearly show the herringbone and other features typical of a chain of secondary craters. Small, sharp craters superposed on other features are also possible Arzachel secondaries. Those in the Müller complex (fig. 28B, locs. 23, 24) were interpreted as volcanic (Howard and Masursky, 1968; Wilhelms and McCauley, 1971), and additional sharp secondary craters may complicate the stratigraphic relations and morphology in other crater groups (fig. 28B, locs. 20, 21).

Several degraded craters are believed likely Nectaris basin secondaries (figs. 27, 28, locs. 14?, 15, 48, 50) on the basis of membership in a group of subequal size (mostly outside the mapped area; see Lunar Orbiter IV photograph H-101) lying about one basin diameter from the Nectaris basin rim crest. However, the Nectaris origin of any single crater is difficult to establish in this Imbrium-affected region.

PRIMARY IMPACT CRATERS

When the secondary craters from all sources are subtracted, surprisingly few craters remain that might be of primary impact origin. Probable primaries younger than Imbrium and larger than 8 km are shown with the diagonal line pattern (fig. 27). The Orientale and Imbrium secondaries reduce the numbers of Imbrian and Eratosthenian primary craters once mapped here (Howard and Masursky, 1968). Twelve recognized probably primaries of Nectarian age have the diameters 21, 24, 30, 31, 32, 33, 36, 38, 47, 100, 115, and 132 km; no Nectarian primary craters smaller than 21 km were recognized. If they exist they are obscured by the

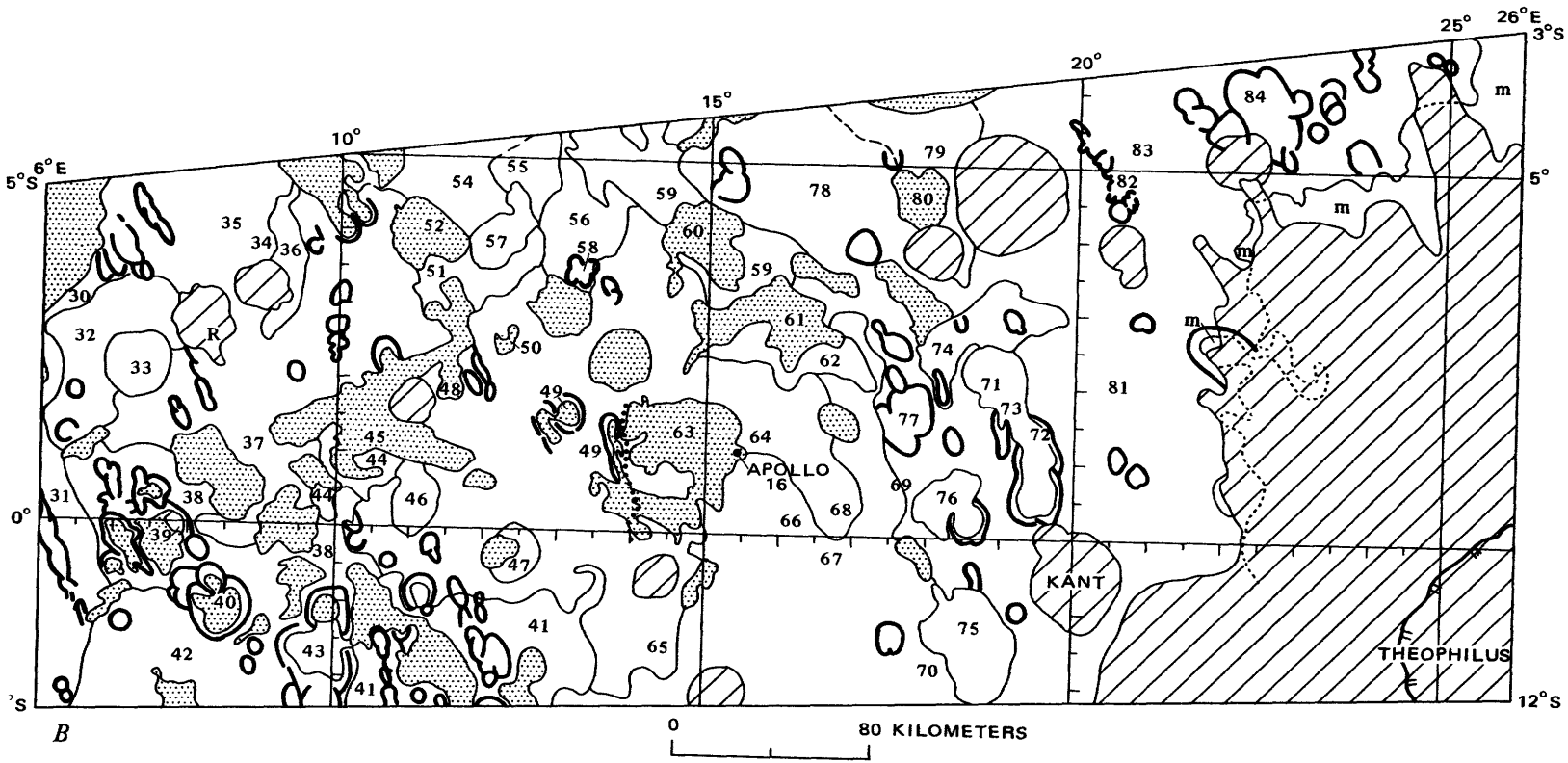
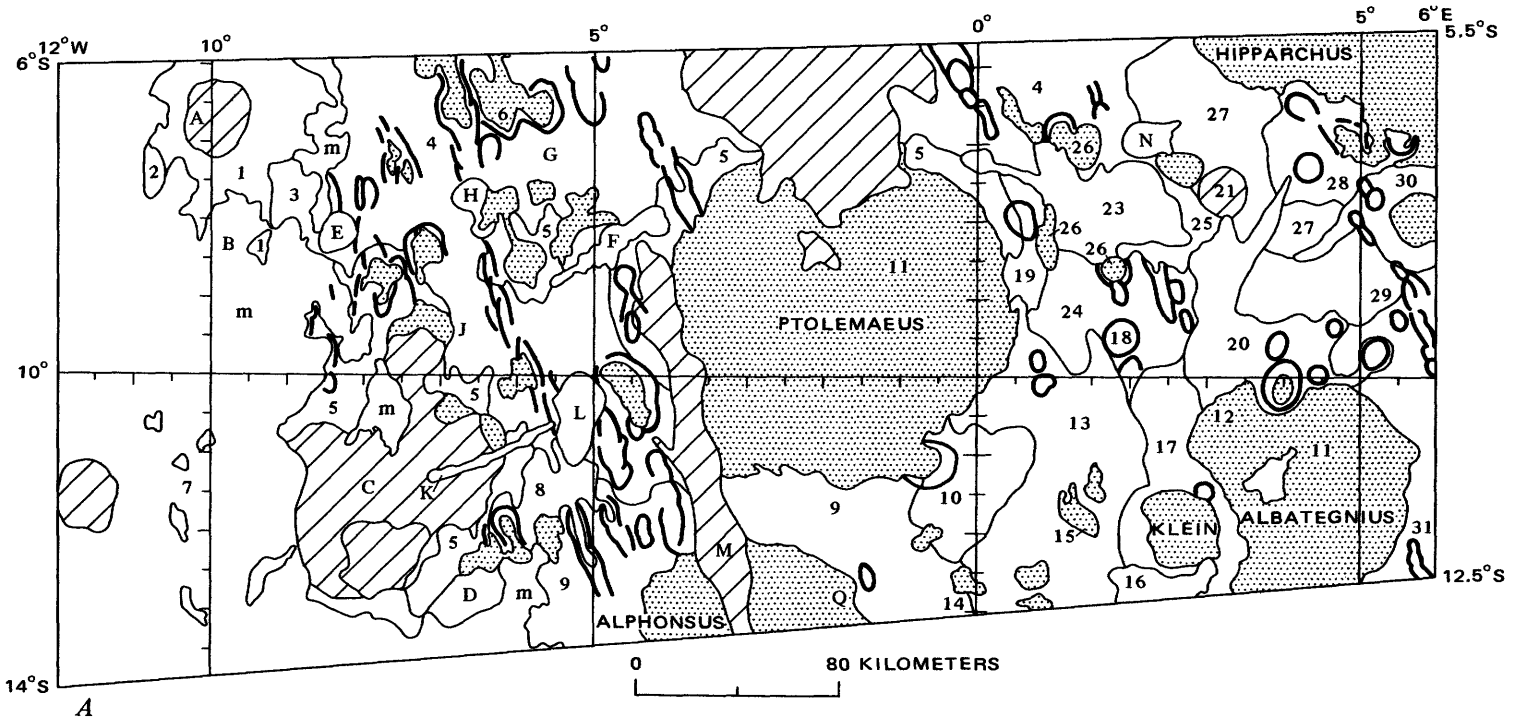


FIGURE 27.—Geologic map of the part of the central highlands covered by vertical photographs taken by the Apollo 16 mapping camera. Geologic symbols as in figure 23. Numbers and capital letters refer to geologic units or features cross-referenced to figure 28 except 14, 52–57 and 78–84, only on figure 27; 22 and 53 omitted. Numbers are concerned with the Imbrium basin; letters, post-Imbrium features. Principal sources of data: Apollo 16 mapping-camera frames 152–173, 430–449, 966–997, 1256–1288, 1650–1682, 1945–1977, 2171–2202, 2798–2819, and 2944–2997. Apollo 16 panoramic-camera frames 4553–4593, 4614–4676, 5371–5408 and Lunar Orbiter IV high-resolution frames 84, 89, 96, 101, 108 and 113 supplemented the Apollo mapping-camera coverage.

The following numbered and lettered localities also appear on figure 28 except as noted.

On figures 28A, B:

1. Thick-appearing hummocky deposits with no visible Imbrium secondary craters.
2. Smooth-appearing hill that may have been overridden by deposits.
3. Deposits and small secondary craters on elevated knobby terrain.
4. (Two localities)—large regions west, northwest, and northeast of Ptolemaeus. Mantling deposits with grooves visible on terrain of intermediate elevation, plains in the depressions. Much of area also finely pitted by more equidimensional craters.
5. (Six localities) The-highest terrain, strongly grooved, has few visible deposits.
6. Ragged, grooved, and mantled north-facing depressions that probably are Imbrium secondaries.
7. Islands in mare are grooved pre-Imbrian terrain like that of "mainland."
8. Extensive deposits in lows between secondary grooves.
9. Inner rim material of Alphonsus consists of small hills and Imbrium secondaries, aligned radially to Imbrium but less strongly than in locs. 5 and 6.

On figure 28B:

10. Southeast rim of Ptolemaeus has a fine knobby texture less strongly indicative of Imbrium effects than other nearby terrain.
11. (Two localities) Imbrium secondary craters buried by plains in the floors of Albatagnius (fig. 31) and Ptolemaeus.
12. Northwest-facing scarp in plains (fig. 31).
13. Sharp grooves on rugged terrain. Plains deposits have flowed to lowest accessible places.
14. Alphonsus B (not on photograph).
15. Elongate plains-filled crater degraded like loc. 6 but radial to Nectaris.
16. Numerous subcircular pits on wall of crater Klein apparently younger than the grooves of loc. 13.
17. Imbrium features on walls of Albatagnius and Klein blurred by downslope movement.
18. Circular crater (Albatagnius G) and irregular, smaller crater adjacent on southeast are probable Imbrium secondaries.
19. Rim of Ptolemaeus seems relatively unaffected by Imbrium here; Imbrium features possibly degraded by downslope movement.
20. Large group of subcircular craters, mostly Imbrium secondaries including Albatagnius B, the large elongate crater filled and embayed by plains. The sharper craters that extend to crater Hipparchus J (loc. 21) are radial to Arzachel and may be its secondaries.

21. Deep crater Hipparchus J of uncertain origin, probably a post-Imbrium primary or an Orientale secondary, older than the Arzachel secondaries(?) of loc. 20 group (22 omitted).

23. The Müller complex.

24. Small, equal-sized craters that continue from highlands to loc. 23, an orientation suggesting Arzachel as source.

25. Mantle superposed on Müller complex.

26. (Three localities) Level plains materials that overlie all craters including the Arzachel secondaries(?) of the Müller complex (loc. 23) and an Imbrium secondary that otherwise resembles loc. 18.

27. Wall and rim of Hipparchus has texture of smoothed-out pits.

28. Low interior of Hipparchus including some large Imbrium secondaries whose rims are degraded into rounded knobs and pitted and partly buried by later deposits.

29. Large, high, level area on which impact features are less distinct than the nearby Imbrium grooves.

On figures 28B, C:

30. Sharply grooved north-facing slope of about 6°.

31. East rim of Albatagnius scored by a large groove-like chain of Imbrium secondaries (see also fig. 31).

On figure 28C:

32. Fairly level shelf between north-facing (loc. 30) and south-facing slopes on which Imbrium grooves are less conspicuous than on either slope.

33. Mounds in crater Hind consisting of Imbrium deposits or material dislodged from the walls by impact of Imbrium ejecta.

34. Imbrium grooves and deposits on lowland.

35. Similar grooves on Hipparchus rim.

36. Sharp furrow-like craters transverse to the Imbrium direction.

37. Strongly grooved terrain of variable slope.

38. (Two localities) Finely grooved texture representing playing out of primary or secondary ejecta flow (compare fig. 29, m).

39. Deeply filled secondary craters encompassing small hills presumably composed of ejecta (compare fig. 26, a–c; fig. 30).

40. Ritchey group of secondaries.

41. (Two localities) Thin, finely lined mantle on secondary craters.

42. Terrain that seems smoothed either by slope movement or secondary deposits.

43. Mound and other materials seemingly superposed on secondary craters (compare fig. 30).

44. Hills that are likely composed of ejecta which has been halted after ground flow.

45. Similar to loc. 44; higher proportion of plains.

46. Andèl M (Imbrium secondary?), filled by thick hummocky deposits.

On figures 28C, D:

47. Knobby deposits resting against wall of crater Andèl (Imbrium secondary or Orientale (compare fig. 29, p).

48. Complexity of the large smoothed-off crater suggests Imbrium or Nectaris secondary origin.

On figure 28D:

49. (Two localities) Degraded probable Imbrium secondaries pitted and filled by plains.

50. Plains fill a very degraded central-peak(?) crater formed either by primary impact or by a coalescence of Imbrium or Nectaris secondaries.

51. Thin mantle over hummocks.

FIGURE 27.—Continued

Outside photographic figures:

52. Thin mantle with some level plains (53 omitted).
 54. Seemingly scoured and mantled area, perhaps produced by a ground flow. Note: locs. 45, 51, 52, 54, and 55 are gradational.
 55. High terrain appearing scoured and thinly mantled.
 56. High terrain appearing scoured by flow of material along the surface.
 57. Bright hills that are pitted and look "clean" as if overriden by deposits.

On figure D:

58. Probable secondary craters with knobby rim intersections; filled by plains in spite of high elevation.
 59. (Two localities, one off photographs) Knobby and planar deposits. Faint grooves suggest ground flow of ejecta.
 60. Similar to loc. 59, but with more plains deposits and fewer knobs.
 61. Patch of plains material with northeast-southwest lineations (compare fig. 29, s).
 62. Thin mantle over hummocks.
 63. Plains at the Apollo 16 site.
 64. Northern Descartes mountains; furrows aligned radial to Imbrium.
 65. Large area similar to loc. 64 west of the crater Descartes. Depressions in this terrain are filled by plains material.
 66. Jumbled hills and furrows of the southern Descartes terrane.
 67. Heavily furrowed parts of the Descartes mountains (hilly unit) resting on rim of crater Descartes. The crater bottoms are quite unfilled by plains, unlike loc. 65.
 68. Relatively uncratered parts of the Descartes mountains (subdued unit of Milton and Hodges, 1972).
 69. Pits like those of Descartes material on surrounding massifs.
 70. Rugged Nectaris basin massifs that have fine Imbrium-radial lineations.
 71. Crater Zöllner.
 72. Complex chain of large probable Imbrium secondaries superposed on Zöllner.
 73. Deposits in Zöllner group of craters.
 74. Small secondaries have impacted the north rim of Zöllner and produced a knobby texture (compare loc. 9 and fig. 25, N).
 75. Morphology like loc. 74 on slope in southern part of depression; lineated deposit in flatter northern part.
 76. A fill similar to loc. 75 perched on a depression at high elevation; pronounced northeast-southwest lineation.
 77. Crater Zöllner D, likely of Imbrium secondary origin, overlain by small Descartes-type pits and partly filled by secondary ejecta or slump.

Not on photographic figures:

78. Taylor is believed to be a primary impact crater because of its central peak.
 79. Pitted terrain. Otherwise not much definite Imbrium effect is visible in this poorly photographed terrain.
 80. Mantling deposits that collected in the low afforded by a pre-Imbrian crater.
 81. Extensive terrain (basically the Nectaris basin rim) east of Imbrium features 71 through 74 over to the Theophilus ejecta has few visible effects of Imbrium except a few pits. The terrain appears gentle and smooth, probably as a result of a mantle of Imbrium deposits, but perhaps as a result of mantling and seismic shaking during formation of the large nearby craters Theophilus, Cyrillus, and Kant.

82. Very bright, sharp Imbrium secondary impact craters. These were previously interpreted as volcanic (Wilhelms and McCauley, 1971) because they seemed too young to be secondaries of Imbrium, but stereoscopic photographs (not shown) suggest that their brightness results from having formed on a scarp.

83. Low terrain has elongate secondaries and deposits.

84. Hypatia and other large secondary craters occur both on the high and low parts of the Nectaris rim. Shallow, small pits also occur on this smoothed terrain. The lowest part may be mantled by dark material of mare affinity.

POST-IMBRIUM FEATURES

On figure 28A:

- A. Lalande A has a large ejecta blanket and is deep so is probably a primary impact crater. Most of the sharp craters that make the adjacent deposit (l) look old are similar in density to those on Lalande A.
 B. Mare-type scarp that also cuts the terra. The southwest side is down.
 C. Davy is much shallower than other craters of its freshness and extent of detectable ejecta (which covers most of the adjacent plains). The floor probably has rebounded, a characteristic of many crater floors near mare-terra contacts (Pike, 1971; Schultz, 1976). Ejecta blanket partly flooded by mare.
 D. Flat area with albedo intermediate between that of terra and mare. Probably results from a very thin cover of mare material on light plains.
 E. Palisa T has an oval shape that suggests secondary impact origin. It is much sharper topographically than Imbrium secondaries in the vicinity and truncates Imbrium grooves; probably a secondary crater of Orientale.
 F. Large group radial to Orientale also sufficiently fresh to be Orientale secondaries. One member of group is filled by some plains.
 G. Three large (5-7 km) and numerous small craters that look like feature E or members of group F and are probably Orientale secondaries.
 H. Palisa C and a similar, smaller crater to the southeast look like the probable Orientale secondaries of features E, F, and G and are superposed on a scarp radial to Imbrium; at least the southern crater is embayed by plains.

J. Four or five craters that look like Orientale secondaries.

K. Catena Davy, a probable secondary crater chain.

L. The compound crater Davy G.

M. Linear herringbone chain is secondary to crater Arzachel.

On figure 28B:

N. A young-looking crater; compound and apparently has eastward-splaying herringbone ejecta suggesting Orientale origin (O and P omitted).

Off photographs:

Q. Volcanic dark-halo craters on floor of Alphonsus.

On figure 28C:

R. Hipparchus C is a primary crater seen stereoscopically to be so deep that it must have penetrated any Imbrium materials present.

On figure 28D:

S. Possible fault (dots) in terra, the only one observed in the area except feature B. However, mantling of pre-existing non-tectonic feature is also likely.

swarm of Imbrium secondaries, but regardless, the total number of Nectarian primaries here and elsewhere is smaller than commonly assumed. The same is true of pre-Nectarian primaries (such as Ptolemaeus and Hipparchus); many of the smaller craters once considered pre-Nectarian may be secondaries of Nectaris and Imbrium (fig. 28C, D, locs. 46, 48, 50, 71).

DESCARTES MOUNTAINS

The origin of the complex of hills, furrows, and craters known as the Descartes mountains (Milton and Hodges, 1972) has long been one of the puzzles of the area. They had been interpreted as hummocky ejecta of the Imbrium basin (Eggleton and Marshall, 1962), but subsequently, endogenic interpretations replaced this impact interpretation (Milton, 1968; Wilhelms and McCauley, 1971; Milton and Hodges, 1972; Head and Goetz, 1972) and led to selection of the base of the mountains as the Apollo 16 landing site (Hiners, 1972).

The returned samples are impact breccias (Lunar Sample Preliminary Examination Team, 1972), and the regional pattern discussed above shows that the landforms must have some relation to Imbrium, as originally believed. The reasons for the jumbled orientation of the furrows and pits and their intimate mixture and mutual superposition with hills in the "hilly unit" (Milton and Hodges, 1972) or Stone Mountain facies of the Descartes terrane (fig. 28D, loc. 66) are still problematical. Explanations include deceleration and jostling by movement of ejecta along the ground, as seen at Orientale (fig. 29, p; Hodges, 1972; Head, 1972; Hodges and others, 1973; Hodges and Muehlberger, in Ulrich and others, 1980), and Imbrium secondary craters superposed on Nectaris ejecta (Wilhelms, 1972d). Hodges and others (1973) proposed that a tongue of Imbrium ejecta moved down a trough that affords a relatively clear path from the Imbrium basin. Part of this deposit has flowed into the crater Descartes (fig. 28D, loc. 67). This interpretation is consistent with the observations of a complex of blocks, striations, mantles, plains, and scoured-looking hills (locs. 54–58) tentatively ascribed here to ground flow in the trough. Moreover, ridges transverse to the Imbrium radial direction (fig. 28D, locs. 61, 66, 76) could be "scum" built up by deceleration of deposits flowing along the ground from Imbrium. A similar feature in another area (fig. 28C, loc. 36) lies transverse to the Imbrium radial direction and might have formed by abrupt slowing of a ground-flowing deposit (loc. 34). Transverse features are common at Orientale (fig. 29, p), though some may not originate by deceleration (fig. 29, upper s). Pits in

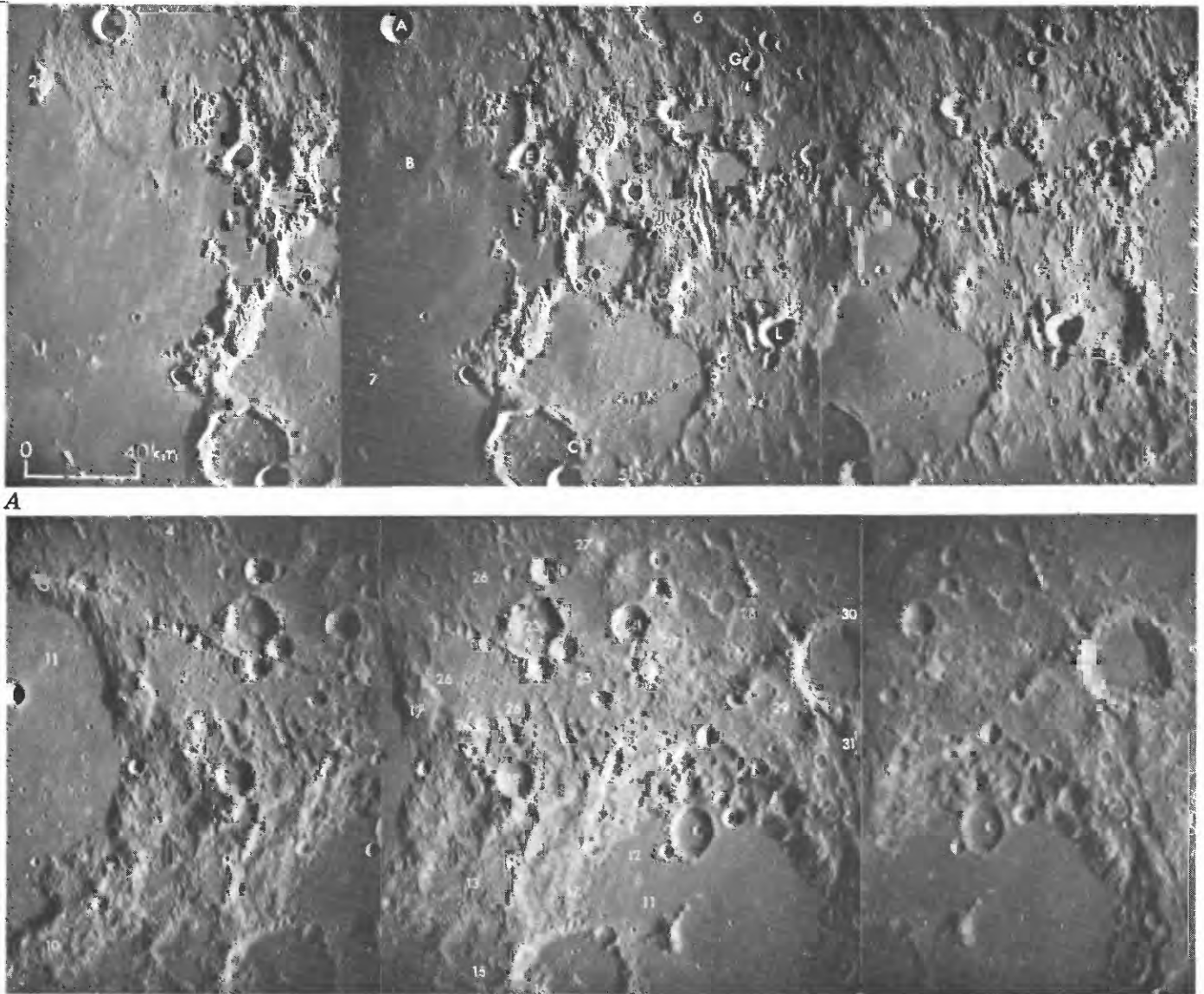
the proposed Descartes flow (loc. 67) do not contain plains deposits like those of the adjacent secondary fields (locs. 64, 65)—plains that are likely to be secondary ejecta, as will be discussed. The weight of evidence, therefore, supports the decelerated-flow origin for the Descartes mountains. However, this conclusion is tempered by the general observation that closely packed secondary impacts can produce a great variety of features and by the gradation of the Descartes morphology with a very likely secondary field (fig. 28D, loc. 64) which continues on high slopes (loc. 69).

OTHER HUMMOCKY DEPOSITS AND HILLS

Other thick-appearing deposits have stratigraphic or morphologic relations suggestive of massive flow along the surface from points nearer the basin. A thick deposit in Andél M (loc. 46) looks like a tongue of ejecta that demolished and flowed over the north rim of that crater and banked up against the south wall (Moore and others, 1974). Similar relations were observed in the crater Julius Caesar north of the mapped area (Morris, 1964; Morris and Wilhelms, 1967; see also fig. 29, p). Knobby deposits in Andél (loc. 47) and Hind (loc. 33) might also result from blocked surface flow. Furthermore, surface flow probably emplaced the large, apparently thick hummocky deposit in the northwest corner of the area (fig. 27A, loc. 1). This deposit has a rolling surface and includes small rather domelike hummocks. It resembles both the outermost terra of Montes Haemus described above, which lies at the same distance (1,350 km) from the center of the Imbrium basin, and the type area of the Fra Mauro Formation (see section on "Southern Oceanus Procellarum").

In addition to the "hummocks" in the deposits, small rounded hills occur in several places. Knobs that are surrounded by plains deposits have been given both "hot" and "cold" interpretations. The former include "volcano or surface expressions of intrusions" (Howard and Masursky, 1968; Wilhelms and McCauley, 1971) and eruptions from hot plains material (Eggleton and Schaber, 1972). "Cold" mechanisms include remnants of buried terrain (Howard and Masursky, 1968; Wilhelms and McCauley, 1971) and fragmental debris (Eggleton and Schaber, 1972), presumably entrained in the impact ejecta flow.

Igneous or quasi-igneous origin is not necessary to explain the hills. Many hills (fig. 28C, D, locs. 39, 44, 45, 59, 60) occur near grooves and apparently scoured surfaces (fig. 27, locs. 54–57), suggesting override by a ground-hugging flow. They might be transported blocks, but in the Orientale analog small hills are composed of ejecta that accumulated against obstacles (fig. 29, p) or in secondary craters (fig. 29, a, c; fig. 30).



B
 FIGURE 28.—Stereoscopic Apollo 16 mapping-camera photographs of part of the central highlands; sun illumination from right (east). A, frames 1676, 1678, 1680 right to left; sun elevation 15° in center. B, frames 1667, 1669, 1671 right to left; sun elevation 24° in center. C,

PLAINS DEPOSITS

In much of the area, rugged terrain is grooved or pitted by secondaries, and adjacent depressions are filled by smooth deposits (fig. 28, locs. 3-8, 13). Some deposits have nearly planar surfaces and appear at least moderately thick (locs. 11, 13, 15, 26, 39, 58, 61, 63); more commonly they have wavy surfaces but are thick enough to conceal Imbrium grooves and other structures (locs. 8, 28, 40, 43, 45, 48, 49, 51-54, 60, 75, 76, 80) or do not conceal underlying features but only "blur" them (25, 62, 68, 81). The planar and wavy deposits seem intergradational.

The prevalence of plains and the necessity to interpret the impact breccias sampled by Apollo 16 in typical plains deposits have led to considerable discussion of the origin of the plains. Imbrian-age plains material was first identified as an outer facies of Imbrium ejecta (Eggleton and Marshall, 1962; Eggleton, 1964, 1965) and later separated from the ejecta unit as the Cayley Formation to avoid premature interpretations (Wilhelms, 1965, 1970). Volcanic interpretations supported before the Apollo 16 mission by relations in Alphonsus (fig. 27, Q), where light plains and volcanic dark mantling materials seem intergradational (Carr, 1969; McCauley, 1969). Howard and Masursky (1968)



C



D

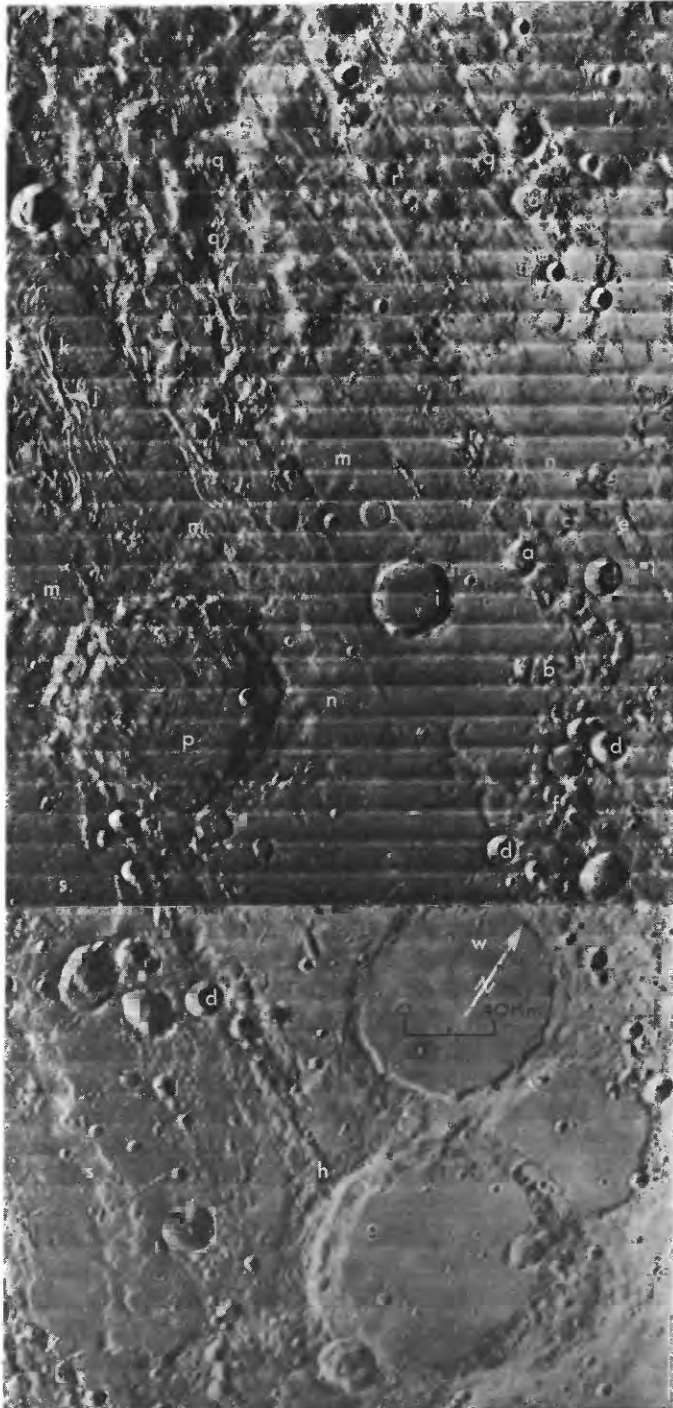
frames 1269, 1271, 1273 right to left; sun elevation 21° in center. *D*, frames 0437, 0439, 0441 right to left, sun elevation 18° in center. See figure 27 caption for explanation of symbols.

and mappers of other areas (summarized by Wilhelms, 1970) recognized the gradation of the plains with mantling material on adjacent higher ground and interpreted the different topographic expressions as the result of ponding and differential compaction of a deposit that fell upon the entire area. Ash-flow tuff was the favored material because of its light color and propensity to differential compaction, though basin ejecta was not excluded (Howard and Masursky, 1968). Plains in the large craters Ptolemaeus, Albategnius, and Hipparchus transect the Imbrium grooves in the crater walls, a stratigraphic relation suggesting that the plains deposits are younger than the Imbrium

basin (summarized by Wilhelms, 1970). Probable Imbrium secondaries also formed inside the craters and were subsequently buried by the surface deposits (fig. 28, locs, 11, 28; fig. 31); Hodges and Muehlberger (in Ulrich and others, 1980) estimated a thickness of 200 m or less for the deposits. These superposition relations seemed more easily explained by volcanic than by basin-ejecta origins. Nevertheless, impact origins now seem required for most plains, as originally suggested (Gilbert, 1893; Eggleton and Marshall, 1962), although volcanism is still favored by some workers for lightly cratered deposits such as those in Albategnius (Neukum and others, 1975b).

It has been suggested that the stratigraphic hiatus implied by the transection of Imbrium sculpture and supported by counts of superposed craters on the plains and adjacent highlands (Soderblom and Boyce, 1972) and young ages of some plains (Neukum and others, 1975b; Boyce and others, 1974, 1975) was caused by deposition of Orientale ejecta on Imbrium ejecta (Chao and others, 1975; Hodges and Muehlberger, in Ulrich

and others, 1980). According to this hypothesis, Orientale deposits have "reset" the ages based on small-crater morphology and density. Some support for the idea was found in this study. Plains embay two craters that seem too deep and sharp to be Imbrium secondaries that close to the basin and thus could be post-Imbrium primary impact craters or Orientale secondaries (fig. 28B, locs. 21, N). Other possible Orientale secondaries were mentioned above including a peculiar pair, embayed by plains (H) and aligned along an Imbrium groove, that is sharper than most other Imbrium secondaries. A post-Imbrium age of some plains is also indicated by several level pools which are cratered by only very sharp, presumably young craters and which apparently embay Arzachel secondaries (fig. 28B, loc. 26). Such plains could be replaced by the Orientale or Arzachel secondaries. They could also be primary Orientale ejecta, because fine-grained ejecta might accumulate without significant cratering and re-ejection of local material (Morgan and others, 1974; Chao and



◀FIGURE 29.—Orientale analogs of many features in the study area. Part of Lunar Orbiter IV frame H-172. Sun illumination from right 16° above horizon. Overlaps with figure 26; letters a-g and w identify the same or similar features as on that figure. Letters l, o, t, u, and v omitted.

- a. Subcircular secondary craters
- b. Intersecting secondaries
- c. Subcircular secondaries flooded by smooth ejecta. These craters could be contemporaneous with a and b craters but were subjected to burial because of their location in depressions
- d. Apparent post-Orientale primary impact crater, but could be Orientale secondary
- e. Groovelike chains of overlapping secondaries
- f. Clusters of small intersecting secondaries
- g. Crater Phocylides filled with smooth deposits that are probably mostly secondary ejecta
- h. High crater rim scored by secondary grooves
- i. Inghirami A, a pre-Orientale primary crater that has survived with relatively little damage except floor flooding by sharp-bordered smooth ejecta
- j. (near upper left edge) Grooves formed within continuous, mostly primary ejecta by rapid flow along the surface
- k. Simultaneous basin-radial and transverse grooves and ridges formed by slowly flowing ejecta; obviously transitional with j
- m. Outer, finely lineated primary ejecta
- n. Smoother continuation of m
- p. Transverse ridges and furrows formed by rapid deceleration of ejecta as it encountered crater floor after flowing rapidly over wall
- q. Additional flow lineations deformed by underlying terrain
- r. Pits, probably Orientale secondaries, that have been overridden by ground-flowing ejecta
- s. (near lower left edge) Lobes of ejecta that have encroached on the secondary craters. Upper occurrence has transverse lineations apparently formed by burial of ridges
- w. Crater Wargentia (85 km diameter) filled with smooth secondary or primary ejecta to higher level than ejecta closer to basin

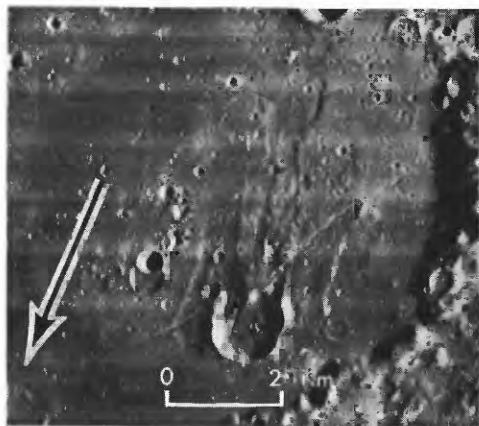


FIGURE 30.—Crater Struve L, 900 km northeast of Orientale basin (direction of arrow). The complex feature resembles loc. 43 (fig. 28) and is clearly of secondary impact origin. The hill that seems superposed on the crater rim was probably formed by interference of closely spaced impacts. Hummocky material in crater floor could be part of the crater-forming projectile or other ejecta that flowed into the crater from Orientale or from other secondaries. Part of Lunar Orbiter IV frame 174-H; sun illumination from right (east) 15° above horizon.

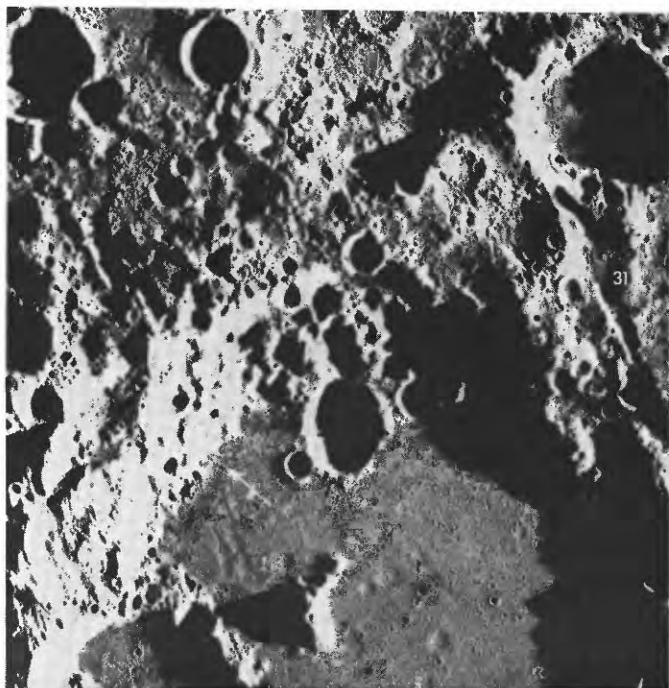
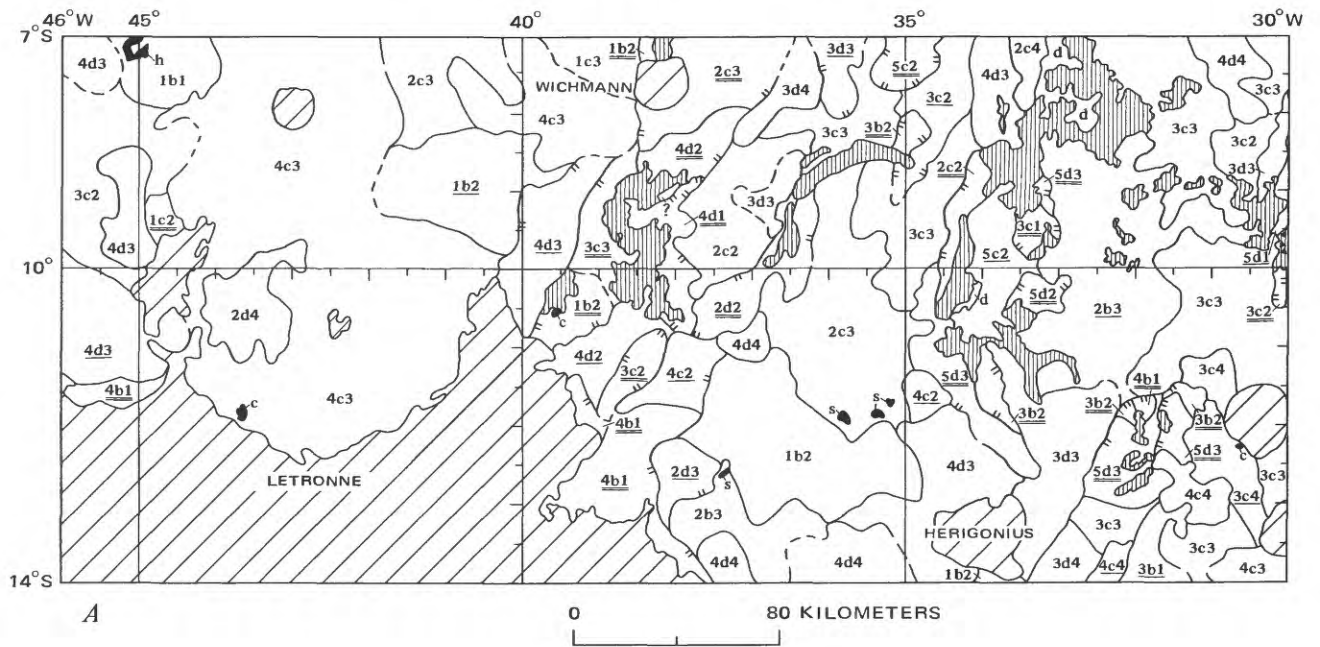


FIGURE 31.—Plains deposits in floor of crater Albategnius appear to have buried Imbrium secondary craters (11). Unburied secondaries are on rim (loc. 31). A ridge (arrow; loc. 12) may indicate marelike deformation or flow of plains material. Part of Apollo 16 mapping frame 449. Sun illumination from right (east) 5° above horizontal.

others, 1975; Hodges and Muehlberger, in Ulrich and others, 1980). Finally, seismic shaking produced by the Orientale impact might have smoothed the plains (Schultz and Gault, 1975).

Nevertheless, the concentration around Imbrium indicates that most plains deposits here must be of Imbrium origin (compare fig. 29, c, g, i, n, w). The stratigraphic gap can be explained as follows even if the entire stratigraphic section and not only the subsurface layers are of Imbrium origin. Except for the deposits in Albategnius (loc. 12, a marelike ridge possibly indicating deformation of a coherent plate) and similar deposits (loc. 26), the gap is not as great as suggested by the frequency counts, because most of the excess craters counted by Soderblom and Boyce (1972) on the highlands are Imbrium secondaries. The counted and buried (fig. 31) secondaries need be only slightly older than the plains to produce the observed age relations, as at Orientale (fig. 29, g-h); only a slight delay of ponding of Imbrium ejecta after formation of the sculpture is required (E. M. Shoemaker, oral commun., 1963). The late-arriving deposit may have been a gas-bearing or otherwise fluidized fraction of Imbrium primary ejecta segregated from the clastic, hummocky ejecta (Eggleton and Schaber, 1972) or a debris surge containing more secondary ejecta than primary ejecta (Oberbeck, 1975; Morrison and Oberbeck, 1975; Oberbeck and others, 1975).

Both primary and secondary ejecta probably compose plains material. Some of the Orientale smooth materials are outward continuations of the textured continuous deposits that presumably are heavily primary (fig. 29, n; Eggleton and Schaber, 1972; Hodges and others, 1973; Moore and others, 1974). The voluminous plains in Ptolemaeus, Albategnius, and Hipparchus and in the trough northwest of the Apollo 16 site, relative to adjacent secondary-pitted highlands, favors predominantly primary origin of these Imbrium plains deposits (Hodges and Muehlberger, in Ulrich and others, 1980). Farther from the basin, plains deposits are less extensive relative to the density of nearby secondaries and probably consist predominantly of secondary ejecta (fig. 28, loc. 65). At Orientale, plains are distal to secondary impact craters (figs. 26, 29, g; fig. 30) and are undoubtedly ejecta of those craters. Both the continuous ejecta and the secondary ejecta plains or Orientale fill secondary craters (fig. 29, c, s) and large depressions (fig. 29, g, w). Thus most plains are related to basins, but sources cannot always be determined because of the similar appearance of plains of primary and secondary-impact origin. Plains around both Orientale and Imbrium are concentrated where the primary regime gives way to the secondary impact regime.



EXPLANATION

- | | |
|---|---|
| <p>5d4 Mare units – Indicated by 3-component symbols, some with underlines; first component is a number indicating color: 1, reddest, 5, bluest; second component is a letter indicating albedo: b, bright, c, intermediate, d, dark; third component is a number indicating age: 1, oldest, 4, youngest. Single underline, probably thin; double underline, very thin</p> <p>d Dark mantling material</p> <p>h^sc Possible endogenic feature – h, hill or cone; c, crater or other depression; s, sinuous rille head</p> <p>▲▲▲ Very red terra</p> | <p> Materials of Imbrian and younger craters</p> <p> Plains material</p> <p> Fra Mauro Formation</p> <p> Probable Imbrium-basin secondary crater</p> <p> Pre-Imbrian crater and terra materials pitted by Imbrium basin secondary craters or smoothed by mass wasting</p> <p>----- Contact – Dashed where approximately located or inferred on the basis of a single property</p> <p> Inferred depositional mare contact along scarp – Ticks on high side</p> |
|---|---|

SOUTHERN OCEANUS PROCELLARUM

Both the terra and mare geology in this region are well shown by the Apollo 16 strip of photographs (figs. 33-35). The stratigraphically complex maria are mapped in the entire region that was photographed west of long 12° W. (fig. 32), and the relations among age, color, overall reflectivity, and thickness were studied in detail. The crater Letronne, an Imbrian-age crater 125 km in diameter, is the major structure in the west half of the mapped area (figs. 32A, 33; Marshall, 1961, 1963). Thin mare units (and mare ridges not mapped) partly trace its submare continuation, and its central peak is partly exposed. In the center of the area is Montes Rhipaeus (figs. 32B, 34; Eggleton, 1965),

which consists of several arcs that must be crater rim crests. Extrapolation of the largest arc gives a diameter of about 200 km. Mare Cognitum (the Ranger 7 impact site; Heacock and others, 1965) must be mostly a fill of this crater or basin. The terrae mostly continue the geological style of the central highlands described above, and only the Fra Mauro Formation and certain exceptionally red terrae will be discussed in this section.

FRA MAURO FORMATION

In the eastern part of the region (figs. 32, 35) is the peninsula that includes the craters Fra Mauro, Bonpland, Parry, and Guericke and the hummocky Fra Mauro Formation. North of the area are the type area

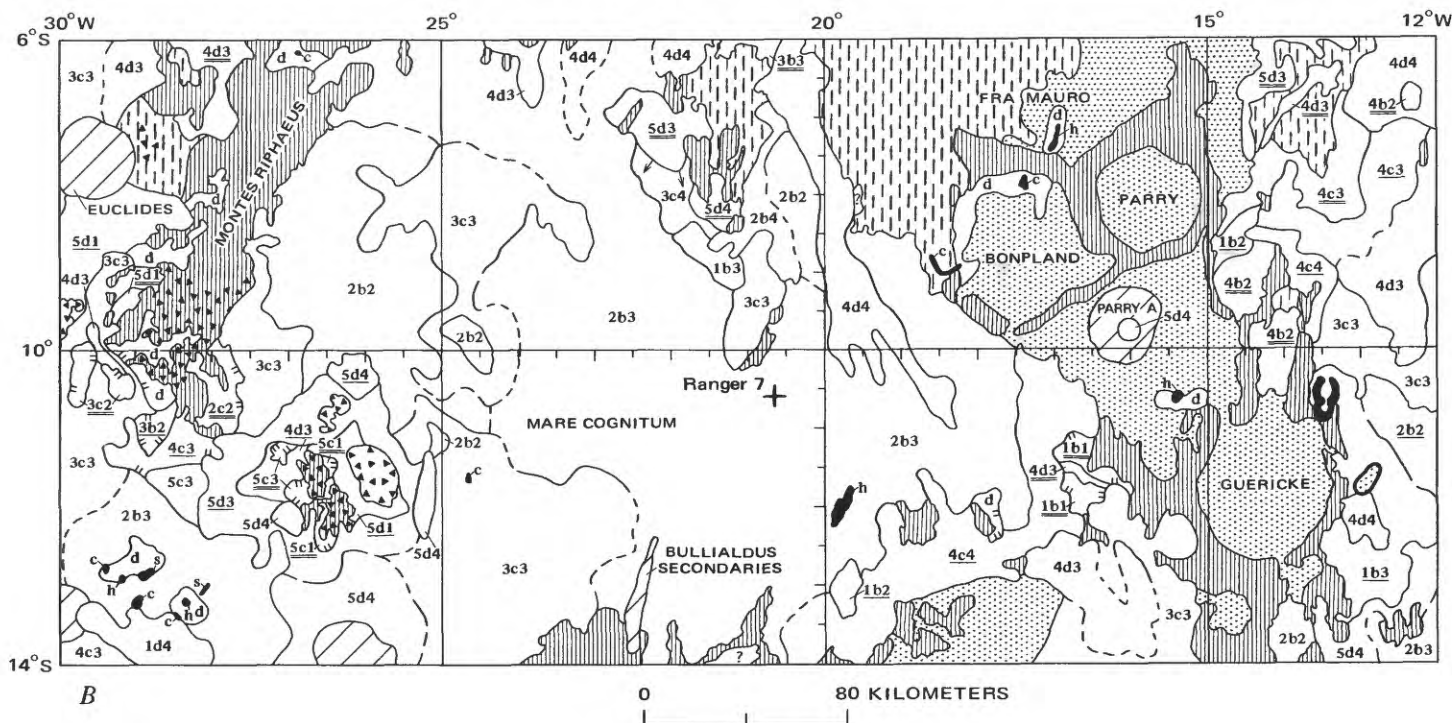


FIGURE 32.—Geologic map of part of southern Oceanus Procellarum. Based on Apollo 16 mapping-camera frames 1680–1689, 1975–1984, 2201–2216, 2816–2842, and 2972–2998.

of this unit (Eggleton, 1964; Wilhelms, 1970) and the Apollo 14 landing site (Eggleton and Offield, 1970; Sutton and others, 1972; Swann and others, 1972, 1977). The Fra Mauro here and the hummocky deposit in the northwest part of figure 28A (loc. 1) are similar and presumably are parts of the same stratigraphic unit.

Although the Imbrium basin origin of the Fra Mauro Formation is clear, the exact manner of emplacement and content of primary and local material are controversial. Early workers (Eggleton, 1964; Wilhelms, 1970) assumed that it is primary ejecta because it resembles continuous, radially ridged deposits of craters that appeared to consist of debris that flowed outward along the surface (for example, fig. 25, K). This conclusion has been disputed by Oberbeck and his coworkers (for example, Oberbeck and others, 1974; Morrison and Oberbeck, 1975; also Head and Hawke, 1975), who believe that local material excavated and redistributed in the ejecta of secondary impact craters should dominate the deposit. These workers believe that the ridges characteristic of continuous ejecta deposits of basins and large craters are formed by the interference of secondary crater ejecta.

Relations in the present area and to the east suggest that the original explanation is more likely than

ballistic emplacement. Ridges and grooves in the Fra Mauro are much less distinct than those in the central highlands, and no distinct secondary craters are visible either in the formation or nearer the basin. The deposits are more like the massive continuous deposits of Orientale closer to the basin (fig. 14), yet they are now adjacent to grooves, ridges, and craters of secondary origin (fig. 35). Thus the deposits probably flowed into the region from a point considerably farther north and therefore contain more primary ejecta than they would if formed by impact of ejecta where they now rest. They are likely to contain more primary material than the adjacent plains, which probably contain appreciable ejecta from the secondary craters on the pre-Imbrian crater rims.

MARE PROPERTIES

AGE

Four ages of maria (4, youngest; 1, oldest) were distinguished. The dating technique of Boyce and others (1974) based on the crater degradation model furnished ages of some of the largest units, but for the many small patches of mare material in this complex region, ages were extrapolated from well-dated units

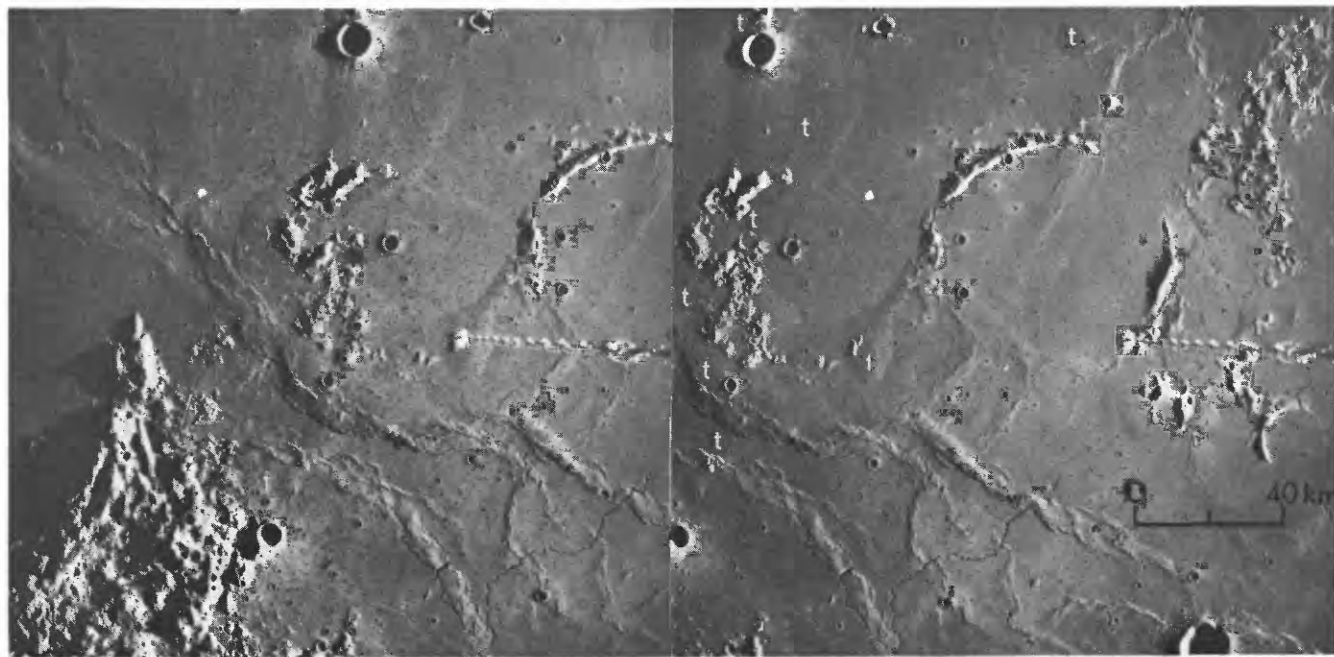


FIGURE 33.—Stereoscopic photographs of central part of area covered by figure 32 (left). Rugged terra at left (west) is east rim of pre-mare crater Letronne. Post-mare crater below scale bar is Herigonius. Abundant kipukas and shelves continue the terra features, probably parts of Letronne and an old basin (Wilhelms and McCauley, 1971), beneath thin mare layers (t—compare double underlines in fig. 32A). Apollo 16 mapping-camera frames 2837 (right) and 2839; sun illumination from right (east) 8° above horizontal in right frame and 6° in left.

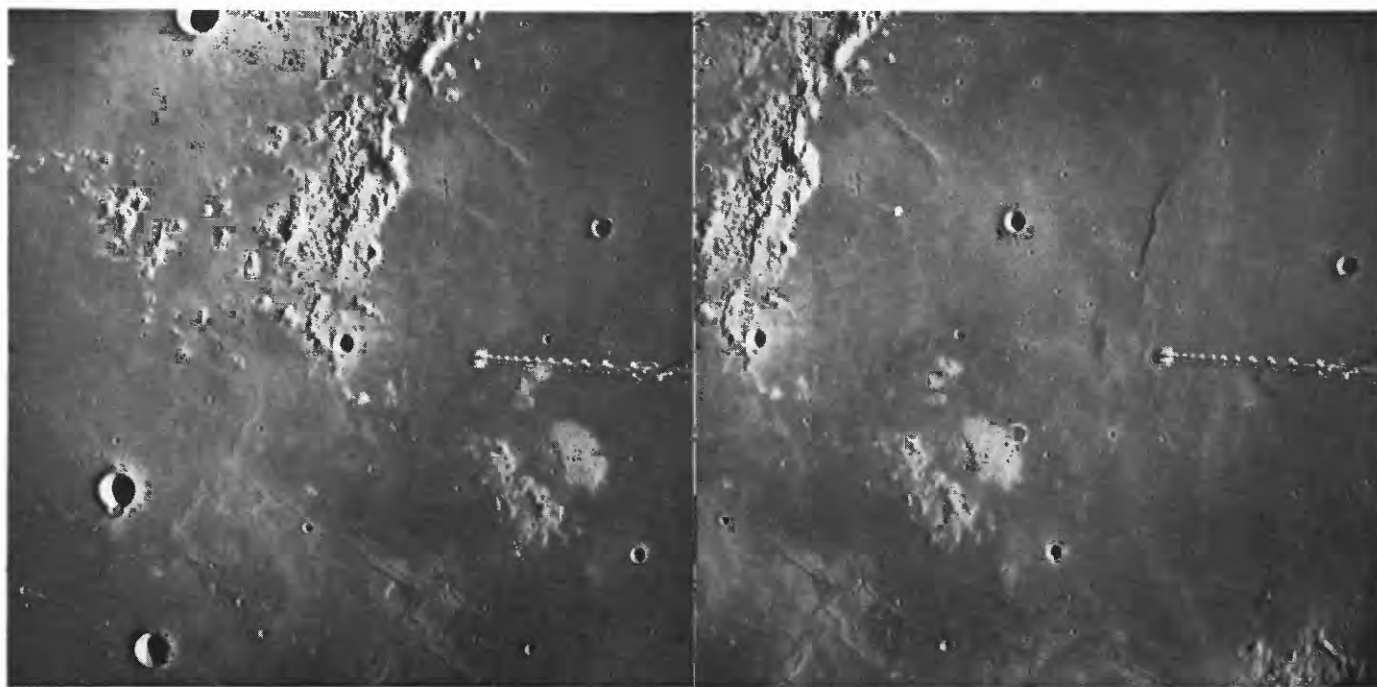


FIGURE 34.—Stereoscopic photographs of western part of area covered by figure 32B. Large, rugged terra feature is Montes Rhipaeus. Shieldlike feature is Darney Chi (D). Same scale as figure 33. Parts of Apollo 16 mapping-camera frames 2829 (right) and 2831; sun illumination from right (east) 17° above horizontal in right frame and 15° in left.

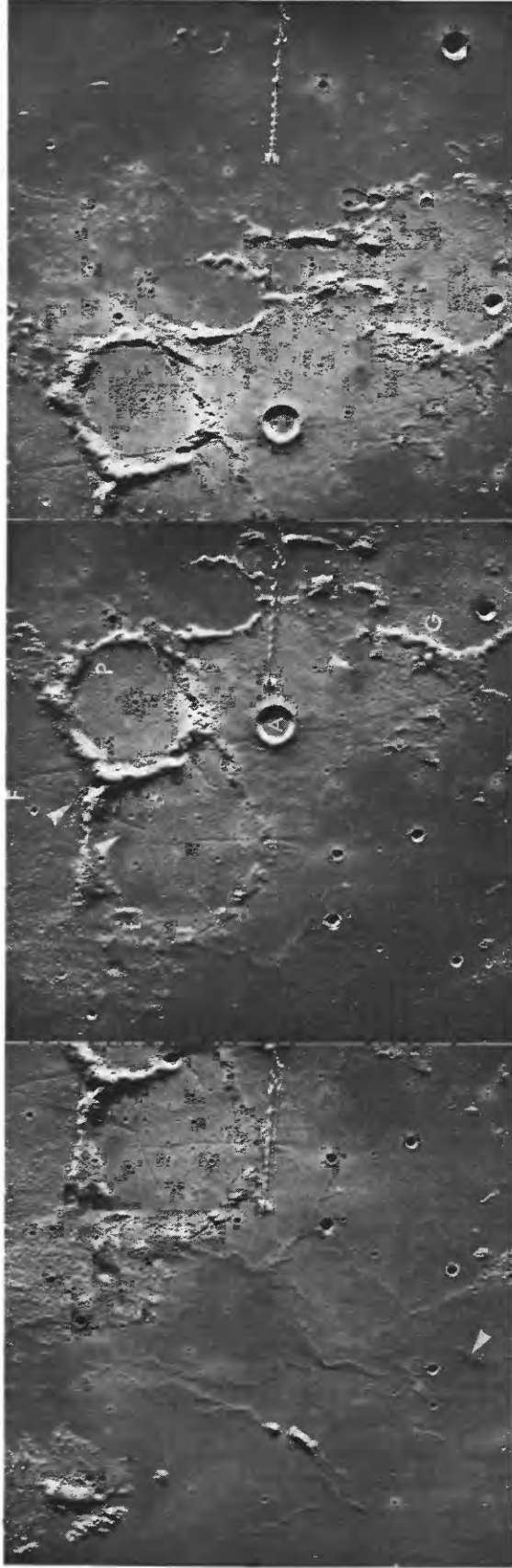


FIGURE 35.—Stereoscopic photographs of eastern part of area covered by figure 32*B*. The terra is informally called the Fra Mauro peninsula. Pre-Imbrian craters are Fra Mauro (F), Bonpland (B), Parry (P), and Guericke (G). Elongation of rims of flooded irregular craters between Parry and Guericke suggests Imbrium secondary origin. Fra Mauro Formaton fills much of crater Fra Mauro and buries an Imbrium secondary at (f). Possible volcanic features shown on geologic map (fig. 32*B*) are indicated by arrowheads. The volcanic features in the center frame could be the sources of the dark smooth materials that surround them; the dark materials thinly mantle the light cratered plains (Cayley Formation), which were once interpreted as older materials of the same type as the dark mantling materials. Imbrium mare-filled primary impact crater Parry A (A) is 14 km in diameter. Apollo 16 mapping-camera frames 2203, 2205, 2207 (right to left); sun illumination from right (east) 13° above horizontal in center.

elsewhere by means of estimated crater densities. Comparison with units mapped in northern Oceanus Procellarum and Mare Imbrium shows that age unit 4 is Eratosthenian (D_L 230 or smaller) and units 2 and 1 are Imbrian (D_L 265 or larger). For age unit 3, of the eight most reliable D_L measurements, two are 265, clearly Imbrian, and the other six are between 230 and 245, in the transition range considered to be either Eratosthenian or Imbrian depending on the weight of other evidence. Parts of age unit 3 apparently embay small Eratosthenian craters as do the northern Eratosthenian units, whereas other parts are older than secondary craters of the crater Bullialdus centered south of the map area, whose Eratosthenian age is shown by embayment by Eratosthenian mare materials and superposition on Imbrian mare materials. Thus age unit 3 probably includes both Eratosthenian and Imbrian materials.

COLOR

Five color divisions were recognized on the color-difference images supplied by E. A. Whitaker (fig. 36; Whitaker, 1966, 1972d). From relatively red to relatively blue, they are numbered from 1 to 5 in the geologic unit symbols.

These colors are primarily a mapping tool, but compositional inferences can be drawn from them if certain

assumptions are made. The pair of wavelengths (0.31–0.40 μm and 0.73–0.90 μm) used to construct the images is sufficiently close to the pair (0.40 and 0.56 μm) used by the remote-sensing group at the Massachusetts Institute of Technology to estimate titanium content of mature soils derived from lunar mare rocks (McCord and others, 1972, 1976; McCord and Adams, 1972; Charette and others, 1974; Pieters and McCord, 1975, 1976). The M.I.T. group relates titanium content to the slope of the curve drawn between those two points on their continuous spectra. Therefore the color-difference photographs are probably reasonable data from which to estimate titanium content of mare soils (Whitaker, 1972b; Zisk and others, 1977) provided the soils are mature and do not contain much pyroclastic glass or other variables.

The M.I.T. workers assume that all mare soils are mature—that is, they contain more than 70 percent of the glass-bonded impact-produced aggregates known as agglutinates, whose production is a function of time (for example, Charette and Adams, 1975; Pieters and McCord, 1976; McCord and others, 1976). As discussed below, this assumption is substantiated by the present study. Therefore, for soils derived from mare lavas, relatively red values (1, 2), which appear bright on the color-difference photographs, generally represent low titanium and blue (dark) values (4, 5) represent high titanium.

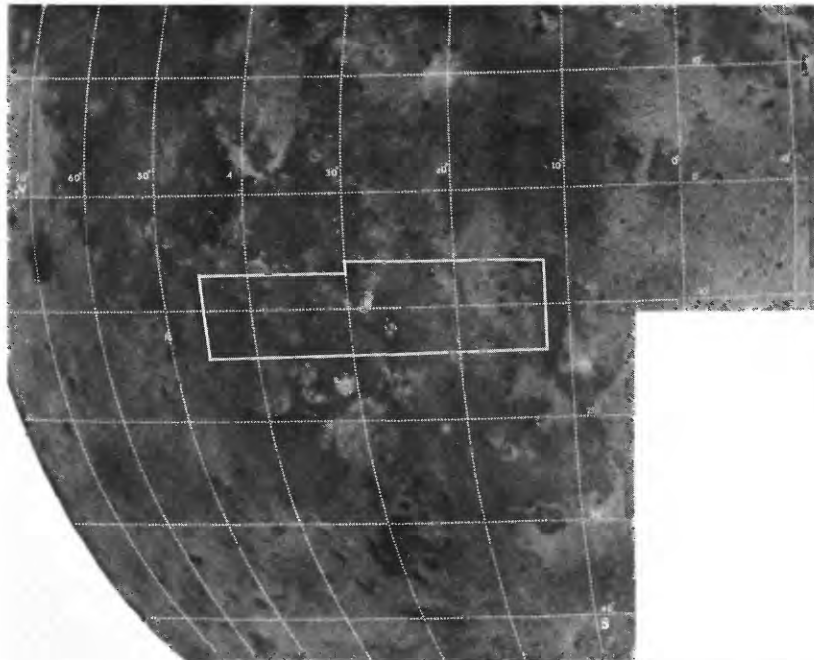


FIGURE 36.—Color-difference photograph of area mapped in figure 32 (outlined). Wavelength pairs are 0.31–0.40 μm and 0.73–0.90 μm . Dark is blue, bright is red. Courtesy of E. A. Whitaker (Whitaker, 1972 b, d).

"Blue" color does not always signify high titanium, however. Immature soils are blue in the wavelength pair 0.56 and 0.95 μm (McCord and others, 1976). Such soils are found on the walls of fresh craters and on other steep slopes where they have not had a chance to become mature because of continual reexposure of fresh material by down-slope movement. Many of the fresh craters in the present area appear blue on the color-difference images (fig. 36). Therefore some bluing effect due to freshness and not composition may be visible on the photographs and must be considered in drawing interpretations.

Soils with a high content of pyroclastic glass may show a different relation between color and composition than do mature mare soils in which most glass is agglutinitic. For the pyroclastic glasses, devitrification is more significant in determining color than is composition (Pieters and others, 1973; Adams and others, 1974; Zisk and others, 1977). For example, the very red and very dark color of the Aristarchus plateau may result from a mixture of one part fresh (orange) glass and two parts devitrified (black) glass of identical (high) titanium content (Zisk and others, 1977), whereas the blue color of the Apollo 17 mantle may result from a higher ratio of devitrified glass (Adams and others, 1974). The effect of pyroclastic glass on the soil colors in the present area cannot normally be distinguished from that of the lava compositions, but certain anomalies in the relation between color and albedo to be discussed do suggest the presence of pyroclastic glass in the soils of some units.

A few complete spectra are available from the southern part of the area (Johnson and others, 1973; Pieters and others, 1975). They confirm that unit 1b2 centered at lat 13° S., long 36° W., has low titanium content. The spectral region which shows as high in titanium covers several of the units mapped here but probably corresponds most closely with the blue units 4d4 and 4d3.

REFLECTIVITY

Three steps of reflectivity have been recognized qualitatively on high-illumination telescopic photographs and to some extent can be seen on the Apollo photographs (figs. 33–35). Almost all maria are darker than the terrae. A few spots in the terrae are darker than the maria (fig. 32, map symbol d; fig. 35). Most such spots are topographically uneven, suggesting that the terra is overlain by only a thin dark mantling deposit, probably pyroclastic. Many such deposits occur on or around probable volcanic craters, hills, or sinuous rille heads (fig. 35, arrowheads). All dark mantles so mapped that are large enough to be detected on the

color-difference images are blue, more like those at the Apollo 17 site than at Aristarchus.

Reflectivity of mare soils without pyroclastic material is generally agreed to be mostly a function of the iron and titanium content of the soil, although the exact nature of the dependence is uncertain (Gold and others, 1977). The M.I.T. group believes that the abundance of agglutinates made opaque and dark by titanium and iron is the controlling factor (Adams and McCord, 1973) whereas others ascribe much of the darkening to an increase in iron and titanium as coatings of other small soil grains as well (Wells and Hapke, 1977; Gold and others, 1977). In either case, soils darken proportionally to time of exposure as the agglutinates or coated grains (probably both) increase in abundance at the expense of the brighter crystalline rock materials, which have the same bulk composition as the lavas from which they are derived. Once maturity is reached, probably no further darkening occurs, and reflectivity of mature soil is a function of titanium and iron content alone. Steep slopes retain their brightness, regardless of the albedo of the source material, because exposure of fresh materials by downslope movement (Shoemaker and Hackman, 1962) is faster than accumulation of agglutinates or other dark soil grains.

THICKNESS

Thickness is a fourth variable which must be taken into account, because reflectivities and colors of thin units seemingly might be altered by contamination with underlying materials. Lateral mixing appears to be ineffective in changing color because many color boundaries are very sharp (Kuiper, 1965), but vertical mixing by impacts is evident in rays and could occur elsewhere. Thickness of the mare units can be estimated from their topography. Thin units are to be expected on shelves bordering terra, on rises that evidently are buried terra features, and in tracts where numerous small terra islands protrude through the mare surface (for example, fig. 33, t). Map symbols of units believed to be thin are underlined, twice if believed to be very thin (fig. 32).

Elevation is also a factor in estimating age. Old units commonly are elevated above young units on a shelf or a kipuka (Nichols and others, 1974). The young units have flowed into depressions that either remained after the old units were thinly draped on rolling topography or that were created by post-depositional subsidence or sagging of the old units, events that are indicated by fracturing of mare material on many of the kipukas. Scarps judged to be depositional are distinguished where possible from fault scarps (fig. 32). Other scarps not mapped here border the special mare structures

known as mare ridges and arches, whose origin is still uncertain (Strom, 1971; Colton and others, 1972; Young and others, 1973a; Hodges, 1973; Lucchitta, 1976).

CORRELATIONS OF MARE PROPERTIES

In order to determine their degree of interdependence, the four variables of age, color, reflectivity, and thickness are plotted against each other in six histograms (fig. 37). The histograms were constructed from a table of units (table 3) that in turn was extracted from the map (fig. 32). The vertical scale of the histo-

grams is an arbitrary one that considers both the areal extent and the number of patches of a unit. Each occurrence of a unit smaller than 1 square degree (900 km²) was given a value of 1. Each occurrence between 1 and 6 square degrees was given a value of 2, and each larger occurrence was given a value 3. Thus, separate occurrences have more weight relative to their area than do large occurrences. Patches that were considered isolated parts of another unit were not counted separately. This procedure was followed because separate eruptions were considered more significant to the volcanic history than voluminous eruptions.

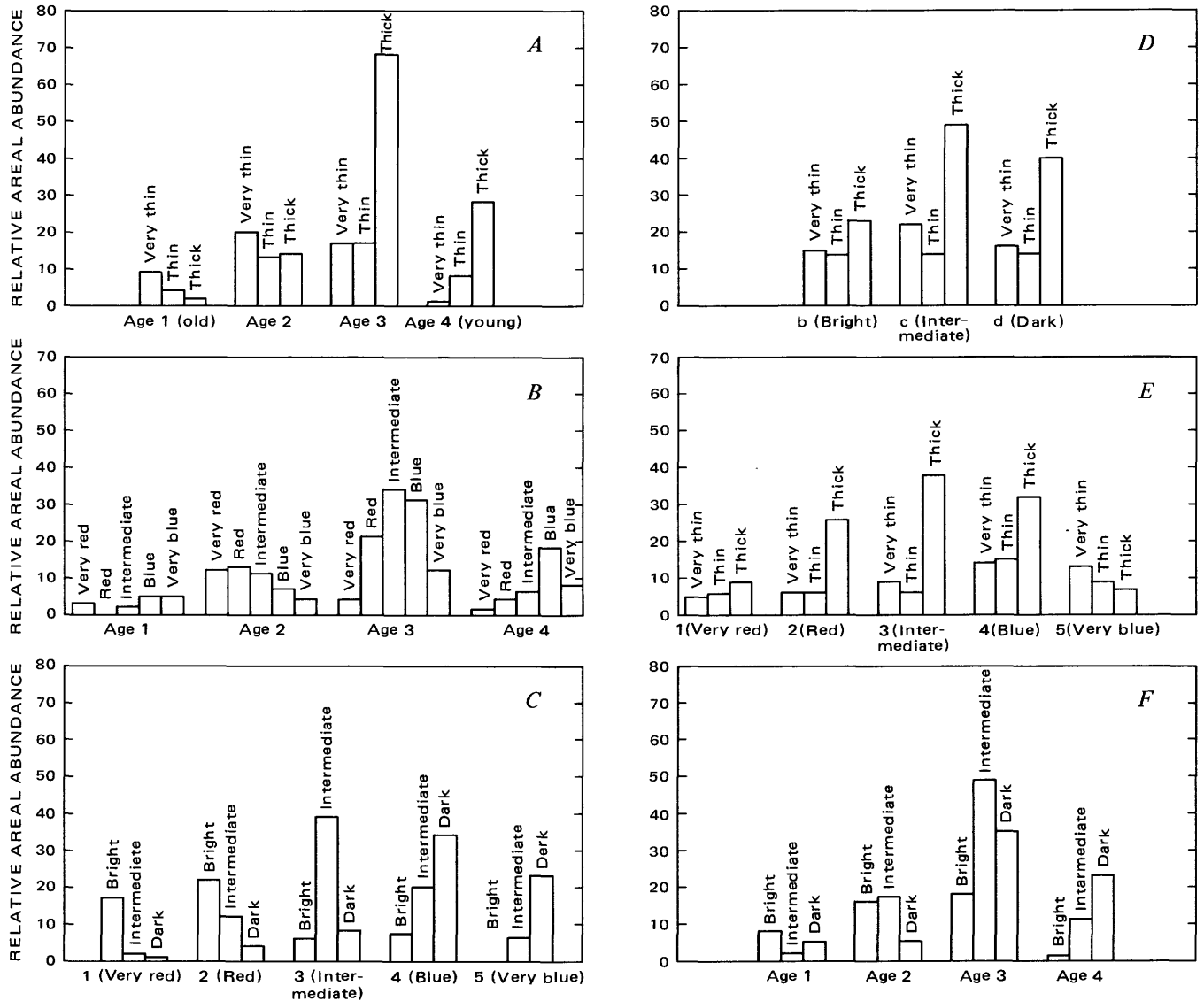


FIGURE 37.—Relations between pairs of mare soils in mapped area (fig. 32; table 3). Ordinate is a measure of areal abundance of mare units in arbitrary units explained in text. A, Age versus thickness. B, Age versus color. C, Color versus reflectivity. D, Reflectivity versus thickness. E, Color versus thickness. F, Age versus reflectivity.

TABLE 3.—List of mare units mapped in figure 32

[First symbol, a number, refers to color: 1, reddest; 5, bluest. Second symbol, a letter, refers to reflectivity: b, bright; c, intermediate; d, dark. Third symbol, a number, refers to age: 1, oldest; 4 youngest. Single underline, probably thin; double underline, very thin. Italic numbers after dash refer to relative abundance (see text)]

Color	Age	Reflectivity								
		Bright			Intermediate			Dark		
		Thick	Thin	Very Thin	Thick	Thin	Very Thin	Thick	Thin	Very Thin
1 (Very red)	4	-----	-----	-----	-----	-----	-----	<i>1d4-1</i>	-----	-----
	3	<i>1b3-1</i>	<u>1b3-2</u>	-----	<i>1c3-1</i>	-----	-----	-----	-----	-----
	2	<i>1b2-4</i>	<u>1b2-4</u>	<u>1b2-3</u>	-----	-----	<u>1c2-1</u>	-----	-----	-----
	1	<i>1b1-2</i>	-----	<u>1b1-1</u>	-----	-----	-----	-----	-----	-----
2 (Red)	4	<i>2b4-1</i>	-----	-----	<i>2c4-1</i>	-----	-----	<i>2d4-2</i>	-----	-----
	3	<i>2b3-10</i>	<u>2b3-4</u>	-----	<i>2c3-5</i>	-----	<u>2c3-2</u>	-----	-----	-----
	2	<i>2b2-5</i>	<u>2b2-2</u>	-----	<i>2c2-2</i>	-----	<u>2c2-2</u>	-----	-----	<u>2d2-2</u>
	1	-----	-----	-----	-----	-----	-----	-----	-----	-----
3 (Intermediate color)	4	-----	-----	-----	<i>3c4-2</i>	<u>3c4-2</u>	-----	<i>3d4-2</i>	-----	-----
	3	-----	-----	<u>3b3-1</u>	<i>3c3-26</i>	-----	<u>3c3-1</u>	<i>3d3-5</i>	<u>3d3-1</u>	-----
	2	-----	<u>3b2-1</u>	<u>3b2-3</u>	<i>3c2-3</i>	<u>3c2-1</u>	<u>3c2-3</u>	-----	-----	-----
	1	-----	<u>3b1-1</u>	-----	-----	-----	<u>3c1-1</u>	-----	-----	-----
4 (Blue)	4	-----	-----	-----	<i>4c4-1</i>	<u>4c4-5</u>	-----	<i>4d4-12</i>	-----	-----
	3	-----	-----	-----	<i>4c3-7</i>	<u>4c3-2</u>	<u>4c3-3</u>	<i>4d3-12</i>	<u>4d3-5</u>	<u>4d3-2</u>
	2	-----	-----	<u>4b2-3</u>	-----	<u>4c2-2</u>	-----	-----	<u>4d2-1</u>	<u>4d2-1</u>
	1	-----	-----	<u>4b1-4</u>	-----	-----	-----	-----	-----	<u>4d1-1</u>
5 (Very blue)	4	-----	-----	-----	-----	-----	-----	<i>5d4-6</i>	<u>5d4-1</u>	<u>5d4-1</u>
	3	-----	-----	-----	<i>5c3-1</i>	-----	<u>5c3-1</u>	-----	<u>5d3-3</u>	<u>5d3-7</u>
	2	-----	-----	-----	-----	<u>5c2-2</u>	<u>5c2-1</u>	-----	-----	<u>5d2-1</u>
	1	-----	-----	-----	-----	-----	<u>5c1-1</u>	-----	<u>5d1-3</u>	<u>5d1-1</u>

AGE VERSUS THICKNESS

Apparent thickness increases with decreasing age (fig. 37A), as expected from the exposure of old units on shelves and kipukas and the fill of the deeper basin centers and other depressions by the younger units. However, the old units also undoubtedly underlie the younger units in the deeper depressions, and so volumetrically, units of ages 1 and 2 might be at least as abundant as units of age 3. The dropoff in abundance in age 4, however, is clearly real, for there is nothing to bury the young units in this area.

AGE VERSUS COLOR

There is some change of color with age (fig. 37B). The oldest group (sparsely exposed) has more blue than red. Reds gain the ascendancy in age unit 2; each of the red categories is about equal to the intermediate color and to the two blues combined. In age unit 3, which has the most exposed materials, the increase is in the three middle colors; in total amount the extremes are as abundant as in age unit 2, although the proportions of red and blue are reversed. The balance in the three middle colors is also shifted to the blue. Age unit 4 is dominated by blue. This progression from dominance

by blue to red and back to blue is the same as the general pattern for the Moon as a whole (Soderblom and Lebovsky, 1972; Soderblom and Boyce, 1976), although it is neither pronounced here nor universally true for the rest of the Moon.

The fact that all colors are represented in all ages indicates that there is no strong purely age-related control such as impact cratering upon color. The changes with age must be a property of the erupted magmas.

COLOR VERSUS REFLECTIVITY

There is a good correlation between color and reflectivity (fig. 37C). Red mare units are bright; blue units are dark; intermediate color correlates with intermediate reflectivity. This correspondence accords with the inference discussed above that composition determines both color and reflectivity in mature, nonpyroclastic soils.

The correlation is even stronger than indicated in the histogram if certain exceptions are evaluated. The bright units of colors 3 (intermediate) and 4 (blue) are all thin (table 3). This may result from contamination by underlying bright terra materials or by fresh, immature materials that are blue. The single very red

unit that is dark is a pronounced anomaly, especially considering that the few reflectivities observed as intermediate for this color are questionable because of the small size of the units or position near rayed craters. The anomaly (unit 1d4), lat 13.5° S., long 28°–30° W., is very smooth and lies near several endogenic features. It could be pyroclastic as proposed for the Aristarchus plateau material that is also dark and red (Zisk and others, 1977). The dark units of color 2 (red) may also be pyroclastic (unit 2d4 in Letronne) or may overlie dark mare units that could contaminate them (unit 2d2 lat 10° S., long 37° W.). Abundant iron is another possible cause of exceptionally dark glasses (Johnson and others, 1973).

REFLECTIVITY VERSUS THICKNESS

A change of reflectivities by contamination is suggested by a plot of reflectivity versus thickness (fig. 37D). Thin and very thin units are more abundant relative to thick units in the bright class than in the other two reflectivity classes. This suggests a brightening by mixing with underlying terra materials.

Although red color and high reflectivity usually correlate, there are some bright units that are blue. As noted above, these blue units are all thin, and so their anomalously high reflectivity could be the result of contamination. Any brightening of the red materials that might occur by mixing could not be detected in the data, because soils derived from red lavas are naturally bright.

COLOR VERSUS THICKNESS

A histogram of color versus thickness (fig. 37E) tests whether colors might be changed by contamination as reflectivities seem to be. The thickness referred to is that of the total estimated mare section down to the terra basement; another mare unit could intervene between the terra and the surface mare unit.

Blue is the dominant color among the thin and very thin units, so the red color of terra units does not seem to affect the mare colors. In the Darney Chi region, some of the bluest material is superposed on some of the reddest terra material. Elsewhere, however, rays change the color of mare units (fig. 10), and so the absence of change noted here is probably due to the lack of sufficiently large impacts.

Thin and very thin units together exceed thick units for the very red and very blue color classes and are almost equal to the thick units for blue unit 4. For the very red units, this correlation is probably a result of the geologic circumstance that the old units remain exposed only where they were emplaced on terra

shelves and kipukas. Thin blue mare units in all age classes occur near terrae, however, as do the dark blue mantling deposits (which differ little in observed properties and possibly lithology from many of the materials mapped as blue mare materials). A possible genetic connection between blueness (high titanium content) and thinness, shallowness of source, or proximity to terra material needs to be further explored.

AGE VERSUS REFLECTIVITY

Low reflectivity had been thought generally diagnostic of young materials, as it indeed seems to be in Mare Imbrium (described above; Wilhelms, 1970), but many dark units are now known to be old because iron and titanium content and not age determine reflectivity of mature soils, as noted above. If soil maturity had not been reached in the age of exposure of the mare units in the present area, reflectivity should vary with age for a given color.

However, reflectivities show much the same trend with age (fig. 37F) that colors do (fig. 37B). This is to be expected in view of the strong correlation between reflectivity and color if soils are mature. There seems to be no other effect of age on reflectivity in the data. Moreover, no anomalously high reflectivities were discovered such as might be produced by other factors such as high feldspar content of the lavas. Therefore even the regoliths on the Eratosthenian units here are probably mature.

VERY RED TERRA

Almost all lunar terrae are redder on the color-difference photographs (fig. 36) than the maria, but some are exceptionally red. Very red areas here are part of southern Montes Rhipaeus, a few terra islands east of that area (fig. 34), and most of the terra material around lat 12° S., long 26° E., including the shieldlike feature Darney Chi (fig. 34; Wood and Head, 1975). These red areas are also very bright. Pieters and others (1975) showed that a feature near the mapped area similar to Darney Chi is compositionally distinct from other terrae (and that it is not red if its whole spectrum is considered). Malin (1974) suggested that the red areas may be pre-mare basalt relatively radioactive and high in potassium, rare earths, and phosphorus (KREEP).

If the Darney Chi plains are composed of old lavas, they would be the only nonmare volcanic lavas yet identified on photographs. They probably are of Imbrian age, as they seem not to be affected by Imbrium secondaries. The rugged highlands of the southern

Montes Rhiphaeus and the other red islands might have been mantled by fire-fountain equivalents of the lavas. Alternatively, both impact and volcanic rocks in the region may have formed from chemically anomalous materials with red color.

SUMMARY AND CONCLUSIONS

The Apollo 15, 16, and 17 mapping cameras photographed representative parts of the two most conspicuous features of the near side of the Moon, the Imbrium multi-ringed circular basin and the maria. Previous studies have shown that the basin is of impact origin and that the maria are composed of basaltic lavas. Limits set by the Apollo 16 samples and comparisons with the Orientale basin have led to the interpretations that most terra landforms in this region were produced by the Imbrium impact. Many of these landforms were previously ascribed to volcanism. The most significant new results for the maria concern their stratigraphic sequence. Working definitions are proposed for the Imbrian-Eratosthenian and Eratosthenian-Copernican system boundaries, and their absolute ages are estimated at 3.3 ± 0.1 and 2.3 ± 0.1 billion years or less, respectively.

IMBRIUM IMPACT

The Imbrium impact contributed more to the Moon's present appearance than any other single event. It uplifted Montes Apenninus, the Moon's largest mountain structure; emplaced masses of ejecta on the Apenninus flank and beyond; mantled, grooved, and cratered outlying highlands; and provided a large basin that was subsequently filled with lava.

Montes Apenninus was formed as part of the rim of the Imbrium basin—the edge of the excavation. Material ejected or thrust from the basin in low trajectories, perhaps without leaving the surface, was deposited close to the rim and formed imbricate blocks. Other more chaotic blocky ejecta may have been transported more violently. Some blocky ejecta of both types grades outward to lineated or smooth material that flowed along the surface, mantled elevated terrain, filled depressions, and banked up against obstacles. The deposits commonly mantle or fill secondary impact craters of Imbrium. These relations are consistent with models of ejection processes whereby ejecta travels outward in a conical curtain whose lower ejecta fragments are deposited first and nearest the basin rim and whose upper fragments, traveling much faster, impact later and farther from the basin. The outer, high-velocity ejecta produces craters larger than the impacting masses,

and the inner, slow ejecta accumulates as thick, continuous deposits that move outward behind the advancing ejecta curtain. Like all high crater walls, the Apennine front was modified by large slumps soon after ejecta deposition and before impact melt inside the basin solidified. Impact melt was also deposited on the mountain flank as it is on crater flanks.

The rest of the terra in the study area was also shaped by Imbrium ejecta, with an outward increase in the proportion of secondary to primary deposits and landforms as expected from the higher impact velocities of the outer ejecta. The complex topography of the interbasin terra east of Mare Serenitatis can be explained, without recourse to endogenic mechanisms, by the interaction of secondary or primary Imbrium ejecta with massifs and deposits of the Serenitatis and Crisium basins, whose structure in turn was probably inherited partly from older basins. Similarly, landforms and stratigraphic relations in the peninsula east of Mare Tranquillitatis, on the northern Nectaris basin rim, and in the central highlands were produced by impact of Imbrium ejecta upon Nectaris-basin deposits and secondary craters and widely spaced Nectarian and pre-Nectarian primary craters. Closely spaced secondary impacts, followed in favorable localities by a debris flow of mixed secondary and primary ejecta, produced most of the Imbrium features in the outer terra. The deposits are grooved, hummocky, rolling, or planar depending on the amount of material and the topography of the terrain over which they moved and on which they came to rest. Some lobes consisting largely of primary ejecta are believed to have flowed large distances from the basin. Certain large basin-radial ridges that were once considered tectonic are now believed to be composed of ejecta. Craters on the ridges and other places protected from the later deposits are sharper than simultaneously formed craters in depressions subject to burial. Inter crater septa, long ridges, grooves, peaks, "domes," and thin and thick deposits were produced by interference of adjacent secondaries and account for numerous landforms once considered volcanic. Groovelike chains of elliptical secondaries formed closest to the Imbrium basin, whereas sharp and degraded subcircular craters up to 30 km in diameter once considered primaries of various ages characterize the more distal terrain.

Non-Imbrium origin is possible for some terra features (besides primary craters) in the study area. Some plains seem to embay scattered Orientale secondaries or post-Imbrium primary craters in the central highlands and could have been emplaced by post-Imbrium impacts. A volcanic origin is not excluded for some plains materials. Certain exceptionally red terra materials of diverse morphology may also be volcanic.

MARE MATERIALS

In northern Oceanus Procellarum and southern Mare Imbrium, the stratigraphic sequence of mare materials and crater materials (from old to young) is: Imbrian System—(1) Imbrium basin, (2) crater Prinz, (3) reddish dark mantle of the Aristarchus region, (4) reddish mare material (two units), (5) crater Krieger, (6) mare material of intermediate color; Eratosthenian System—(7) crater Lambert, (8) crater Eratosthenes, (9) crater Timocharis, (10) bluish mare material, (11) crater Euler, (12) crater Delisle, (13) bluish mare material (two units), (14) crater Diophantus; Copernican System—(15) crater Copernicus, (16) crater Phytneas, (17) crater Kepler, and (18) crater Aristarchus.

The colors of the mare units (as seen on certain color-difference images) have been shown by other workers to result from the titanium content of the regolith derived from the lava. Blue colors indicate high titanium, red colors indicate low titanium. Thus the above sequence progresses from low to high titanium. Blue units older than this sequence occur along the margins of southern Serenitatis and northern Tranquillitatis, and young blue units are common in western Oceanus Procellarum. This has led to the suggestion that lunar lavas follow a general east-west progression in time from high titanium to low and back to high. A rough blue-red-blue progression applies to the detailed stratigraphy in southern Oceanus Procellarum, where thick red units of late Imbrian age fill the deepest depressions as in the northern basins. However, there are exceptions in all areas. For example, red mare as old or older than the blue occurs in Sinus Amoris, Mare Imbrium, and Oceanus Procellarum, and Eratosthenian red or intermediate-color materials occur in Mare Serenitatis, Mare Vaporum, and southern Oceanus Procellarum.

The proposal was made early that lunar surface materials darken with time, for crater rays fade with time and steep slopes, where relatively fresh rock presumably is exposed, are bright. This proposal plus the observed progression from bright to dark of lavas in regions like northern Procellarum and southern Imbrium led to the suggestion that the youngest mare lavas and dark mantling materials were always the darkest. The dark, blue lavas and the mantles along the Serenitatis-Tranquillitatis border were accordingly considered young until the Apollo photographs showed otherwise. Now it is believed that the darkening is caused by the production of dark glassy particles and coatings on other particles in the regolith at the expense of brighter crystalline rock fragments and that this darkening progresses only to a point of equilibrium. In mature regoliths, reflectivity is a function of

titanium and iron content. This relation seems confirmed by comparison of properties in southern Oceanus Procellarum, where reflectivity correlates with color for most units, indicating that soils are mature and that composition is normally the only determinant of reflectivities of mare regoliths. Departures from this relation may be due to pyroclastic (lava-droplet) particles or to contamination by materials of underlying units by cratering. Other workers have shown that anomalously low reflectivities of red mantling units, in particular, may indicate high contents of titanium- or iron-rich glasses in certain states of devitrification. Anomalously high reflectivities of some blue units (all thin) may be due to impact contamination from underlying, perhaps crystalline materials.

There is evidence that the early stages of mare formation included eruption of much pyroclastic material, some of which reached high elevations. Thick deposits of red and blue dark mantling material occur high on Montes Haemus along the Serenitatis border, thin blue mantles are common in all areas, a new red deposit was found on the Crisium basin rim, and the terra margins of all maria are darkened patchily in a way that suggests dark mantles were once abundant and have become inconspicuous only because of mixing with underlying terra materials by impact and downslope movement. Perhaps many small maria are merely accumulations in depressions or on flat surfaces of "fire-fountained" lava droplets.

Almost all conspicuous patches of dark mantling material surround or adjoin irregular craters, rilles, sinuous rille "cobra heads," cones, crater chains, or other features of undoubted internal origin. These features presumably were sources for the pyroclastic materials. Some of them occur at high elevations on the terra. Visible sources of lavas are much rarer. "D-caldera" in Montes Apenninus surmounts one of the highest known occurrences of mare material, a dome-shaped swell of young blue material. Other sources are inferred from the high level of certain pools of mare material, from which a steplike cascading to lower levels has occurred. Thus there is no common hydrostatic level of mare material.

REFERENCES CITED

- Adams, J. B., and McCord, T. B., 1973, Vittrification darkening in the lunar highlands and identification of Descartes material at the Apollo 16 site: Proc., Lunar Sci. Conf., 4th, Geochim. et Cosmochim. Acta, supp. 4, v. 1, p. 163-177.
- Adams, J. B., Pieters, Carle, and McCord, T. B., 1974, Orange glass: Evidence for regional deposits of pyroclastic origin on the Moon: Proc., Lunar Sci. Conf., 5th, Geochim. et Cosmochim. Acta, supp. 5, v. 1, p. 171-186.

- Aggarwal, H. R., and Oberbeck, V. R., 1974, Roche limit of a solid body: *Astrophys. Jour.*, v. 191, p. 577-588.
- Baldwin, R. B., 1949, *The face of the Moon*: Chicago, Ill., Univ. Chicago Press, 239 p.
- 1963, *The measure of the Moon*: Chicago, Ill., Univ. Chicago Press, 488 p.
- Boyce, J. M., 1976, Age of flow units in the lunar nearside maria based on Lunar Orbiter IV photographs: *Proc., Lunar Sci. Conf.*, 7th, *Geochim. et Cosmochim. Acta*, supp. 7, p. 2717-2728.
- Boyce, J. M., and Dial, A. L., Jr., 1973, Relative ages of some nearside mare units based on Apollo 17 metric photographs: *Apollo 17 Prelim. Sci. Rept.*, NASA SP-330, p. 29-26 to 29-28.
- 1975, Relative ages of flow units in Mare Imbrium and Sinus Iridum: *Proc., Lunar Sci. Conf.*, 6th, *Geochim. et Cosmochim. Acta*, supp. 6, v. 3, p. 2585-2595.
- Boyce, J. M., Dial, A. L., and Soderblom, L. A., 1974, Ages of the lunar near side light plains and maria: *Proc., Lunar Sci. Conf.*, 5th, *Geochim. et Cosmochim. Acta*, supp. 5, v. 1, p. 11-23.
- 1975, A summary of relative ages of lunar nearside and far-side plains: *Astrogeology* 66, U.S. Geol. Survey interagency report (open file), 26 p.
- Brennan, W. J., 1975, Modification of preare impact craters by volcanism and tectonism: *The Moon*, v. 12, p. 449-461.
- Bryan, W. B., and Adams, M.-L., 1973, Some volcanic and structural features of Mare Serenitatis: *Apollo 17 Prelim. Sci. Rept.*, NASA SP-330, p. 30-9 to 30-12.
- Carr, M. H., 1965, Geologic map and section of the Timocharis region of the Moon: U.S. Geol. Survey Misc. Geol. Inv. Map I-462, scale 1:1,000,000.
- 1966, Geologic map of the Mare Serenitatis region of the Moon: U.S. Geol. Survey Misc. Geol. Inv. Map I-489, scale 1:1,000,000.
- 1969, Geologic map of the Alphonsus region of the Moon: U.S. Geol. Survey Misc. Geol. Inv. Map I-599, scale 1:1,000,000.
- Carr, M. H., Howard, K. A., and El-Baz, Farouk, 1971, Geologic maps of the Apennine-Hadley Region of the Moon, Apollo 15 pre-mission maps: U.S. Geol. Survey Misc. Geol. Inv. Map I-723, scales 1:250,000 and 1:50,000.
- Chao, E. C. T., 1974, Impact cratering models and their application to lunar studies—A geologist's view: *Proc., Lunar Sci. Conf.*, 5th, *Geochim. et Cosmochim. Acta*, supp. 5, v. 1, p. 35-52.
- 1977, The Ries crater of southern Germany, a model for large basins on planetary surfaces: *Geologisches Jahrbuch*, Series A, no. 43, 85 p.
- Chao, E. C. T., Hodges, C. A., Boyce, J. M., and Soderblom, L. A., 1975, Origin of lunar light plains: *U.S. Geol. Survey Jour. Research*, v. 3, no. 4, p. 379-392.
- Charette, M. P., and Adams, J. B., 1975, Mare basalts: Characterization of compositional parameters by spectral reflectance, in *Papers presented at conference, Origin of mare basalts*, Houston, Texas, Nov. 1975: *Lunar Sci. Inst. contr.* 234, p. 25-28.
- Charette, M. P., McCord, T. B., Pieters, Carle, and Adams, J. B., 1974, Application of remote spectral reflectance measurements to lunar geology classification and determination of titanium content of lunar soils: *Jour. Geophys. Research*, v. 79, no. 11, p. 1605-1613.
- Colton, G. W., Howard, K. A., and Moore, H. J., 1972, Mare ridges and arches in southern Oceanus Procellarum: *Apollo 16 Prelim. Sci. Rept.*, NASA SP-315, p. 29-90 to 29-93.
- Dence, M. R., 1971, Impact melts: *Jour. Geophys. Research*, v. 76, p. 5552-5565.
- Eggleton, R. E., 1964, Preliminary geology of the Rhiphaeus quadrangle of the Moon and definition of the Fra Mauro Formation, in *Astrogeologic Studies Annual Progress Report*, Aug. 1962-July 1963, pt. A: U.S. Geol. Survey open-file report, p. 46-63.
- 1965, Geologic map of the Rhiphaeus Mountains region of the Moon: U.S. Geol. Survey Misc. Geol. Inv. Map I-458, scale 1:1,000,000.
- Eggleton, R. E., and Marshall, C. H., 1962, Notes on the Apenninian Series and pre-Imbrian stratigraphy in the vicinity of Mare Humorum and Mare Nubium, in *Astrogeologic Studies Semiannual Progress Report* Feb. 1961 to Aug. 1961: U.S. Geol. Survey open-file report, p. 132-137.
- Eggleton, R. E., and Offield, T. W., 1970, Geologic maps of the Fra Mauro region of the Moon, Apollo 14 pre-mission maps: U.S. Geol. Survey Misc. Geol. Inv. Map I-708, scale 1:25,000 and 1:250,000.
- Eggleton, R. E., and Schaber, G. G., 1972, Cayley Formation interpreted as basin ejecta: *Apollo 16 Prelim. Sci. Rept.*, NASA SP-315, p. 29-7 to 29-16.
- El-Baz, Farouk, 1973, "D-caldera": New photographs of a unique feature: *Apollo 17 Prelim. Sci. Rept.*, NASA SP-330, p. 30-13 to 30-17.
- Elston, D. P., 1972, Geologic map of the Colombo quadrangle of the Moon: U.S. Geol. Survey Misc. Geol. Inv. Map I-714, scale 1:1,000,000.
- Fielder, Gilbert, and Fielder, J., 1968, Lava flows in Mare Imbrium: Boeing Science Research Laboratory document D1-82-0749, 36 p.
- Gault, D. E., 1974, Impact cratering, in *Greeley, R., and Schultz, P. H., eds., A primer in lunar geology*: Mountain View, Calif., NASA Ames Research Center (Comment edition), p. 137-175.
- Gault, D. E., Quaide, W. L., and Oberbeck, V. R., 1968, Impact cratering mechanics and structures, in *French, B. M., and Short, N. M., eds., Shock metamorphism of natural materials*: Baltimore, Mono Book Corp., p. 87-99.
- Gilbert, G. K., 1893, The Moon's face, a study of the origin of its features: *Philos. Soc. Washington Bull.*, v. 12, p. 241-292.
- Gold, Thomas, Bilson, E., and Baron, R. L., 1977, The search for the cause of the low albedo of the Moon: *Jour. Geophys. Research*, v. 82, p. 4899-4908.
- Greeley, Ronald, 1973, Comparative geology of crater Aratus CA (Mare Serenitatis) and Bear Crater (Idaho): *Apollo 17 Prelim. Sci. Rept.*, NASA SP-330, p. 30-1 to 30-6.
- Greeley, Ronald, and Carr, M. H., eds., 1976, *A geological basis for the exploration of the planets*: National Aeronautics and Space Administration, NASA SP-417, 109 p.
- Hackman, R. J., 1962, Geologic map and sections of the Kepler region of the Moon: U.S. Geol. Survey Misc. Geol. Inv. Map I-355, scale 1:1,000,000.
- 1964, Stratigraphy and structure of the Montes Apenninus quadrangle of the Moon, in *Astrogeologic Studies Annual Progress Report*, Aug. 1962-July 1963, pt. A: U.S. Geol. Survey open-file report, p. 18.
- 1966, Geologic map of the Montes Apenninus region of the Moon: U.S. Geol. Survey Misc. Geol. Inv. Map I-463, scale 1:000,000.
- Hackman, R. J., and Mason, A. C., 1961, Engineer special study of the surface of the Moon: U.S. Geol. Survey Misc. Geol. Inv. Map I-351, scale 1:3,800,000.
- Hartmann, W. K., 1963, Radial structures surrounding lunar basins, I: The Imbrium system: *Arizona Univ. Lunar and Planetary Lab. Commun.*, v. 2, no. 24, p. 1-15.
- 1964, Radial structures surrounding lunar basins, II: Orientale and other systems; Conclusions: *Arizona Univ. Lunar and Planetary Lab. Commun.* v. 2, no. 36, p. 175-191.
- 1972, Interplanet variations in scale of crater morphology—Earth, Mars, Moon: *Icarus*, v. 17, p. 707-713.
- Hartmann, W. K., and Kuiper, G. P., 1962, Concentric structures surrounding lunar basins: *Arizona Univ. Lunar and Planetary Lab. Commun.*, v. 1, no. 12, p. 51-66.

- Hartmann, W. K., and Wood, C. A., 1971, Moon: Origin and evolution of multi-ring basins: *The Moon*, v. 3, no. 1, p. 4-78.
- Heacock, R. L., Kuiper, G. P., Shoemaker, E. M., Urey, H. C., and Whitaker, E. A., 1965, Ranger VII. Part II. Experimenters' analyses and interpretations: Pasadena, Calif., Jet Propulsion Lab. Tech. Report 32-700, 154 p.
- Head, J. W., 1972, Small-scale analogs of the Cayley Formation and Descartes mountains in impact-associated deposits: *Apollo 16 Prelim. Sci. Report*, NASA SP-315, p. 29-16 to 29-20.
- 1974a, Morphology and structure of the Taurus-Littrow highlands (Apollo 17): Evidence for their origin and evolution: *The Moon*, v. 9, p. 355-395.
- 1974b, Lunar dark-mantle deposits: Possible clues to the distribution of early mare deposits: *Proc., Lunar Sci. Conf.*, 5th, *Geochim. et Cosmochim. Acta*, supp. 5, v. 1, p. 207-222.
- 1974c, Orientale multi-ringed basin interior and implications for the petrogenesis of lunar highland samples: *The Moon*, v. 11, p. 327-356.
- 1976, Evidence for sedimentary origin of Imbrium sculpture and lunar basin radial texture: *The Moon*, v. 15, p. 445-462.
- 1977, Origin of rings in multi-ringed basin: Evidence from morphology and ring spacing, in Roddy, D. J., Pepin, R. O., and Merrill, R. B., eds., *Impact and explosion cratering*: London, Pergamon Press, p. 563-573.
- Head, J. W., and Goetz, A. F. H., 1972, Descartes region: Evidence for Copernican-age volcanism: *Jour. Geophys. Research*, v. 77, no. 8, p. 1368-1374.
- Head, J. W., and Hawke, B. R., 1975, Geology of the Apollo 14 region (Fra Mauro): Stratigraphic history and sample provenance: *Proc., Lunar Sci. Conf.*, 6th., *Geochim. et Cosmochim. Acta*, supp. 6, v. 3, p. 2483-2501.
- Heiken, G. H., McKay, D. S., and Brown, R. W., 1974, Lunar deposits of possible pyroclastic origin: *Geochim. et Cosmochim. Acta*, v. 38, p. 1703-1718.
- Hinners, N. W., 1972, Apollo 16 site selection: *Apollo 16 Prelim. Sci. Report*, NASA SP-315, p. 1-1 to 1-3.
- 1973, Apollo 17 site selection: *Apollo 17 Prelim. Sci. Report*, NASA SP-330, p. 1-1 to 1-5.
- Hodges, C. A., 1972, Descartes highlands: Possible analogs around the Orientale basin: *Apollo 16 Prelim. Sci. Rept.*, NASA SP-315, p. 29-20 to 29-24.
- 1973, Mare ridges and lava lakes: *Apollo 17 Prelim. Sci. Rept.*, NASA SP-330, p. 31-12 to 31-21.
- Hodges, C. A., Muehlberger, W. R., and Ulrich, G. E., 1973, Geologic setting of Apollo 16: *Proc., Lunar Sci. Conf.*, 4th, *Geochim. et Cosmochim. Acta*, supp. 4, v. 1, p. 1-25.
- Hodges, C. A., and Wilhelms, D. E., 1976, Formation of lunar basin rings: Abstracts, *Internat. Geol. Congress*, Sydney, Australia, 1976, p. 612-613.
- Howard, K. A., 1974, Fresh lunar impact craters: Review of variations with size: *Proc., Lunar Sci. Conf.*, 5th, *Geochim. et Cosmochim. Acta*, supp. 5, v. 1, p. 61-69.
- 1975, Geologic map of the crater Copernicus: *U.S. Geol. Survey Misc. Geol. Inv. Map I-840*, scale 1:250,000.
- Howard, K. A., Carr, M. H., and Muehlberger, W. R., 1973, Basalt stratigraphy of southern Mare Serenitatis: *Apollo 17 Prelim. Sci. Rept.*, NASA SP-330, p. 29-1 to 29-12.
- Howard, K. A., and Larsen, B. R., 1972, Lineaments that are artifacts of lighting: *Apollo 15 Prelim. Sci. Rept.*, NASA SP-289, p. 25-58 to 25-62.
- Howard, K. A., and Masursky, Harold, 1968, Geologic map of the Ptolemaeus quadrangle of the Moon: *U.S. Geol. Survey Misc. Geol. Inv. Map I-566*, scale 1:1,000,000.
- Howard, K. A., and Muehlberger, W. R., 1973, Lunar thrust faults in the Taurus-Littrow region: *Apollo 17 Prelim. Sci. Rept.*, NASA SP-330, p. 31-22 to 31-25.
- Howard, K. A., Wilhelms, D. E., and Scott, D. H., 1974, Lunar basin formation and highland stratigraphy: *Reviews Geophysics and Space Physics*, v. 12, no. 3, p. 309-327.
- Howard, K. A., and Wilshire, H. G., 1975, Flows of impact melt at lunar craters: *U.S. Geol. Survey Jour. Research*, v. 3, no. 2, p. 237-251.
- Johnson, T. V., Matson, D. L., Phillips, R. J., and Saunders, R. S., 1975, Vidicon spectral imaging: Color enhancement and digital maps: *Proc., Lunar Sci. Conf.*, 6th, *Geochim. et Cosmochim. Acta*, supp. 6, v. 3, p. 2677-2688.
- Johnson, T. V., Pieters, Carle, and McCord, T. B., 1973, Mare Humorum: An integrated study of spectral reflectivity: *Icarus*, v. 19, no. 2, p. 224-229.
- Karlstrom, T. N. V., 1974, Geologic map of the Schickard quadrangle of the Moon: *U.S. Geol. Survey Misc. Geol. Inv. Map I-823 (LAC-110)*, scale 1:1,000,000.
- Kuiper, G. P., 1954, On the origin of the lunar surface features: *Natl. Acad. Sci. Proc.*, v. 40, no. 12, p. 1096-1112.
- 1959, The exploration of the Moon, in Alperin, Morton, and Gregory, H. F., eds., *Vistas in astronautics*: New York, Pergamon, v. 2, p. 272-312.
- 1965, Interpretation of Ranger VII records, in Ranger VII—Part II. Experimenters' analyses and interpretations: Pasadena, Calif., Jet Propulsion Laboratory Tech. Rept. 32-700, p. 9-73.
- Lindsay, J. F., 1976, Lunar stratigraphy and sedimentology: New York, Elsevier, 302 p.
- Lucchitta, B. K., 1973, Photogeology of the dark material in the Taurus-Littrow region of the Moon: *Proc., Lunar Sci. Conf.*, 4th, *Geochim. et Cosmochim. Acta*, supp. 4, v. 1, p. 149-162.
- 1976, Mare ridges and related highland scarps—Result of vertical tectonism?: *Proc., Lunar Sci. Conf.*, 7th, *Geochim. et Cosmochim. Acta*, supp. 7, p. 2761-2782.
- Lucchitta, B. K., and Sanchez, A. G., 1975, Crater studies in the Apollo 17 region: *Proc., Lunar Sci. Conf.*, 6th, *Geochim. et Cosmochim. Acta*, supp. 6, v. 3, p. 2427-2441.
- Lucchitta, B. K., and Schmitt, H. H., 1974, Orange material in the Sulcius Gallus Formation at the southwestern edge of Mare Serenitatis: *Proc., Lunar Sci. Conf.*, 5th, *Geochim. et Cosmochim. Acta*, supp. 5, v. 1, p. 223-234.
- Lunar Sample Preliminary Examination Team, 1972, Preliminary examination of lunar samples: *Apollo 16 Prelim. Sci. Rept.*, NASA SP-315, p. 7-1 to 7-58.
- 1973, Preliminary examination of lunar samples: *Apollo 17 Prelim. Sci. Rept.*, NASA SP-330, p. 7-1 to 7-46.
- McCaughey, J. F., 1967, The nature of the lunar surface as determined by systematic geologic mapping, in Runcorn, S. K., ed., *Mantles of the Earth and terrestrial planets*: New York, John Wiley & Sons, p. 431-460.
- 1968, Geologic results from the lunar precursor probes: *Am. Inst. Aeronautics Astronautics Jour.*, v. 6, no. 10, p. 1991-1996.
- 1969, Geologic map of the Alphonsus GA region of the Moon: *U.S. Geol. Survey Misc. Geol. Inv. Map I-586*, scale 1:1,000,000.
- 1977, Orientale and Caloris: *Physics Earth and Planetary Interiors*, v. 15, p. 220-250.
- McCord, T. B., and Adams, J. B., 1972, Progress in remote optical analysis of lunar surface composition: *The Moon*, v. 7, p. 453-474.
- McCord, T. B., Charette, M. P., Johnson, T. V., Lebofsky, L. A., and Pieters, Carle, 1972, Lunar spectral types: *Jour. Geophys. Research*, v. 77, no. 8, p. 1349-1359.
- McCord, T. B., Pieters, Carle, and Feierberg, M. A., 1976, Multispectral mapping of the lunar surface using ground-based telescopes: *Icarus*, v. 29, p. 1-34.

- Malin, M. C., 1974, Lunar red spots: Possible pre-mare materials: *Earth and Planetary Sci. Letters*, v. 21, p. 331-341.
- Marshall, C. H., 1961, Thickness of the Procellarian System, Letronne region of the Moon: U.S. Geol. Survey Prof. Paper 424-D, p. D208-D211.
- 1963, Geologic map and sections of the Letronne region of the Moon: U.S. Geol. Survey Misc. Geol. Inv. Map I-385, scale 1:1,000,000.
- Milton, D. J., 1968, Geologic map of the Theophilus quadrangle of the Moon: U.S. Geol. Survey Misc. Geol. Inv. Map I-546, scale 1:1,000,000.
- Milton, D. J., and Hodges, C. A., 1972, Geologic maps of the Descartes region of the Moon, Apollo 16 pre-mission maps: U.S. Geol. Survey Misc. Geol. Inv. Map I-748, scales 1:250,000 and 1:50,000.
- Milton, D. J., and Roddy, D. J., 1972, Displacements within impact craters: *Internat. Geol. Cong. Rept. Sess. 24th*, p. 119-24.
- Moore, H. J., 1965, Geologic map of the Aristarchus region of the Moon: U.S. Geol. Survey Misc. Geol. Inv. Map I-465, scale 1:1,000,000.
- 1967, Geologic map of the Seleucus quadrangle of the Moon: U.S. Geol. Survey Misc. Geol. Inv. Map I-527, scale 1:1,000,000.
- 1971, Craters produced by missile impacts: *Jour. Geophys. Research*, v. 76, no. 23, p. 5750-5755.
- 1976, Missile impact craters (White Sands, New Mexico) and applications to lunar research: U.S. Geol. Survey Prof. Paper 812-B, 47 p.
- Moore, H. J., Hodges, C. A., and Scott, D. H., 1974, Multiringed basins—Illustrated by Orientale and associated features: *Proc. Lunar Sci. Conf.*, 5th, *Geochim. et Cosmochim. Acta*, supp. 5, v. 1, p. 71-100.
- Morgan, J. W., Ganapathy, R., Higuchi, Hideo, Krahenbuhl, Urs, and Anders, Edward, 1974, Lunar basins: Tentative characterizations of projectiles, from meteoritic elements in Apollo 17 boulders: *Proc., Lunar Sci. Conf.*, 5th, *Geochim. et Cosmochim. Acta*, supp. 5, v. 2, p. 1703-1736.
- Morris, E. C., 1964, Stratigraphic relations in the vicinity of the crater Julius Caesar, in *Astrologic Studies Annual Progress Report*, Aug. 1962-July 1963, pt A.: U.S. Geol. Survey open-file report, p. 31-32.
- Morris, E. C., and Wilhelms, D. E., 1967, Geologic map of the Julius Caesar quadrangle of the Moon: U.S. Geol. Survey Misc. Geol. Inv. Map I-510, scale 1:1,000,000.
- Morrison, R. H., and Oberbeck, V. R., 1975, Geomorphology of crater and basin deposits—Emplacement of the Fra Mauro Formation: *Proc. Lunar Sci. Conf.*, 6th, *Geochim. et Cosmochim. Acta*, supp. 6, v. 3, p. 2503-2530.
- Muehlberger, W. R., 1974, Structural history of southeastern Mare Serenitatis and adjacent highlands: *Proc., Lunar Sci. Conf.*, 5th, *Geochim. et Cosmochim. Acta*, supp. 5, v. 1, p. 101-110.
- Muehlberger, W. R. and 29 coauthors, 1972, Preliminary geologic investigation of the Apollo 16 landing site: Apollo 16 Prelim. Sci. Rept., NASA SP-315, p. 6-1 to 6-81.
- Muehlberger, W. R., and 19 coauthors, 1973, Preliminary geologic investigation of the Apollo 17 landing site: Apollo 17 Prelim. Sci. Rept., NASA SP-330, p. 6-1 to 6-91.
- Mutch, T. A., 1973 *Geology of the Moon—A stratigraphic view*: Princeton, N. J., Princeton Univ. Press, 391 p. (2d ed.).
- Neukum, Gerhard, and König, Beate, 1976, Dating of individual lunar craters: *Proc., Lunar Sci. Conf.*, 7th, *Geochim. et Cosmochim. Acta*, supp. 7, p. 2867-2881.
- Neukum, Gerhard, König, Beate, and Arkani-Hamed, J., 1975a, A study of lunar impact crater size-distributions: *The Moon*, v. 12, p. 201-229.
- Neukum, Gerhard, König, Beate, Fechtig, H., and Storzer, D., 1975b, Cratering in the earth-moon system: Consequences for age determination by crater counting: *Proc. Lunar Sci. Conf.*, 6th, *Geochim. et Cosmochim. Acta*, supp. 6, v. 3, p. 2597-2620.
- Nichols, D. J., Young, R. A., and Brennan, W. J., 1974, Lunar kipukas as evidence for an extended tectonic and volcanic history of the maria [abs.]: *Lunar Sci. Conf.*, 5th, Houston, Texas, Lunar Sci. Inst., p. 550-552.
- Oberbeck, V. R., 1973, Simultaneous impact and lunar craters: *The Moon*, v. 6, p. 83-92.
- 1975, The role of ballistic erosion and sedimentation in lunar stratigraphy: *Rev. Geophys. and Space Physics*, v. 13, no. 2, p. 337-362.
- Oberbeck, V. R., Hörz, F., Morrison, R. H., Quaide, W. L., and Gault, D. E., 1975, On the origin of the lunar smooth-plains: *The Moon*, v. 12, p. 19-54.
- Oberbeck, V. R., and Morrison, R. H., 1974, Laboratory simulation of the herringbone pattern associated with lunar secondary crater chains: *The Moon*, v. 9, p. 415-455.
- 1976, Candidate areas for *in situ* ancient lunar materials: *Proc. Lunar Sci. Conf.*, 7th, *Geochim. et Cosmochim. Acta*, supp. 7, p. 2983-3005.
- Oberbeck, V. R., Morrison, R. H., Hörz, F., Quaide, W. L., and Gault, D. E., 1974, Smooth plains and continuous deposits of craters and basin: *Proc., Lunar Sci. Conf.*, 5th, *Geochim. et Cosmochim. Acta*, supp. 5, v. 1, p. 111-136.
- Page, N. J., 1970, Geologic map of the Cassini quadrangle of the Moon: U.S. Geol. Survey Misc. Geol. Inv. Map I-666, scale 1:1,000,000.
- Pieters, Carle, Head, J. W., McCord, T. B., Adams, J. B., and Zisk, S. H., 1975, Geochemical and geological units of Mare Humorum: Definition using remote sensing and lunar sample information: *Proc., Lunar Sci. Conf.*, 6th, *Geochim. et Cosmochim. Acta*, supp. 6, v. 3, p. 2689-2710.
- Pieters, Carle, and McCord, T. B., 1975, Classification and distribution of lunar mare basalt types, in *Papers presented at conference, Origin of mare basalts*, Houston, Texas, Nov. 1975: Lunar Sci. Inst. contribution 234, p. 125-129.
- 1976, Characterization of lunar mare basalt types: 1. A remote sensing study using reflection spectroscopy of surface soils: *Proc., Lunar Sci. Conf.*, 7th, *Geochim. et Cosmochim. Acta*, supp. 7, v. 3, p. 2677-2690; also frontispiece of v. 1.
- Pieters, Carle, McCord, T. B., Zisk, S. H., and Adams, J. B., 1973, Lunar black spots and the nature of the Apollo 17 landing area: *Jour. Geophys. Research*, v. 78, no. 26, p. 5867-5875.
- Pike, R. J., 1971, Genetic implications of the shapes of martian and lunar craters: *Icarus*, v. 15, no. 3, p. 384-395.
- Reed, V. S., and Wolfe, E. W., 1975, Origins of the Taurus-Littrow massifs: *Proc., Lunar Sci. Conf.*, 6th, *Geochim. et Cosmochim. Acta*, supp. 6, v. 3, p. 2443-2461.
- Roberts, W. A., 1966, Shock—A process in extraterrestrial sedimentology: *Icarus*, v. 5, p. 459-477.
- Schaber, G. G., 1969, Geologic map of the Sinus Iridum quadrangle of the Moon: U.S. Geol. Survey Misc. Geol. Inv. Map I-602.
- 1973, Lava flows in Mare Imbrium: Geologic evaluation from Apollo orbital photography: *Proc., Lunar Sci. Conf.*, 4th, *Geochim. et Cosmochim. Acta*, supp. 4, v. 1, p. 73-92.
- Schaber, G. G., Boyce, J. M., and Moore, H. J., 1976, The scarcity of mappable flow lobes on the lunar maria: Unique morphology of the Imbrium flows: *Proc., Lunar Sci. Conf.*, 7th, *Geochim. et Cosmochim. Acta*, supp. 7, p. 2783-2800.
- Schaber, G. G., Thompson, T. W., and Zisk, S. H., 1975, Lava flows in Mare Imbrium: An evaluation of anomalously low earth-based radar reflectivity: *The Moon*, v. 13, p. 395-423.
- Schultz, P. H., 1976, Floor-fractured lunar craters: *The Moon*, v. 15, p. 241-273.

- Schultz, P. H., and Gault, D. E., 1975, Seismic effects from major basin formations on the Moon and Mercury: *The Moon*, v. 12, p. 159-177.
- Scott, D. H., 1972a, Structural aspects of Imbrium sculpture: Apollo 16 Prelim. Sci. Rept., NASA SP-315, p. 29-31 to 29-33.
- 1972b, Geologic map of the Maurolycus quadrangle of the Moon: U.S. Geol. Survey Misc. Geol. Inv. Map I-695, scale 1:1,000,000.
- 1972c, Geologic map of the Eudoxus quadrangle of the Moon: U.S. Geol. Survey Misc. Geol. Inv. Map I-705, scale 1:1,000,000.
- 1973a, Mare Serenitatis cinder cones and terrestrial analogs: Apollo 17 Prelim. Sci. Rept., NASA SP-330, p. 30-7 to 30-8.
- 1973b, Small structures of the Taurus-Littrow region: Apollo 17 Prelim. Sci. Rept., NASA SP-330, p. 31-25 to 31-28.
- 1974, The geologic significance of some lunar gravity anomalies: Proc., Lunar Sci. Conf., 5th, *Geochim. et Cosmochim. Acta*, supp. 5, v. 3, p. 3025-3036.
- Scott, D. H., Diaz, J. M., and Watkins, J. A., 1975, The geological evaluation and regional synthesis of metric and panoramic photographs: Proc., Lunar Sci. Conf., 6th, *Geochim. et Cosmochim. Acta*, supp. 6, v. 3, p. 2531-2540.
- Scott, D. H., Lucchitta, B. K., and Carr, M. H., 1972, Geologic maps of the Taurus-Littrow region of the Moon—Apollo 17 pre-mission maps: U.S. Geol. Survey Misc. Geol. Inv. Map I-800, scales 1:250,000 and 1:50,000.
- Scott, D. H., McCauley, J. F., and West, M. N., 1977, Geologic map of the west side of the Moon: U.S. Geol. Survey Misc. Geol. Inv. Map I-1034, scale 1,500,000.
- Scott, D. H., and Pohn, H. A., 1972, Geologic map of the Macrobius quadrangle of the Moon: U.S. Geol. Survey Misc. Geol. Inv. Map I-799, scale 1:1,000,000.
- Sekiguchi, Naosuke, 1970, On the fissions of a solid body under influence of tidal force; with application to the problem of twin craters on the Moon: *The Moon*, v. 1, p. 429-439.
- Shoemaker, E. M., 1959, Address to earth sciences session: Proc. Lunar Planetary Explor. Colloquium, v. 2, no. 1, p. 20-28.
- 1962, Interpretation of lunar craters, in Kopal, Zdeněk, ed., *Physics and astronomy of the Moon*: New York, Academic Press, p. 283-359.
- 1965, Preliminary analysis of the fine structure of the lunar surface in Mare Cognitum, in *Ranger VII—Part II. Experimenters' analyses and interpretations*: Pasadena, Calif., Jet Propulsion Laboratory Tech. Rept. 32-700, p. 75-134.
- Shoemaker, E. M., Batson, R. M., Holt, H. E., Morris, E. C., Rennison, J. J., and Whitaker, E. A., 1968, Television experiments from Surveyor VII, in *Surveyor VII mission report: Part II, Science results*: Pasadena, Calif., Jet Propulsion Lab. Tech. Report 32-1264, p. 9-76.
- Shoemaker, E. M., and Hackman, R. J., 1962, Stratigraphic basis for a lunar time scale, in Kopal, Zdeněk, and Mikhailov, Z. K., eds., *the Moon—Symposium 14, International Astronomical Union, Leningrad, 1960*: London, Academic Press, p. 289-300.
- Short, N. M., and Forman, M. L., 1972, Thickness of impact crater ejecta on the lunar surface: *Modern Geology*, v. 3, p. 69-91.
- Soderblom, L. A., and Boyce, J. M., 1972, Relative ages of some near-side and far-side terra plains based on Apollo 16 metric photography: Apollo 17 Prelim. Sci. Rept., NASA SP-315, p. 29-3 to 29-6.
- 1976, Distribution and evolution of global color provinces on the Moon, in *Lunar Science VII, Abstracts 7th Lunar Science Conference*: Houston, Texas, Lunar Sci. Inst., p. 882-824.
- Soderblom, L. A., and Lebofsky, L. A., 1972, Technique for rapid determination of relative ages of lunar areas from orbital photography: *Jour. Geophys. Research*, v. 77, no. 3, p. 279-296.
- Strom, R. G., 1964, Analysis of lunar lineaments, I: Tectonic maps of the Moon: *Commun. Lunar and Planetary Lab., Univ. Arizona*, v. 2, no. 39, p. 205-216.
- 1971, Lunar mare ridges, rings and volcanic ring complexes: *Modern Geology*, v. 2, p. 133-157.
- Stuart-Alexander, D. E., and Howard, K. A., 1970, Lunar maria and circular basins—A review: *Icarus*, v. 12, no. 3, p. 440-456.
- Stuart-Alexander, D. E., and Wilhelms, D. E., 1975, The Nectarian System, a new lunar time-stratigraphic unit: U.S. Geol. Survey Jour. Research, v. 3, no. 1, p. 53-58.
- Sutton, R. L., Hait, M. H., and Swann, G. A., 1972, Geology of the Apollo 14 landing site: Proc., Lunar Sci. Conf., 3d, *Geochim. et Cosmochim. Acta*, supp. 3, v. 1, p. 27-38.
- Swann, G. A., and 19 coauthors, 1972, Preliminary investigation of the Apollo 15 landing site: Apollo 15 Prelim. Sci. Rept., NASA SP-289, p. 5-1 to 5-112.
- Swann, G. A., Bailey, N. G., Batson, R. M., Eggleton, R. E., Hait, M. H., Holt, H. E., Larson, K. B., Reed, V. S., Schaber, G. G., Sutton, R. L., Trask, N. J., Ulrich, G. E., and Wilshire, H. G., 1977, Geology of the Apollo 14 landing site in the Fra Mauro highlands: U.S. Geol. Survey Prof. Paper 880, 103 p.
- Thompson, T. W., Howard, K. A., Shorthill, R. W., Tyler, G. L., Zisk, S. H., Whitaker, E. A., Schaber, G. G., and Moore, H. J., 1973, Remote sensing of Mare Serenitatis: Apollo 17 Prelim. Sci. Rept., NASA SP-330, p. 33-3 to 33-10.
- Trask, N. J., 1970, Geologic maps of early Apollo landing sites: Supp. to U.S. Geol. Survey Misc. Geol. Inv. Maps I-616 to I-627.
- Ulrich, G. G., Hodges, C. A., and Muehlberger, W. R., eds., 1980, *Geology of the Apollo 16 area, central lunar highlands*: U.S. Geol. Survey Prof. Paper 1048 (in press).
- Varnes, D. J., 1974, The logic of geological maps, with reference to their interpretation and use for engineering purposes: U.S. Geol. Survey Prof. Paper 837, 48 p.
- Wells, Ed, and Hapke, Bruce, 1977, Lunar soil: Iron and titanium bands in the glass fraction: *Science*, v. 195, no. 4282, p. 977-979.
- Whitaker, E. A., 1966, The surface of the Moon, in Hess, W. M., Menzel, D. H., and O'Keefe, J. A., eds., *The nature of the lunar surface*: Baltimore, Johns Hopkins Press, p. 79-98.
- 1972a, Mare Imbrium lava flows and their relationship to color boundaries: Apollo 15 Prelim. Sci. Rept., NASA SP-289, p. 25-83 to 25-84.
- 1972b, Lunar color boundaries and their relationship to topographic features: A preliminary survey: *The Moon*, v. 4, p. 348-355.
- 1972c, Color contrasts in Mare Nubium and the southern Oceanus Procellarum: Apollo 16 Prelim. Sci. Rept., NASA SP-315, p. 29-104 to 29-105.
- 1972d, An unusual mare feature: Apollo 15 Prelim. Sci. Rept., NASA SP-289, p. 25-84 to 25-85.
- Wilhelms, D. E., 1965, Fra Mauro and Cayley Formations in the Mare Vaporum and Julius Caesar quadrangles, in *Astrogeologic Studies Annual Progress Report, July 1964-July 1965, pt. A*: U.S. Geol. Survey open-file report, p. 13-28.
- 1968, Geologic map of the Mare Vaporum quadrangle of the Moon: U.S. Geol. Survey Misc. Geol. Inv. Map I-548, scale 1:1,000,000.
- 1970, Summary of lunar stratigraphy—Telescopic observations: U.S. Geol. Survey Prof. Paper 599-F, p. F1-F47.
- 1972a, Geologic map of the Taruntius quadrangle of the Moon: U.S. Geol. Survey Misc. Geol. Inv. Map I-722, scale 1:1,000,000.
- 1972b, Geologic mapping of the second planet: Interagency report *Astrogeology 55*, U.S. Geol. Survey open-file rept., 36 p.
- 1972c, Preliminary geologic map of the region around the Candidate Proclus Apollo landing site: Apollo 15 Prelim. Sci. Rept., NASA SP-289, p. 25-72 to 25-75.

- 1972d, Reinterpretations of the northern Nectaris basin: Apollo 16 Prelim. Sci. Rept., NASA SP-315, p. 29-27 to 29-30.
- 1973, Geologic map of the northern Crisium region: Apollo 17 Prelim. Sci. Rept., NASA SP-330, p. 29-29 to 29-34.
- 1976, Secondary impact craters of lunar basins: Proc., Lunar Sci. Conf., 7th, *Geochim. et Cosmochim. Acta*, supp. 7, p. 2883-2901.
- Wilhelms, D. E., Hodges, C. A., and Pike, R. J., 1977, Nested-crater model of lunar ringed basins, *in* Roddy, D. J., Pepin, R. O., and Merrill, R. B., eds., *Impact and explosion cratering*: London, Pergamon Press, p. 539-562.
- Wilhelms, D. E., and McCauley, J. F., 1971, Geologic map of the near side of the Moon: U.S. Geol. Survey Misc. Geol. Inv. Map I-703, scale 1:5,000,000.
- Wolfe, E. W., and Bailey, N. G., 1972, Lineaments of the Apennine Front—Apollo 15 landing site: Proc., Lunar Sci. Conf., 3d, *Geochim. et Cosmochim. Acta*, supp. 3, v. 1, p. 15-25.
- Wolfe, E. W., Lucchitta, B. K., Reed, V. S., Ulrich, G. E., and Sanchez, A. G., 1975, Geology of the Taurus-Littrow valley floor: Proc., Lunar Sci. Conf., 6th, *Geochim. et Cosmochim. Acta*, supp. 6, v. 3, p. 2463-2482.
- Wolfe, E. W., and Reed, V. S., 1976, Geology of the massifs at the Apollo 17 landing site: U.S. Geol. Survey Jour. Research, v. 4, no. 2, p. 171-180.
- Wood, C. A., and Head, J. W., 1975, Geologic setting and provenance of spectrally distinct pre-mare material of possible volcanic origin, *in* Papers presented at conference, Origin of mare basalts, Houston, Texas, Nov. 1975: Lunar Sci. Inst. Contr. 244, p. 190-193.
- Young, R. A., Brennan, W. J., Wolfe, R. W., and Nichols, D. J., 1973a, Analysis of lunar mare geology from Apollo photography: Proc., Lunar Sci. Conf., 4th, *Geochim. et Cosmochim. Acta*, supp. 4, v. 1, p. 57-71.
- 1973b, Volcanism in the lunar maria: Apollo 17 Prelim. Sci. Rept., NASA SP-330, p. 31-1 to 31-11.
- Zisk, S. H., Hodges, C. A., Moore, H. J., Shorthill, R. W., Thompson, T. W., Whitaker, E. A., and Wilhelms, D. E., 1977, The Aristarchus-Harbinger region of the Moon: Surface geology and history from recent remote-sensing observations: *The Moon*, v. 17, 59-99.

